ABSTRACT

FRENCH, ADAM JAMES. The Initiation and Evolution of Multiple Modes of Convection Within a Meso–Alpha Scale Region. (Under the direction of Matthew D. Parker.)

On 30 March 2006 a convective episode occurred featuring isolated supercells, a mesoscale convective system (MCS) with parallel stratiform (PS) precipitation, and an MCS with leading stratiform (LS) precipitation. These three distinct convective modes occurred simultaneously across the same region in eastern Kansas. Multi-modal events, are especially challenging for forecasters given the wide range of severe weather threats that accompany the different convective modes. In order to better understand the mechanisms that govern such events, this study examined the 30 March 2006 episode through a combination of an observation-based case study and numerical simulations. From the results of this study we conclude that, for this event, localized environmental variations were largely responsible for the eventual convective mode, with the method of storm initiation having only limited effects. The resultant mode was very sensitive to both the environmental thermodynamic and wind shear profiles, as variations in either lead to different convective modes within the numerical simulations. Finally, we conclude that while the individual modes each developed within an environment distinctly favorable for that mode, they were able to persist in close proximity to one other due to a "middle ground" environment permissive of all three. Strong vertical shear and moderate instability led to the development of supercells in western Oklahoma and similarly strong shear oriented parallel to a surface dryline coupled with with dry air in the mid and upper levels led to the development of the PS linear MCS in central Kansas. Meanwhile, moderate wind shear coupled with high instability and strong linear forcing led to the development of the

LS MCS in eastern Kansas. Without this linear forcing, the moderate shear environment in eastern Kansas was supportive of both linear and isolated supercell modes, resulting in the storms that moved into this region maintaining their original organization.

The Initiation and Evolution of Multiple Modes of Convection Within a Meso–Alpha Scale Region

by

ADAM JAMES FRENCH

A thesis submitted to the Graduate Faculty of

North Carolina State University

in partial fulfillment of the

requirements for the Degree of

Master of Science

Marine, Earth, and Atmospheric Sciences

Raleigh, North Carolina

2007

APPROVED BY:

Matthew D. Parker, Chair of Advisory Committee

Gary Lackmann

Sandra Yuter

Dedication

To the men and women of my generation, and of generations past who instead of spending their late teens and early twenties pursuing higher education and enjoying college life, spent them around the world protecting our freedom. Without you, none of this work would have been possible, and I am forever indebted.

Biography

Adam French was born and raised in Manchester, Connecticut where he got to experience a wide variety of weather, from summer thunderstorms to winter nor'easters. This sparked an interest in the weather at an early age, however it was not until he wrote his 11th grade honors thesis on severe weather in Connecticut that Adam decided he wanted to become a meteorologist.

Adam attended Valparaiso University in northern Indiana from 2001-2005, where he received his B.S. in meteorology. While at Valpo, Adam was also a member of Christ College, an interdisciplinary honors college, from which he earned a minor in humanities, and graduated as a Christ College scholar. In the summer of 2004, Adam participated in the National Weather Center Research Experience for Undergraduates in Norman, Oklahoma where he analyzed data from the SPC/NSSL Spring Program. During his senior year at Valpo, Adam served as president of the Northwest Indiana Chapter of the National Weather Association and played a main role in the organization and running of the 3rd Annual Great Lakes Meteorology Conference. Following graduation from Valparaiso in 2005, Adam came to North Carolina State University and began pursuing a Masters degree as one of the inaugural members of the Convective Storms Group under Dr. Matthew Parker.

In his spare time, Adam enjoys hiking and camping with his girlfriend Miranda and hound dog Dixie. He is also an avid aviation photographer, and enjoys traveling to air shows to take pictures whenever his schedule allows.

Acknowledgments

I would first like to thank my adviser, Dr. Matthew Parker, both for taking me on as a Masters student and also for all of the guidance that he provided and knowledge that he shared with me through the course of this project. Also, my committee members, Dr's. Gary Lackmann and Sandra Yuter for their help and insights along the way. I also want to thank my parents, Jonathan and Loyola and sister Molly for their continued love and support in all of my endeavors. Thank you to my wonderful girlfriend, Miranda for helping me keep my sanity these last two years, you are amazing. Thank you to the members of the Convective Storms Group, especially Jerilyn Billings, Ben Baranowski and Billy Booth for all your help and for the countless discussions throughout the course of this research. Finally, last, but not least, I need to thank my dog, Dixie, as our daily walks always managed to lift my spirits whenever I became frustrated with a model run or developed a case of writers block. This research was funded by NSF Grant ATM0552154.

Contents

List of Figures

List of Tables

Chapter 1

Introduction

1.1 Motivation

A principle element of a severe weather forecast is the determination of the mode that the convective storms will take upon initiation, as different modes tend to be associated with different severe weather threats (Johns and Doswell 1992; Doswell and Evans 2003; Kain et al. 2006). In general, supercell storms can feature tornadoes, hail and severe winds, (e.g. Doswell and Burgess 1993; Davies-Jones et al. 2001) while linear modes, specifically bow echoes, tend to favor damaging straight line winds (e.g. Fujita 1978; Przybylinski 1995; Wakimoto 2001). In addition, linear mesoscale convective systems (MCSs) with line-parallel (hereafter PS) and line-leading (hereafter LS) stratiform precipitation can result in a larger threat for flash flooding due to either their slower motion (for LS systems, e.g. Pettet and Johnson 2003) or training of cells over one area (for PS systems, e.g. Parker and Johnson 2000; Schumacher and Johnson 2005). Given this association between storm mode and severe weather threat, an accurate prediction of mode can help forecasters to better prepare for a severe weather event, leading to better situational awareness and better warnings (McNulty 1995).

However, despite its importance in the formulation of an accurate severe weather forecast, convective mode remains difficult to anticipate and is an area of continuing research and focus (Kain et al. 2006). In line with past research, forecasters generally rely on analysis of vertical wind shear to determine the mode that storms will take (McNulty 1995; Edwards et al. 2002). This approach, however, can become complicated as different convective modes can occur within environments exhibiting similar wind profiles (e.g. Bluestein and Jain 1985; Bluestein and Weisman 2000; Doswell and Evans 2003; Parker 2007a; b). It becomes complicated further in cases where two or more of these modes are present at the same time. One such event occurred on 30 March 2006 and is the focus of this study. This event featured isolated supercells, as well as linear MCSs with parallel and leading stratiform precipitation evolving simultaneously over eastern Kansas (Fig. 1.1). Accompanying the various modes, a variety of severe weather was observed as well. Large hail and tornadoes, including a long-track (25 km) F-2 in southeast Kansas were observed with several of the supercell storms (Fig. 1.2). Additionally, the PS line produced numerous hail reports, as well as damaging wind reports late in its evolution as it was transitioning toward the trailing stratiform (TS) mode. Given this wide range of severe weather, the 30 March 2006 case underscores the importance of improved understanding of multi-mode episodes while providing a well developed example of one such event.

In light of the complex nature of multi-mode events, the goal of this study, is to examine the mechanisms behind one such event and determine both how all three modes developed, and subsequently how all three evolved in close proximity to each other. This two-pronged approach will be echoed throughout this thesis, as various results will be focused on storm initiation, examining initial storm formation during the first 30-60 minutes, while others will focus on storm evolution following initiation. This can be seen

in terms of the forecasting problem of not just determining the initial severe weather threat based on how storms will organize upon initiation, but then how that threat will evolve over time as storm organization evolves. Additionally, a broader goal of this study is to apply the findings from this single multi-mode case to the larger problem of anticipating convective mode in similar moderate-high wind shear environments. Namely the goal is to identify various features that favor the development of each mode within the larger-scale moderate-high shear environment.

1.2 Structure of this thesis

Chapter 2 provides a general review of past literature regarding convective mode as well the specific modes that will be detailed in the remainder of this study. Chapter 3 details the methods and results of the observed case study, setting the stage for the numerical simulations, which are detailed in chapter 4. Chapter 5 then discusses and synthesizes the results of the case study and simulations and revisits the broader theme of multiple modes of convective storms in localized regions. This final chapter closes by summarizing these conclusions and suggesting possible avenues for future work.

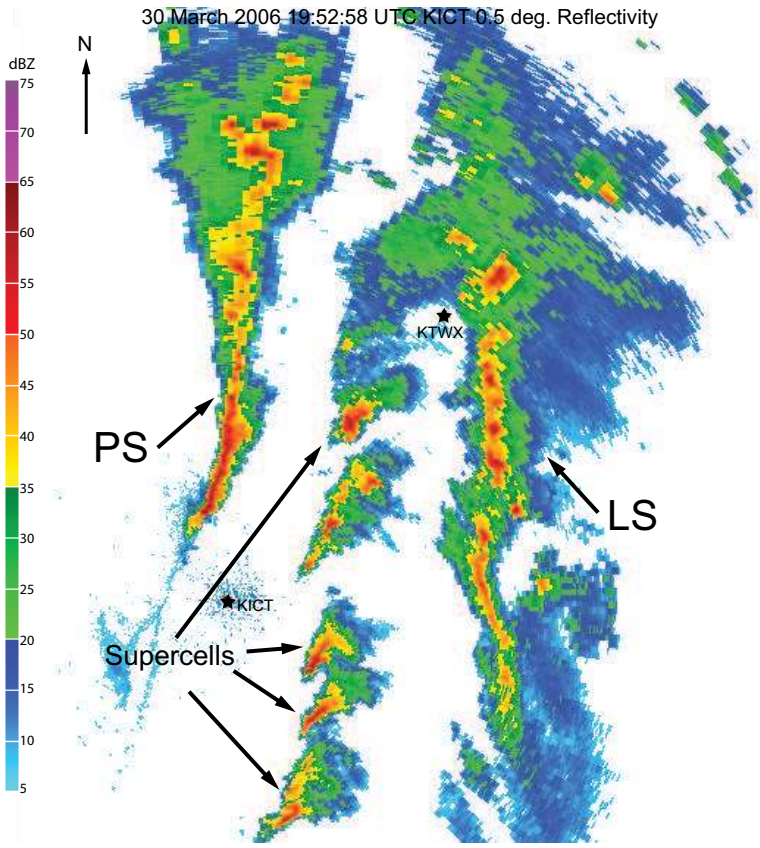

Figure 1.1: Extended range base reflectivity from Wichita, Kansas at 1957 UTC 30 March 2006. Three modes of convection (PS, supercell, LS) are labeled for reference.

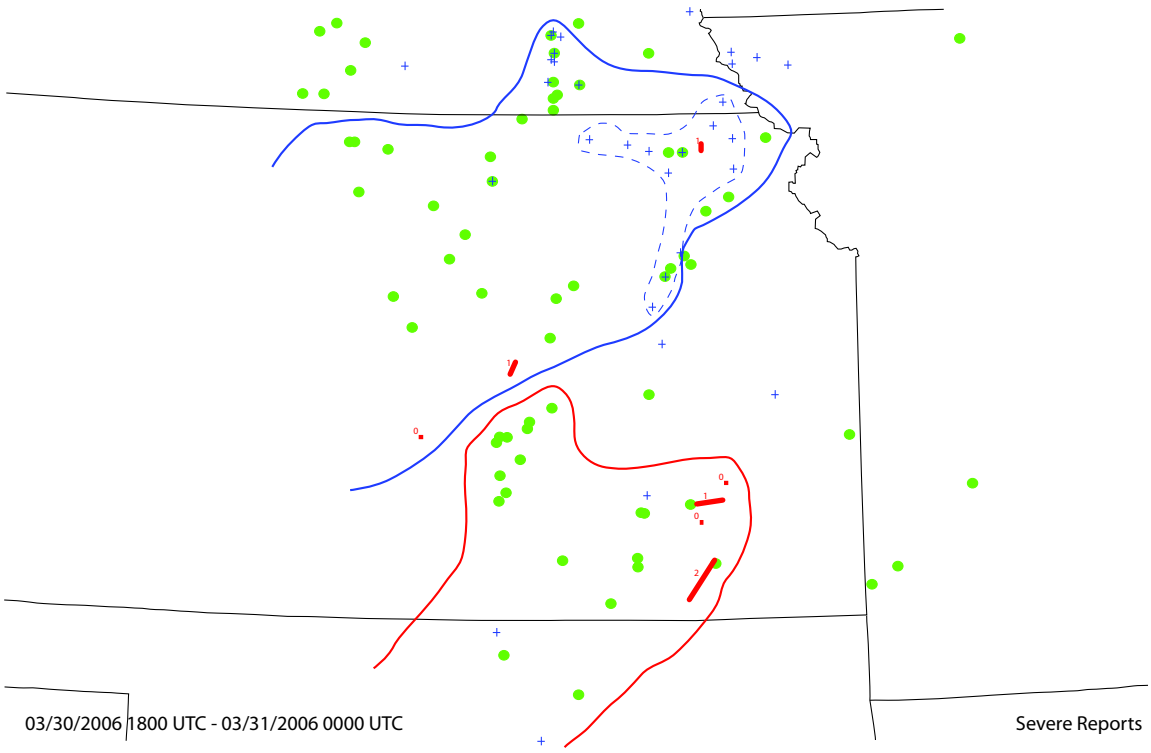

Figure 1.2: Storm reports received by the Storm Prediction Center in Norman, Oklahoma between 1800 UTC 30 March 2006 and 0000 UTC 31 March 2006. Green dots denote hail reports, blue pluses severe wind, and small red crosses or lines denote tornadoes and tornado tracks. Numbers plotted next to tornado reports refer to Fujita scale intensity rating. Blue outline signifies storm reports associated with the PS squall line, with the dashed blue indicating reports during and after transition to the TS structure. Red outline signifies reports associated with supercells.

Chapter 2

Background

Convective storms can be organized in a variety of shapes and sizes with varying degrees of complexity. However, the most basic element of organization is the convective cell. At the simplest end of the organizational spectrum lies the ordinary cell described by Byers and Braham (1949). These tend to be rather short lived, with a typical lifespan on the order of 30-60 minutes during which the cell progresses through three stages of development shown in Figure 2.1. Somewhat more organized and complex are multicell storms characterized by several cells in various stages of maturity (Figures 2.2a and 2.2b). These storms are characterized by new cells developing along the gust front, a mature storm located rearward of this new cell and dissipating cells that have moved further rearward with respect to the storm's motion as discussed by Browning (1977). This process repeats as the new cells continue to move rearward, leading to long-lived multicellular convection. Finally, at the most complex end of the organizational spectrum one finds the long-lived supercell storm, first identified by Browning (1964). These storms tend to be long-lived and characterized by a single, quasi-steady, rotating updraft and generally move to the right of the mean wind (Figure 2.3)(Lemon and Doswell 1979). Groups of these various types of cells can organize into a larger group of storms that develops its

own mesoscale circulations a contiguous gust front, called a mesoscale convective system (MCS) (Maddox 1980). However, the convective cell forms the primary building block of organized convection.

The ultimate organization of a convective system, consisting of one or more convective cells, is here referred to as the storm's organizational mode. Convective mode has been defined in many ways over a broad spectrum of scales. Some delineate between convective modes based on the dynamical structure of the cells that make up a given storm, essentially whether the system consists of ordinary, multi or supercells (Weisman and Klemp 1984). Some consider convective mode to refer to the meso-beta scale storm characteristics dealing with storm organization and appearance on radar, such as whether storms appear isolated, clustered (e.g. a multicell cluster) or linear in nature (Kain et al. 2006). Still others make more precise divisions among subsets of a larger group of storms, such as mesoscale convective systems with trailing, linear, and parallel stratiform precipitation (Parker and Johnson 2000). And yet others determine variations in mode based on storm formation, such as the different means for isolated severe storm development along the dryline outlined by Bluestein and Parker (1993) or different modes of mesoscale convective line development discussed by Bluestein and Jain (1985).

In any case, convective mode generally refers to a differentiation between various types of storms, largely based on observed organizational characteristics. For the purposes of this study, convective mode will refer to the meso-beta scale organizational characteristics, with supercell thunderstorms, linear MCSs with trailing stratiform precipitation, linear MCSs with leading stratiform precipitation and linear MCSs with parallel stratiform stratiform precipitation all representing unique modes. The interest, thus, is not just in differentiating between isolated and linear modes (i.e. supercells vs. squall lines), but also between the various linear modes. This further delineation is useful, as the various

linear modes can each be associated with different types of severe weather (as discussed in Chapter 1). In order to best introduce the scientific problem at hand, this section will first look at the individual modes of interest in detail, then discuss the differences in environment and dynamics that result in said modes.

2.1 Convective Modes in Detail

2.1.1 Supercells

The supercell is considered to be the most intense in the spectrum of cellular convection. First identified in the 1960s (Browning 1964), these storms have been the subject of intense study over the past 40 years, likely due to their close association with severe weather and tornadoes (Doswell 2001). The key feature of the supercell storm is the presence of a rotating mesocylone located near or within the storm's updraft, that can advect hydrometeors around the updraft leading to the distinctive hook-shaped radar echo (Doswell 2001). Supercells tend to be favored in environments that contain high instability and strong vertical wind shear, and will typically move to the right or left of the mean wind, with right-moving storms favored in environments characterized by clockwise turning hodographs (Weisman and Klemp 1982, 1984). Given this favored environment, most supercells tend to be isolated in nature, either as a lone storm, or as a group of storms with minimal interactions, although they can occur embedded within a squall line or cluster of storms (Rotunno et al. 1988). The high wind shear environment also aides in the development of vertical pressure gradients that can result in dynamically enhanced updrafts. This, in addition to strong buoyant forcing, will cause a supercell to have a significantly stronger updraft than an ordinary or multicell storm (Weisman and Klemp 1984). While not all severe weather results from supercell storms, high impact

severe weather events (e.g. hail $>$ 5 cm, winds $>$ 33 m/s, tornadoes $>$ F2) do tend to be associated with these storms resulting in an increased severe weather threat associated with supercells (Doswell 2001).

2.1.2 Squall Lines

While the term squall line has historically been used to refer to a variety of meteorological phenomena, with regard to convective storms, "squall line" refers a to linearly oriented MCS (Bluestein and Jain 1985). More specifically, squall lines consist of multiple, interacting, convective cells that share a common leading edge and appear as a line or arc with no breaks in precipitation between the cells (Doswell 2001). These cells can range from short-lived ordinary cells, which would require the frequent triggering of new cells to sustain the system, to organized supercells which would result in a squall line of long-lived individual cellular elements (Bluestein and Jain 1985). However, many squall lines are made up of elements that behave similarly to multicell storms, with periodic regeneration of new cells as old ones decay (Houze et al. 1989). In addition to cellular convection, there are also cases wherein a squall line consists of a swath of contiguous lifting, referred to as *slabular lifting* (James et al. 2005). This type of lifting tends to occur in conditions wherein a strong cold pool is present to create a broad area of lift.

The squall line, like the supercell, is very dependent on the buoyancy and shear profiles within its environment. Obviously, an unstable environment is necessary for convective storm development, although squall line environments do not always possess the large amount of instability that tends to be seen with supercells (Bluestein and Jain 1985). Environmental wind shear is also important to squall line development, however the importance tends to lie in the orientation of the vertical wind shear relative to the squall line, and its distribution with height (Weisman et al. 1988). While the magnitude

and orientation of environmental wind shear does play a role in the organization of cells within the squall line (i.e. whether the line contains ordinary cells or supercells) it also also plays an important role in squall line longevity (Rotunno et al. 1988). In a long-lived squall line, low level wind shear balances the cold pool circulation generated by the gust front as the cold pool spreads beneath the storm. Without shear the gust front would just move away from the storm, resulting in no new convective development and a short-lived storm. However, with low level wind shear to oppose this cold pool motion, the gust front remains close to the storm and a shear-induced circulation balances the cold pool circulation resulting in new convective development and a long-lived storm. In the optimal case where the shear and cold pool balance each other, this will lead to an upright updraft, and a strong, long-lived storm (Figure 2.4) (Rotunno et al. 1988).

In general, squall line formation necessitates some means to force linear organization. Such organization can come from synoptic scale features such as fronts and drylines, wherein a broad region of forcing is present. Oftentimes convection will be initiated along one of these boundaries in isolated pockets and then grow along the line as the initial cells grow in size and new ones form between them (Bluestein and Jain (1985)'s broken line). In other cases, an isolated cell or group of cells along a boundary will evolve into a line through repeated new cell development occurring upstream (with respect to cell motion) along the line that then merges with the old cell (Bluestein and Jain (1985)'s backbuilding). Squall lines can also form in the absence of strong synoptic forcing, such as from the mergers of two or more isolated cells, such as supercells (e.g. Bluestein and Weisman 2000; Finley et al. 2001). In these cases the merger will often result in the strengthening of surface outflow, leading to development of new convection in a more linear organization along the outflow boundary.

Once the squall line has formed, generation of a cold pool and outflow will allow it to

be maintained through consistent lifting along the leading edge of the gust front and the generation of new cells as older cells mature and decay while moving rearward, similar to the multicell regeneration process (Houze et al. 1989). As this process continues it will lead to a region of intense convective precipitation, along with a broad area of weaker stratiform precipitation. Figure 2.5 shows the classic trailing stratiform (TS) structure that is found in many squall lines. Intense convection is found at the leading edge of the line in the region of strongest ascent along the gust front with a broad region of stratiform precipitation behind the line due to to hydrometeors being advected rearward over the cold pool by an ascending front to rear flow (Houze et al. 1989). Since this front to rear flow is favored in systems with strong cold pools (Rotunno et al. 1988), it makes sense that linear MCSs with strong cold pools favor, and ultimately evolve towards, the TS structure. While the trailing stratiform structure tends to be the most common type of squall line, two other modes have been identified based on the structure of their stratiform regions; the leading stratiform linear MCS, wherein the stratiform region precedes the convective region of the line, and the parallel stratiform linear MCS, wherein the stratiform region is oriented parallel to the convective line (Figure 2.6) (Parker and Johnson 2000).

2.1.2.1 Convective Lines With Leading Stratiform Precipitation

A linear MCS with leading stratiform precipitation (LS) is characterized by the majority of its stratiform precipitation being located ahead of, or leading the convective line (Parker and Johnson 2000). Observations of the near storm environment for LS MCSs, as well as idealized numerical simulations, suggest that upper level line-perpendicular shear, directed from rear to front, is key to hydrometeor transport extending ahead of the convective line and creating the leading stratiform region (Parker and Johnson 2004a). Two

types of LS systems have been observed in nature: rear-fed LS and front-fed LS. The key difference between the two types is the source of inflow, with rear-fed systems being sustained by inflow from behind the line (Pettet and Johnson 2003) while front-fed LS systems are sustained by inflow from ahead of the line that passes through the stratiform region (Parker and Johnson 2004c). Given that the front fed systems are more numerous in nature, they have received more attention in the literature, and the majority of the knowledge regarding LS systems relates to this type.

LS MCSs can largely be approximated as 2-D entities as evidenced by Parker and Johnson (2004c) (Figure 2.7). A key dynamical feature of these systems is an overturning updraft wherein inflowing air enters from ahead of the line, ascends through the updraft and then is accelerated downshear ahead of the line (Parker and Johnson 2004a). This acceleration is due to transient accelerations generated by buoyancy, as well as linear and non-linear pressure fields (Parker and Johnson 2004a). The leading precipitation eventually causes a transition to the trailing stratiform (TS) structure, as buoyancy-induced pressure perturbations lead to a decrease in vertical wind shear in the pre-line region. This, combined with a strengthening cold pool, result in a rearward sloping of the updraft and eventual transition to a TS system (Parker and Johnson 2004b). This evolution from LS to TS occurs a majority of the time (Parker and Johnson 2004c), especially for long-lived cases and was indeed seen within some of the LS simulations performed in this study, namely those initiated with a significantly colder initial cold box.

2.1.2.2 Convective Lines With Parallel Stratiform Precipitation

A linear MCS with parallel stratiform precipitation (PS) is characterized by the majority of its stratiform precipitation being located parallel to the convective line, typically

to the left of the storm's motion vector with a strong reflectivity gradient to either side of the convective line itself (Parker and Johnson 2000). Observations of the near storm environment for PS MCSs suggest a very shallow layer of line-perpendicular storm-relative winds in the low levels, and a deep layer of along-line storm-relative winds through the mid and upper levels resulting in the along-line transport of hydrometeors (Parker and Johnson 2000). These findings were further solidified by more in depth observations by Parker (2007a) and through idealized model simulations by Parker (2007a,b) showing that line perpendicular shear in the low levels and deep-layer line parallel shear are equally important in developing the PS structure (Figure 2.8) . Parker (2007b) determined that line perpendicular shear in the low levels is necessary to maintain upright updrafts along the leading edge of the convective line by balancing the cold pool circulation as per Rotunno et al. (1988). Meanwhile, the deep-layer line-parallel shear aids in developing the parallel stratiform region through upper level hydrometeor transport to the left of the storm motion (generally to the north Parker 2007a). Line parallel shear to the left of the storm motion in the lower troposphere, along with spreading by the surface cold pool drives the back building mechanism (described by Bluestein and Jain 1985) that causes growth of the convective line (Parker 2007a). As with the LS systems described above, PS systems eventually tend towards TS systems due to a strengthening cold pool and a decrease in line parallel flow (Parker 2007a). As a result of the along line hydrometeor transport, convective cells seed neighboring cells, generating a great deal of precipitation fallout close the the gust front. This causes PS systems to rapidly generate strong cold pools which can ultimately lead to a faster transition to the TS systems (Parker 2007a).

Parker and Johnson (2004b) showed that the environments for LS systems and supercells overlap, and Parker (2007a) noted that the environments for PS systems and supercells overlap. In other words, environments with moderate to strong vertical wind

shear may permit three distinguishable primary structures. This makes it less surprising that all three modes were observed on 30 March 2006, however it does not answer the question of how all three managed to be simultaneously present in close proximity to each other. To continue to get to the root of this problem, some of the mechanisms that drive convective mode in more general terms will now be reviewed.

2.2 Delineation Between Modes

Given the differences between between these various modes, the key environmental factors that delineate between them have received much attention in the literature. Two early studies in this regard are those of Weisman and Klemp (1982, 1984) who used idealized model simulations to examine the sensitivity of storm mode to environmental shear and buoyancy. The first of these studies, Weisman and Klemp (1982), utilized a three-dimensional cloud model to simulate convective storms in environments with varying buoyancy and two-dimensional shear profiles. Through a series of experiments wherein the wind shear profile was varied, the authors found a general trend towards greater organization with increasing wind shear. No wind shear resulted in a short pulse of convection that did not last very long and showed little organization, akin to the ordinary cell described by Byers and Braham (1949). Low to moderate shears resulted in what the authors termed secondary development storms, wherein new cells developed along the gust front of previous storms which is similar to multicell structures observed in nature. Finally, in moderate to strong shears long-lived splitting storms, qualitatively similar to supercell storms seen in nature, were observed. The authors noted, though, that the mirror image splits (one storm moved to the right and one to the left) they observed are not typically seen in nature, and were likely due to the two dimensional

nature of the flow fields.

This first study offered a great deal of insight into some of the environmental factors that effect convective storm type, however the authors admitted that there were some shortcomings, namely that the two dimensional shear profile failed to account for directional wind shear, which at the time was suggested to play an important role in storm structure, especially for supercell storms. To address this, the authors did another study in 1984, this time using a three dimensional wind field which allowed for directionally varying wind shear. When directional shear was added to the model, the authors still found an increase in organization with increasing shear. They observed a spectrum of storms from short-lived isolated convection to multicells to supercells as shears progressed from low to moderate to high. They did find, though, that the storm structures varied somewhat compared to the previous study. For instance, with a clockwise turning hodograph supercell development was favored on the right flank of storms, while the left flank tended towards more of a multicell development. In moderate shears these two modes evolved together, which the authors pointed out is similar to what is sometimes observed in nature where a supercell will be present at the southern end of a squall line (Weisman and Klemp 1984).

The addition of directional shear allowed Weisman and Klemp (1984) also to examine some of the dynamics associated with the simulated storms, and resulted in the authors offering classification criteria based on these dynamical differences. In this vein, the authors found that the supercell storms that developed on the right flank consisted of one quasi-steady updraft that propagated to the right of the mean wind. Up to 60% of the strength of this updraft was due to dynamic forcing from vertical pressure gradients on the right flank of the storm. The location of the updraft also correlates strongly with cyclonic vertical vorticity in the lowest 8 km of the storm. On the other hand, the multicell left

flank storms consist of multiple short-lived updrafts that generally move with the mean wind. These updrafts are initially forced by a surface gust front, and 60-70% of their strength is attributed to buoyancy forcing. Mid-level vorticity maxima are found with these storms as well, but they do not correlate strongly with the updraft locations. Given these differences, the authors suggest two main modes of storms, multicells and supercells, based on the dynamical differences described above. Larger organized convective systems such as squall lines are then seen as consisting of a combination of these two types. Since these features largely depend on vertical wind shear and buoyancy, the authors suggest that these factors continue to be the keys in determining convective mode.

One of the shortcomings of the Weisman and Klemp (1982) and Weisman and Klemp (1984) papers is that their study fails to account for changes in the buoyancy and shear profile shapes. They used a variety of shear and buoyancy profiles, however did little to test the vertical distributions of said shear and buoyancy and how that might effect storm structure. A study by McCaul and Cohen (2002) tested the shape of the shear and buoyancy profiles in environments that were both favorable for supercells as well as those in the transition range between multicells and supercells. In this study it was found that in high shear cases supercells still tended to be favored almost universally, while within the transition range the ultimate mode did appear to depend on the shape of the buoyancy profile, as well as the lifting condensation level (LCL) and level of free convection (LFC) heights. One result from this was the development of supercells from relatively low CAPE environments where a multicellular mode would traditionally be expected. This suggests that at either end of the spectrum shear and buoyancy can be the determining factor between modes (as seen in the Weisman and Klemp papers), however for shears in the more moderate range the vertical structure of buoyancy as well as other factors such as LCL and LFC height can be the determining factor, sometimes

with rather surprising results.

Similarly, the vertical moisture profile can play a role in convective mode. The low level moisture can play a significant role in mode selection by having an impact on the environmental instability, which as been shown by McCaul and Weisman (2001) and McCaul and Cohen (2002) to effect the mode that evolves from that environment. Additionally, the presence of dry air aloft in an environment can also play a role in mode selection. Dry air in the low and middle levels of the atmosphere can enhance cold pool development through evaporational cooling, leading to colder, broader cold pools that favor slabular lifting and linear modes (James et al. 2006). As with the variations in the buoyancy profile noted above, the effects of variations in the moisture profile on storm mode also depend on shear, although in a different way. James et al. (2006) suggest that drier air aloft can lead to stronger cold pools, which can then more effectively balance, or even overwhelm stronger values of wind shear leading to more upright, intense updrafts as described by Rotunno et al. (1988). In cases where the cold pool locally overwhelms the wind shear (i.e. segments along a larger squall line) bow echoes can form, leading to enhanced damaging wind potential (James et al. 2006). Dry air aloft has also been shown to have an effect on supercell thunderstorms as well, although in a more detrimental manner. In supercells, the enhancement of downdrafts and creation strong surface outflow by dry air aloft can lead to the storm becoming outflow dominated, which is typically detrimental to mesocyclone and storm longevity (Gilmore and Wicker 1998; McCaul and Cohen 2002). The presence of drier air in the middle troposphere may have played an important role in the 30 March 2006 event to be studied herein, as two of the modes (the supercells and PS line) formed in environments characterized by almost identical values of 0-6 km wind shear, however one of the key differences between these environments was the amount of dry air aloft.

While it is clear from the above studies that shear and buoyancy play an important role in determining convective mode, the presence of linear boundaries such as outflow boundaries and dry lines can be important as well, especially when considered along with wind shear[1]. This is not a new idea, having been introduced by Bluestein and Jain (1985) wherein the authors speculated as to why they observed both supercells and backbuilding squall lines forming in similar environments, and in similar proximity to surface boundaries. The authors hypothesized that the orientation of the vertical shear with respect to the boundary may be important, however their limited investigations using observed data met with little success. Fifteen years later, Bluestein and Weisman (2000) examined the effect of varying the orientation of wind shear vectors with respect to a line of forcing (in their case a dryline) on numerically simulated supercells. The study used idealized model simulations that included a pseudo dryline as well as a line of supercells initiated using warm bubbles, to which the authors introduced wind shear that was perpendicular, oblique (45°), and parallel to the line. They found that for shear perpendicular to the line, the simulation generated a squall line with right and left moving supercells at either end. For shear oblique to the line, the result was a line of isolated (i.e. not interacting) right moving supercells. Finally for shear parallel to the line, the authors found a right moving supercell at the downshear end of the line, along with a left moving supercell that has some multicell characteristics, and most of the rest of the cells along the line devolved to ordinary cells after interacting with their neighbors (Bluestein and Weisman 2000). This suggests that when a linear forcing mechanism such as a dryline is present, just the mere presence of shear is not enough to determine the mode, but rather how that shear is oriented with respect to the line matters as well.

[1]In this sense boundary refers to mesoscale boundaries such as drylines or outflow boundaries. For more synoptic-scale features such as fronts, the vertical wind profile would be assumed to be in thermal wind balance suggesting that the shear would always be parallel to the boundary and thus the orientation of the shear relative to the boundary would be unchanging.

In the simulations, curved hodographs indicative of supercells were used in every case, however, the results show that depending on the shear's orientation to the simulated dryline, different modes can result despite the presence of a "supercell environment".

The role of synoptic boundaries in determining convective mode was also examined in a study by Dial and Racy (2004) wherein they found that the orientation of the 2-6 km or 2-8 km mean wind compared to the boundary and the component of the shear in those levels perpendicular to the boundary were key parameters with regards to convective mode. They determined that when the 2-6 or 2-8 km flow and boundary were nearly parallel, the result was a rapid transition to a more linear mode, due to mergers and interactions between storms being aided by the mean flow. This flow parallel to the boundary can also advect hydrometeors along the line, seeding new updrafts and aiding in the production of precipitation, which in turn can lead to stronger cold pool development and favor linear modes (Parker 2007a). The nature of the boundary also provided a means for discrimination among modes, as cold fronts tended to develop squall lines faster than drylines or other boundaries, and boundaries characterized by strong convergence also tended to favor linear modes due to the development of more storms, allowing for faster mergers (Dial and Racy 2004). It is also important to note that boundaries can have relevance to convective mode well past the initial development of the storms. Jewett and Wilhelmson (2006) found that the inclusion of a simulated cold front in idealized squall line simulations had a significant effect on storm evolution, resulting in enhanced (diminished) longevity of cyclonic (anticyclonic) storms and an overall increase in cell count and storm longevity. This suggests that the presence of a boundary or forcing mechanism can play an important role in determining convective mode, both during storm initiation, as well as while the storm is evolving. Thus in addition to their importance in interactions with wind shear, boundaries can play a key

role in determining convective mode by themselves.

In addition to their discussion of the importance of shear relative to a boundary, Bluestein and Weisman (2000) also discussed the importance of cell interactions in determining convective mode. For most cases within their simulations, when a cell encountered another cell or its outflow, it tended to lose its supercellular characteristics and multiple interactions often led to the development of a squall line. Simulations by Finley et al. (2001) demonstrated the role that cell mergers can play in the transition of a high-precipitation supercell to a bow echo. In the simulated event, the merger of a pair of supercells led to increased precipitation resulting in cold pool intensification and the transition to a bow echo structure. Thus cell interactions can have a significant effect on convective mode when multiple storms are present.

Finally, while vertical shear continues to be a key parameter with regards to convective mode, new ways of understanding this shear have emerged. For instance, in examining proximity soundings in an attempt to distinguish between derecho and supercell environments, Doswell and Evans (2003) determined that different hydrometeor distributions resulting from variations in the mid and upper level storm relative winds were a key differentiator. This differs from the bulk shear analysis of Weisman and Klemp (1982, 1984), however, given that the storm-relative flow is related to the vertical shear profile, shear is still playing a role in mode determination, it is just being analyzed differently. This different analysis is of use in cases where the bulk shear values are the same, as in the comparison of two high-shear modes such as bow echos and supercells described by Doswell and Evans (2003). The bulk shear values for many of these events showed little skill at discriminating between the two modes, as both tend to form in high shear environments. However, when storm motion and hodograph shape are taken into account, different storm-relative flow fields emerge, leading to a means to discriminate between

these two modes.

Thus, an increasing body of work suggests that the vertical wind shear is of primary importance to the determination of convective mode. However, in addition to the bulk shear within the environment, its orientation with respect to mesoscale boundaries and in the storm relative sense can be key as well. Furthermore, there are other factors related to the thermodynamic profile such as buoyancy and moisture distribution that can be just as important as the shear profile, if not more so, especially within environments characterized by moderate shear (i.e. between the multicell and supercell ranges). However, to date little has been done to examine the mechanisms at play in cases where multiple modes of convection are present in a localized area as was witnessed on 30 March 2006. The present study will seek to address this issue, using an observational case study as well as numerical simulations to determine and evaluate the mechanisms that govern one such event.

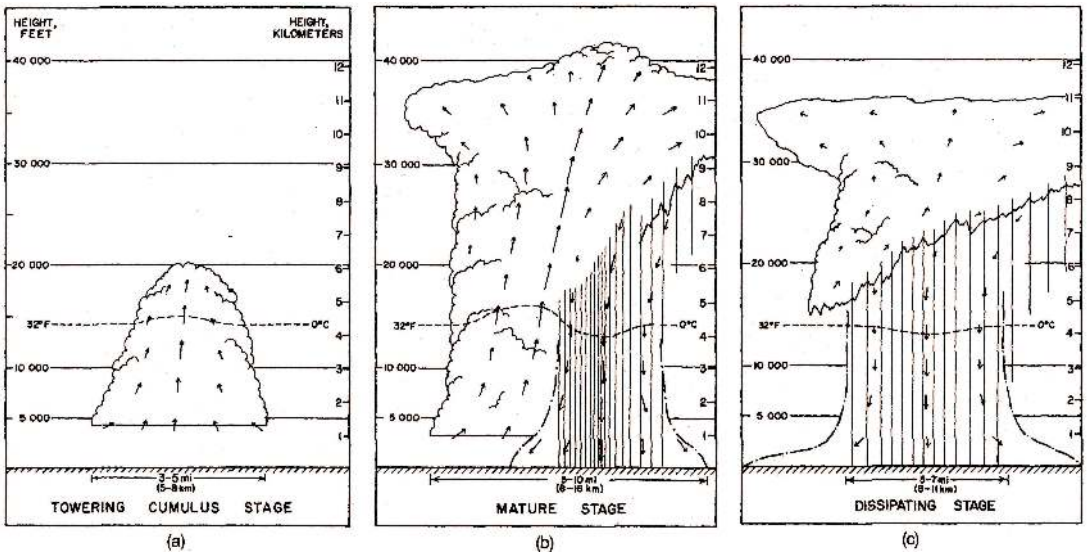

Figure 2.1: Life cycle of an ordinary cell thunderstorm: a)towering cumulus stage dominated by updrafts, b) mature stage containing updrafts and downdrafts, c) dissipating stage dominated by downdrafts (adapted from Byers and Braham, 1949).

Figure 2.2: Cross section through a multicell storm over the course of 20 minutes. Note the new cells developing on the left flank of the storm (cell 5), while old cells are dissipating to the right (cell 1) (from Doswell, 1985).

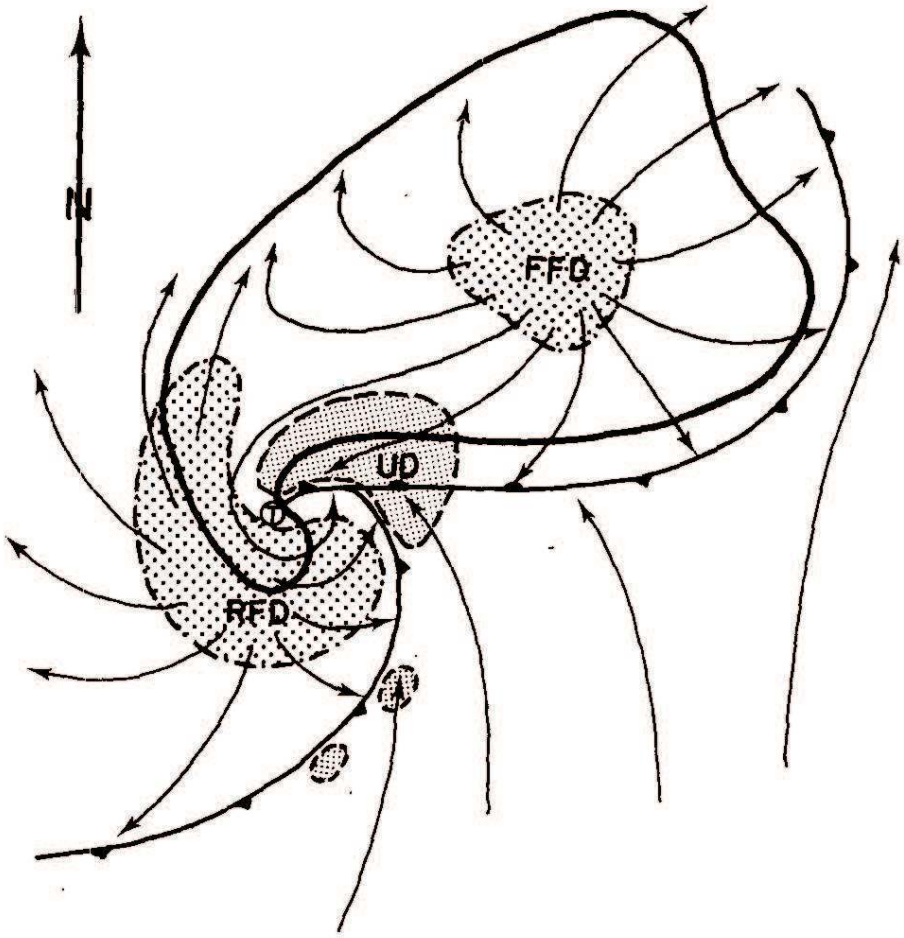

Figure 2.3: Schematic of a supercell thunderstorm noting the location of prominent updrafts, downdrafts and airflows as well as outlining a typical radar signature (from Lemon and Doswell, 1979).

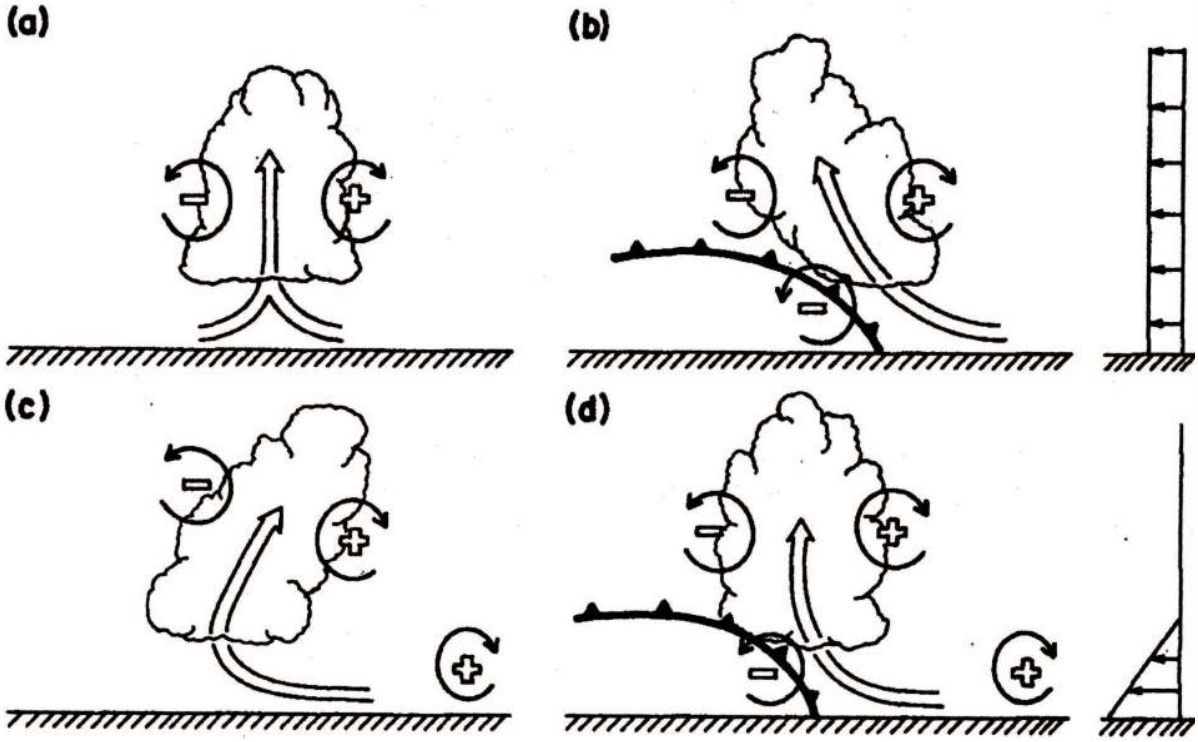

Figure 2.4: The effects of wind shear and cold pool induced circulations on a squall line updraft. a) No shear or cold pool results in a vertical updraft. b) No shear with a cold pool results in an updraft that tilts rearward over the cold pool. c) Shear with no cold pool results in an updraft that tilts forward. d) Shear and cold pool in optimal balance results in vertical updraft. (from Rotunno et al. 1988).

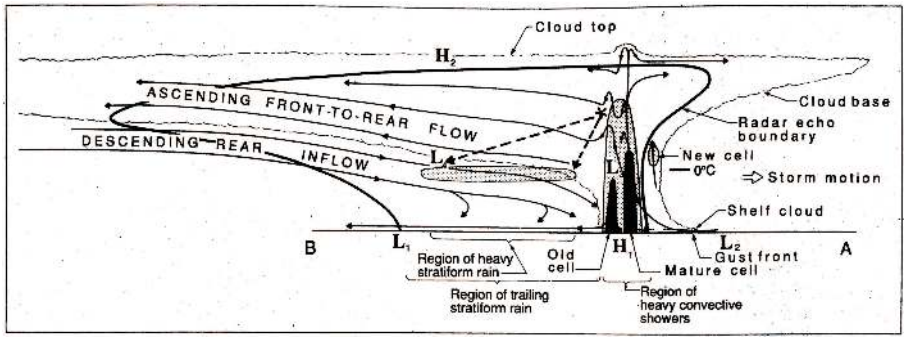

Figure 2.5: Vertical cross section of a squall line with trailing stratiform precipitation (from Houze et al., 1989).

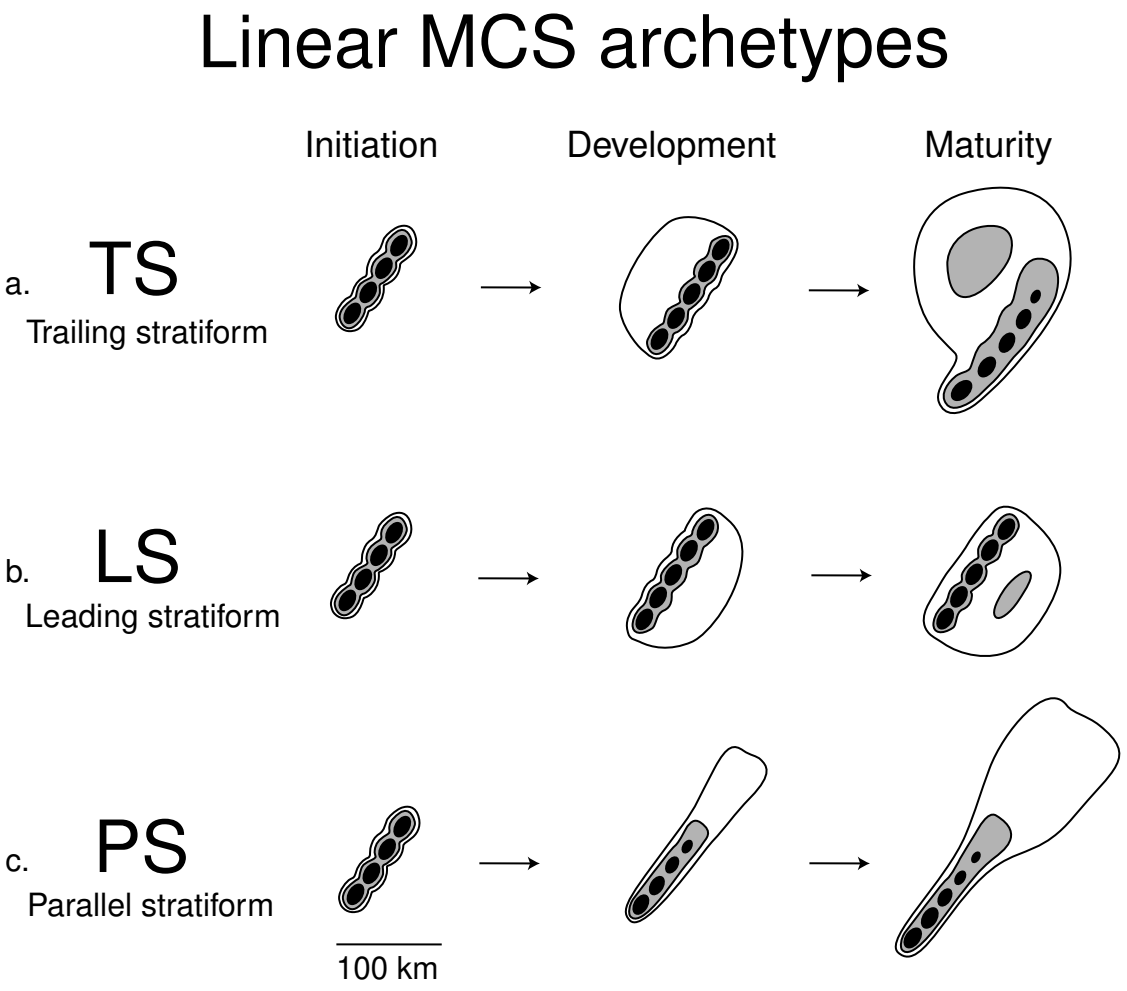

Figure 2.6: Schematic plan views of linear MCSs with trailing, leading and parallel stratiform regions from initiation through maturity (from Parker and Johnson (2000)).

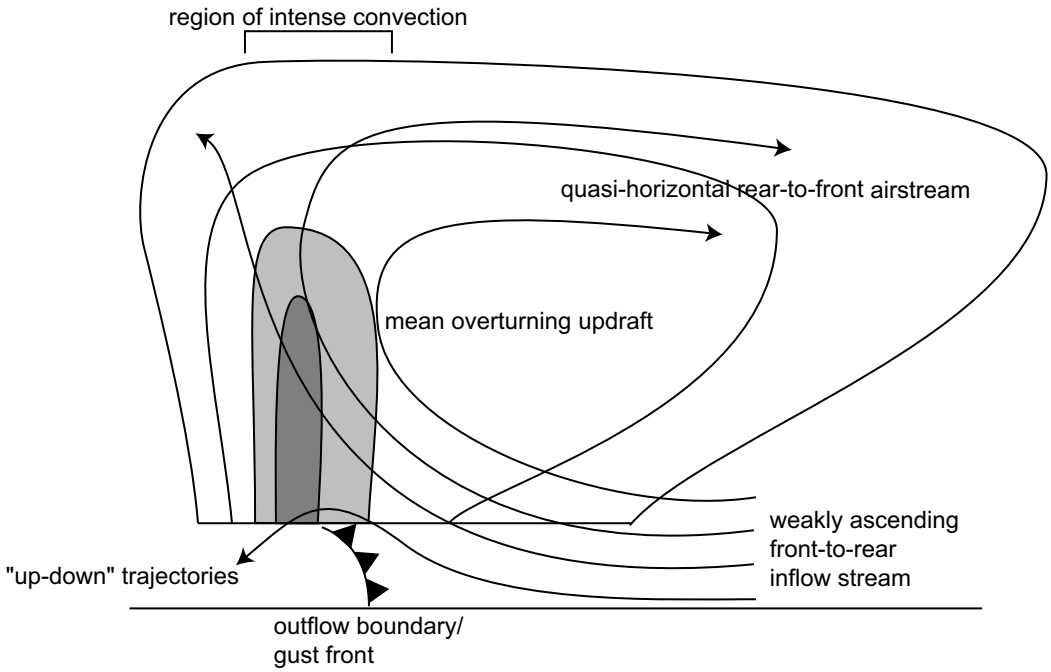

Figure 2.7: Cross-sectional schematic of an MCS with leading stratiform precipitation (from Parker and Johnson, 2004c).

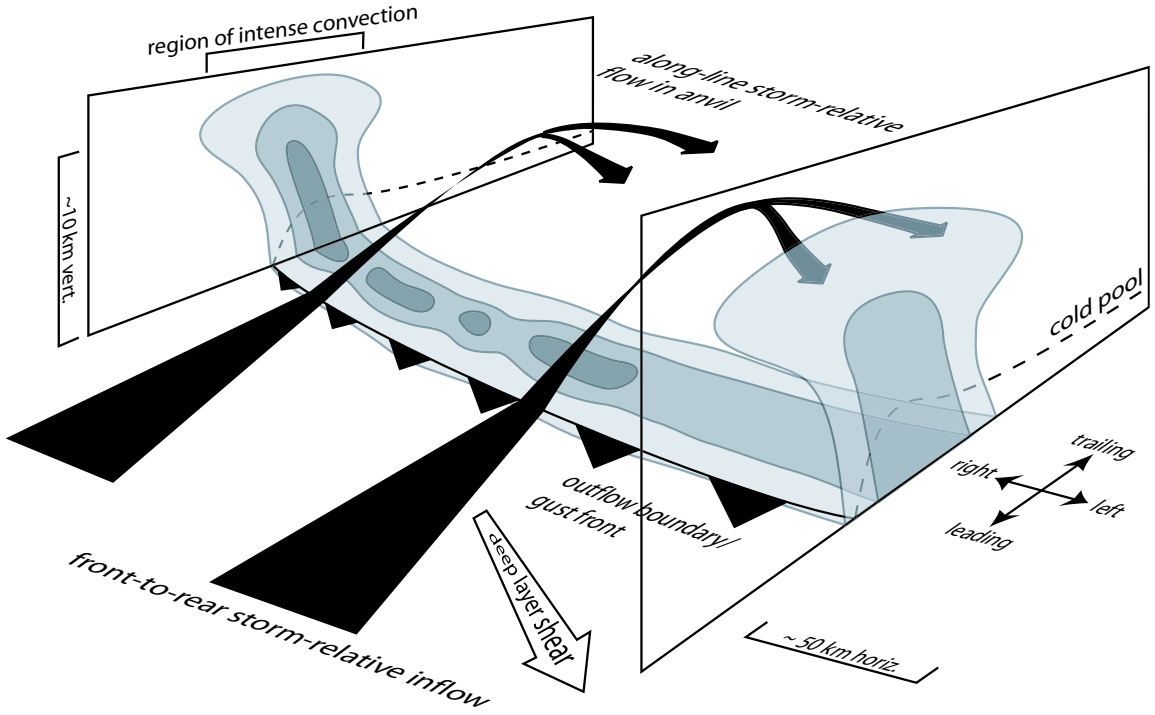

Figure 2.8: Three-dimensional schematic of an MCS with parallel stratiform precipitation (from Parker, 2007a).

Chapter 3

Observational Case Study

The aforementioned case of 30 March 2006 will serve as the basis for the observational case study and subsequent numerical simulations, as it is a prime example of a multi-modal event, with supercells, an LS MCS and a PS MCS present over a localized region (Fig.1.1). The data and methods used in the case study will be discussed first, followed by a discussion of the results of this portion of the study.

3.1 Case Study Methodology

The observational case study consisted entirely of data available from operational platforms for the date in question. The background synoptic conditions for this case were determined from isobaric charts and skew-T ln-P plots generated from radiosonde observations from the operational observing network taken at 1200 and 1800 UTC on 30 March, and 0000 UTC on 31 March (Fig. 3.1). Regional ASOS surface observations taken hourly were used to identify surface features within the region. WSR-88D radar observations from Wichita, Kansas (KICT), Topeka, Kansas (KTWX), Vance Air Force Base, Oklahoma (KVNX) and Kansas City, Missouri (KEAX) provided base reflectivity

and Doppler velocity observations covering the scope of the event (Fig. 3.1). Finally, the radiosonde wind profiles were supplemented by hourly observations from regional NOAA Wind Profiler sites (Fig. 3.1).

In addition to these actual observations from the day in question, the North American Regional Reanalysis (NARR, Mesinger et al. 2006) was used to supplement the observations because of its enhanced coverage and resolution. This resulted in a more complete picture of the event, especially in the vertical, and allowed for cross-sectional analyses of important features such as the surface dryline. In order to ensure accuracy, the NARR data were compared to available observations at both 1200 and 1800 UTC on 30 March as well as 0000 UTC on 31 March, and were found to be representative of regional soundings and surface observations. This collection of observations and NARR data was analyzed both objectively and subjectively to gain a detailed picture of the storms and their environments throughout the duration of the event.

The decision was made to focus on a single case rather than multiple cases largely to allow for an in-depth analysis of each of the individual storms and the small-scale environmental features across the region. Thus rather than focusing on a few key parameters over a broader range of events, the goal of this study was to perform a very detailed analysis of the one event in order to highlight all of the features and mechanisms that were relevant to the development and evolution of all three modes. The 30 March 2006 case was chosen in particular as it provided a rather unique opportunity to examine three distinct modes in what was largely the same synoptic scale environment. Instead of looking at individual cases of each convective mode from different events, the 30 March case provided a quasi-controlled event wherein all three modes were present within the same large-scale environment. Thus, the focus could then be turned to the mesoscale features that were key in mode delineation. Furthermore, the case was chosen

as a somewhat unique example of a multi-mode event. Dial and Racy (2004) found, in a study of 37 cases, that mixed-mode events (defined as consisting of linear and isolated modes) occurred approximately 19% of the time for their parameter space. This suggests that while not an everyday occurrence, these multi-mode events occur often enough to be of concern to forecasters, especially given their wide-ranging severe weather threat.

3.2 Case Study Results

The case of 30 March 2006 included three distinct modes of convection: an MCS with parallel stratiform precipitation in central Kansas, an MCS with leading stratiform precipitation in far eastern Kansas, and a group of isolated supercells in east central Kansas (Fig. 1.1). All were present at the same time and within an area of less than 400 km x 500 km.

3.2.1 Background environment

Key features of the pre-storm synoptic environment are summarized in Fig. 3.2 . This environment was characterized by a large amplitude, diffluent, middle and upper level trough over the Rocky Mountains evident at 500 hPa (Fig. 3.2b). A 35 m/s jet curved around the base of this trough from the west coast into the southern plains, with an embedded 45 m/s jet streak over New Mexico and Arizona (Fig. 3.2a). At lower levels, an 850 hPa 25 m/s southwesterly low level jet was transporting warm moist air into Oklahoma and Kansas (Fig. 3.2c). The key surface feature for this event was a dryline that extended from a low pressure center in north central Kansas southward into northern Texas (Fig.3.3). Ahead of this dryline, temperatures had warmed into the 18-20°C range by 1800 UTC with dew points around 15°C along a narrow band from southeast Texas

into south-central Kansas. West of the dryline temperatures were approximately 5°C higher while dew points were significantly lower, with a narrow axis of very dry air extending from southwest Kansas through central New Mexico. The 1800 UTC upper air soundings from around the region indicated a moderately unstable (CAPE of 1000-2000 J/kg), weakly capped environment to the east of the dryline (Fig.3.4) characterized by moderate to strong vertical wind shear (Fig.3.5).

Taken as a whole, these features indicate an environment primed for convective storms. Synoptic-scale sources of lift were present in the form of the upper level trough and jet streak, as well as large scale low level warm advection. The surface dryline provided a localized focus for lifting in the boundary layer. CAPE values in the 1000-2000 J/kg range suggested that storms would have ample instability to fuel their development, while the moderate (15-20 m/s) to high ($>$ 20 m/s) wind shear suggested supercells or squall lines were possible (Rasmussen and Blanchard 1998; Evans and Doswell 2001). Thus the background environment for this case was very favorable for organized, strong convective storms. In such a case, an operational forecaster might be led to expect one predominant convective mode to emerge; but instead several unique and long-lasting storm types occurred.

3.2.2 Radar Analysis

The multi-mode event of 30 March 2006 began with storms that would eventually become isolated supercells developing along the dryline in western Oklahoma at approximately 1630 UTC. By 2000 UTC isolated supercells, a linear MCS with parallel stratiform precipitation (hereafter "PS line") and a linear MCS with leading stratiform precipitation (hereafter "LS line") were present over eastern Kansas (Fig. 3.6c). All three remained present for 2-3 hours (e.g. Fig. 3.6c-d), with the last of the storms dissipating by 2230

UTC. During the course of this time period the storms involved affected central and eastern Kansas, most of northern Oklahoma and parts of western Missouri. Each convective mode's formation and evolution will now be described in turn.

The storms that would evolve into the isolated supercells on 30 March 2006 event were initiated along and just ahead of a surface dryline in western Oklahoma at approximately 1630 UTC (Fig. 3.7). While the initial storms consisted of both isolated and broken linear structures, they quickly moved northeastward off of the dryline, becoming increasingly isolated in nature while intensifying and developing supercellular characteristics (Fig. 3.6a). By 1845 UTC these had become a collection of isolated storms oriented northeast to southwest from eastern Kansas into central Oklahoma, with well-developed mesocyclones and hook-echo structures evident (Fig. 3.8a,b). A range-height indicator (RHI) scan through one these storms reveals a bounded weak echo region (BWER), further indicating the supercell mode. Additionally, these storms produced numerous reports of severe hail greater than 1" in diameter, as well as several tornado reports (Fig. 1.2). The isolated supercellular organization of these storms remained until their eventual dissipation in eastern Kansas and Oklahoma.

Around 1730 UTC, several cells were initiated in close proximity to one another along the northern portion of the dryline in central Kansas (Fig. 3.9). A few of these initially developed supercell characteristics, with weak mesocyclones and hook echo structures, however the cells quickly merged into a small line, which then began backbuilding southward along the dryline (Fig. 3.6b). It is of note that the PS squall line simulated of Parker (2007a, b) initially developed supercell structures before evolving into the PS line as well, suggesting that this occurrence may not be that uncommon given the similar environments that favor these modes. This line matured into a linear MCS with parallel stratiform precipitation, having a narrow convective line extending north/south through

central Kansas, and a region of stratiform precipitation located at the northern end of this line (Fig. 3.10a). Range-Height Indicator (RHI) plots taken in both the across and along-line directions further illustrate the PS structure, indicating little stratiform precipitation ahead of or behind the line (Fig. 3.10c), and substantial stratiform precipitation north of the strongest convection, parallel to the convective line (Fig. 3.10b). This MCS was fairly similar in structure to the 2 May 1997 PS MCS analyzed by Parker (2007a), including a radar-indicated fine line structure extending south of the line (Fig. 3.10a). In the present case, this appears to be an indication of the surface dryline, based on surface observations taken as the feature passed.

The PS system progressed eastward across Kansas, remaining just ahead of this surface dryline, and eventually evolved into a linear MCS with trailing stratiform precipitation (TS) by 2100 UTC (Fig. 3.11) as is often observed with this convective mode (Parker and Johnson 2000; Parker 2007a). After the transition to the TS mode, the MCS began to weaken as it crossed northeastern Kansas and southeastern Nebraska, losing most of its organization by approximately 2330 UTC. During its evolution, this MCS generated severe hail, with reports of greater than 2" diameter hailstones (Fig. 1.2). These hail reports came first from the initial cells near the northern edge of the line, which exhibited higher reflectivities, and continued to contain weak mesocyclones throughout the first 1-2 hours of PS evolution, although scattered severe hail was also reported along the remainder of the convective line throughout the course of the event. Additionally, the PS line was not associated with any severe wind reports until after it had transitioned to the TS mode in northeastern Kansas.

Meanwhile, just after 1900 UTC, as the supercells and PS squall line were evolving to the west, a new squall line (that would become the LS line) began rapidly developing just east of the supercells in eastern Kansas (Fig. 3.6b). Rather than being forced along

the dryline, as was the case with the supercells and PS line, these storms appear to have been forced by a collision between two outflow boundaries. Surface observations in this area were sparse, however earlier observations in the vicinity of the supercells recorded temperature drops of 6°C within the storms and 2-3°C near their periphery, suggesting at least some weak outflow from these storms. Observations to the east where the LS line formed also show slightly (1°C) cooler temperatures suggesting an area of weak outflow that resulted from the passage of earlier convection (visible near KTWX in figure 3.6a, b). The strongest evidence of this outflow collision, though, can be seen in the radar data which shows two fine lines, indicative of boundaries, that appeared to merge as this line developed (Fig. 3.12). Following the merger, a squall line rapidly back built to the south, and eventually produced leading stratiform precipitation (Fig. 3.13a). An RHI plot, taken in the across-line direction at 2103 UTC shows two key elements of the front-fed LS structure (Parker and Johnson 2004c); the leading stratiform region in the reflectivity field (Fig. 3.13b), as well as the characteristic pre-line structure of low level flow toward the convective line, with mid and upper level flow away from the convective line (Fig. 3.13c). Unlike the supercells and PS MCS, the LS line produced very little in the way of severe weather, with only some very widely scattered reports of severe hail during its evolution. The storm maintained its leading stratiform structure as it moved east into Missouri, where it eventually began dissipating by 2230 UTC.

3.2.3 Environmental and Initiation Variations

The aim of this study was to understand the mechanisms that led to these three distinct convective modes within the same area on 30 March 2006. Because the supercells and PS line both developed along the dryline, this discussion will first focus on key differences between the local environments of these two modes. The focus will then turn

to the environment in eastern Kansas where the LS line formed, and eventually where all three modes were present. Finally, some differences in storm initiation mechanism and their possible implications with regards to convective mode will be discussed as well.

3.2.3.1 Mid-Level Winds

One important difference between the supercell and PS environments is the variation in the direction of the mid-level winds in relation to the dryline due to the location of the upper level trough. To the south, across Oklahoma, winds were more westerly above the dryline whereas to the north, they were more southerly and more nearly parallel to the dryline (Fig. 3.14). This can also be seen in figure 3.15 as a stronger v-component of the 500 hPa environmental wind is evident farther to the north, suggesting a larger dryline-parallel component of the wind in this region. A larger along-line component of the mid-level flow would allow the storms to remain close to the boundary and its associated linear forcing, likely favoring more linear evolution like the PS system in central Kansas. A larger across-line component would likely cause cells to move off the dryline and away from the linear forcing, favoring more isolated storms such as the supercells in western Oklahoma. Figure 3.16 illustrates that this was indeed the case. By around 1900 UTC, the supercells had moved well off the dryline, while the PS line was anchored just ahead of it.

Boundary-relative flow aloft also plays a role in the interactions among neighboring convective cells insofar as it relates to the direction of the deep layer shear vector. Bluestein and Weisman (2000) determined that for shear vectors oriented 45° from a linear boundary, developing cells will interact little with their neighbors and will move off of the boundary as isolated supercells (provided the shear is sufficient for supercells). On 30 March 2006, the 0-6 km shear vectors in western Oklahoma were indeed close to

a 45° angle with the dryline (Fig. 3.17), and the initial cells and broken lines moved off of the dryline and evolved into isolated supercells. In contrast, an environment with a larger along-line component tends to favor linear modes as along-line shear tends to result in cell mergers, which have been shown to be detrimental to long-lived isolated structures and instead favor linear modes (Bluestein and Weisman 2000). Furthermore, this can lead to the seeding of hydrometers into downstream cells aloft expediting cold pool development, and leading to a strong, broad cold pool favoring a linear mode (e.g. Dial and Racy, 2004; Parker, 2007a). Such an environment, containing along-line shear was present farther north along the dryline where the PS line developed (Fig. 3.17). While there were no observations of fine enough scale to determine specific hydrometeor motions, radar animations do indicate the presence of cell collisions during the developmental stages of the PS line. As well, given the along-line hydrometeor transport that is necessary for the formation of a region of parallel stratiform precipitation it is also likely that seeding occurred, much as was seen in the PS simulations of Parker (2007a; b).

3.2.3.2 Dry Air Aloft

Another difference between the supercell and PS environments is the presence of drier air aloft to the north. This is shown quite dramatically in a north-south cross section created from the 1800 UTC NARR data (Fig. 3.15) with moist air to the south across Oklahoma, and north over Nebraska, and an intrusion of drier air over Kansas. A region of very dry air at the surface from western Kansas southwest into New Mexico at 1800 UTC (Fig. 3.2d) is likely the surface indication of this elevated zone of dry air aloft, with deep mixing bringing the drier air down to the surface behind the dryline. The elevated layer of dry air is evident on the 0000 UTC Topeka, Kansas raob (Fig. 3.4c), which was taken just ahead of the dryline, suggesting a similar environment would have

been present ahead of the dryline in west-central Kansas 6 hours earlier.

The presence of dry air aloft in the region where the squall line formed is significant, as dry air can enhance cold pool development due to evaporational cooling. This would favor the development of linear modes as stronger cold pools tend to spread and interact, resulting in a broad region of linear lifting along the leading edge of the cold pool. Some evidence of this stronger cold pool development in the region of the PS line (relative to that seen with the supercells to the south) was evident on 30 March 2006. Just after 1900 UTC the observations from Concordia and Salina Kansas, in the vicinity of the PS line, both registered temperature decreases of approximately 6°C, with the colder temperatures remaining in place for close to an hour. Salina also recorded a 2 hPa increase in pressure during this time. Observations from Newton, Kansas taken as one of the supercells passed near the observing station also show a 6°C temperature decrease, however the areal extent of this cold pool was much smaller, as nearby stations in Wichita recorded temperature decreases of only 2-3°C, and these were of shorter duration than the observed decreases in Salina and Concordia. Furthermore, there were no discernible pressure changes with the passage of the supercell, suggesting that while the precipitation had a cooling effect on the lower levels, the cold pool was not as strong as that seen farther north with the PS line. These observations would suggest that the lack of dry air aloft farther south resulted in weaker, smaller cold pools, aiding in the maintenance of an isolated mode.

3.2.3.3 Initiation Mechanisms

In addition to the variations in environment that have been highlighted thus far, it is also important to note that there were some differences in how the storms were initiated as well. Most notably, the supercells and PS line were initiated along the dryline, while

the LS line developed along an apparent outflow collision, suggesting two distinct forcing mechanisms. Looking closer at the supercells and PS line, further variations emerge, as the supercells were initiated as more widely spaced isolated and broken linear entities while the PS line developed from several closely spaced cells. Orientation of these initial cells is important to note as well, as the initial storms that led to the supercells were initially oriented in a more southwest-northeast line, while those that developed the PS line were in a more north-south line. These variations in initial cell orientation may have been an important part of the 30 March event, as Bluestein and Weisman (2000) demonstrated that cell orientation relative to the vertical wind shear vector can have important effects on storm mode. These differences in cell orientation will be investigated further using the idealized model simulations discussed in chapter 4.

3.2.3.4 Moderate Shear Environment

A final environmental variation that likely played a role in the evolution of the 30 March 2006 event was the presence of a region of weaker vertical wind shear across eastern Kansas where the LS line formed. The environments that spawned the supercells and PS MCS were both characterized by high 0-6 km wind shears of approximately 25 m/s, which is understandable given that both modes are favored in high-shear environments (Parker 2007a). However, the environment over eastern Kansas, characterized by the 18 UTC Topeka radiosonde observation, contained a more moderate 0-6 km wind shear of 18 m/s (Fig. 3.5b). This suggests an environment that could sustain both multicell and supercell storms (as documented in the simulations of Weisman and Klemp 1984), playing an important part in the evolution of the 30 March event in two ways.

First, the moderate shear environment played at least a supporting role in the development of the LS MCS during the event. The 18 UTC Topeka hodograph was similar

in shape to that from Lamont (Fig. 3.5a,b), however, the weaker 0-6 km wind shear in Topeka made it less favorable for supercells. This environment was combined with the strong linear forcing of the colliding outflow boundaries, favoring linear modes even more. Outflows are typically associated with 'slabular,' or layer-like, lifting (James et al. 2005), so the collision of outflows is likely to result in a strong preference for slabular lifting (Fig. 3.12), as opposed to the more isolated cellular lifting that was seen along the dryline, where the supercells and PS line formed (Fig. 3.6a). Given that the MCS that developed was oriented largely north-south, the environmental shear vectors ended up being directed largely across-line, thus ruling out the development of the PS mode. And while the shear was less than seen in the supercell and PS environments, it was still strong enough to favor the LS precipitation structure (Parker and Johnson 2004c).

The moderate shear environment is also a key factor in the evolution of all three modes during this event. While the initial storms developed in three distinct environments, as outlined above, eventually all three were present in eastern Kansas within an hour of the 1800 UTC Topeka, Kansas radiosonde observation. Given the close proximity of the three modes to each other, and the presence of all three modes in the region within an hour of the 1800 UTC observation, it can be assumed that all three modes were evolving through a similar environment characterized by this observation. This finding provides the basis for the working hypothesis that its presence as a "middle of the road" environment allowed all three modes observed on 30 March 2006 to be sustained in close proximity to one another. Upon initiation in their respective environments, the supercells and PS line both moved into the moderate shear environment in eastern Kansas where the LS line was developing. All three modes then proceeded to evolve through this environment for the remainder of the event. During this time, each mode largely maintained their original organizational characteristics despite being in close proximity to two other distinctly different modes

of convection. It is hypothesized that this was made possible by this moderate shear environment containing enough wind shear to support the on-going supercells, while not containing so much shear that the linear MCSs evolved into more isolated or supercellular structures.

The results of the observational case study, suggest several hypotheses regarding the 30 March 2006 case. Two hypotheses emerge to with regards to the initiation of the various convective modes observed in this case. It appears that either the presence of three distinct environments with different thermodynamic and wind shear structures played a key part in the development of multiple modes of convection, or that differences in the means of storm initiation, both in the type of forcing and the spacing of initial cells governed the determination of convective mode. These two hypotheses stem from the key differences observed between the different modes, namely that each mode originated from a unique environment, and that each was initiated in a slightly different manner. With regards to storm evolution, one hypothesis was formulated from the observations; that the moderate shear environment in eastern Kansas provided an environment favorable to the evolution of all three modes, and thus accounts for the multi-mode evolution seen in this case. It is important to stress, once again, the delineation between the initiation portion of this event, and the evolution portion of the event. As the various modes initiated across the Kansas/Oklahoma region, they all initiated in three different environments, as outlined above. Then, as the storms moved into eastern Kansas and began to evolve in close proximity to each other, beginning around 1900 UTC, they had moved into a single environment. Essentially the supercells and PS line had progressed out of their initial, different, environments and into a third environment where the LS line was continuing to develop. All three modes then remained in this environment as they progressed across eastern Kansas. This progression leads to the moderate shear environment hypothesis

regarding the evolution of all three modes. The hypotheses outlined in this section cannot be completely examined and tested using just observations, and thus they were tested through the use of numerical simulations, which will be discussed next.

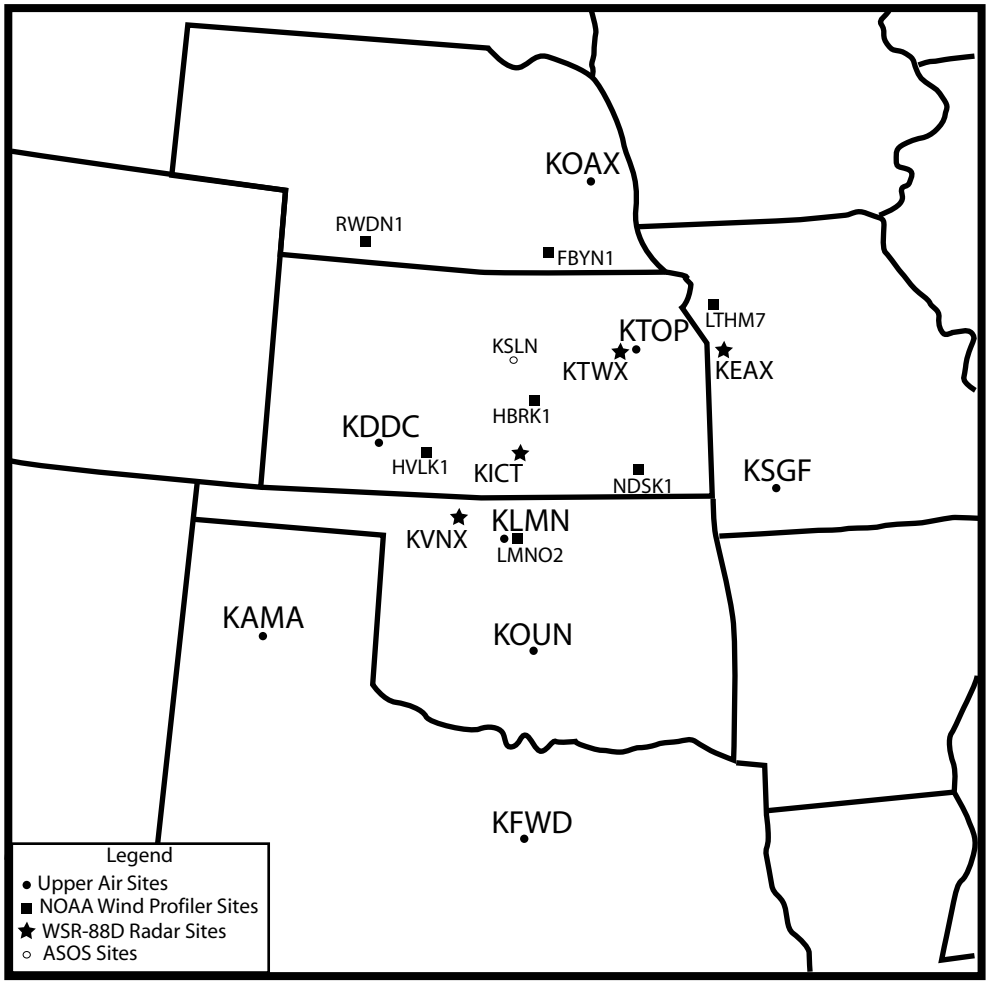

Figure 3.1: Map detailing the locations of upper air observation sites that launched 18 UTC soundings on 30 March 2006 (dots with large text), WSR-88D Doppler radar sites (stars), NOAA Wind Profiler sites (squares) and key ASOS sites (circles). It should be noted that this is not an exhaustive map of all sites in the region (e but rather these are the sites for data used in this study.

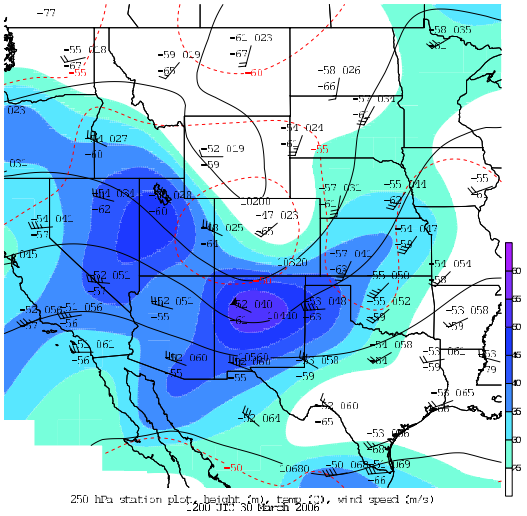

(a)

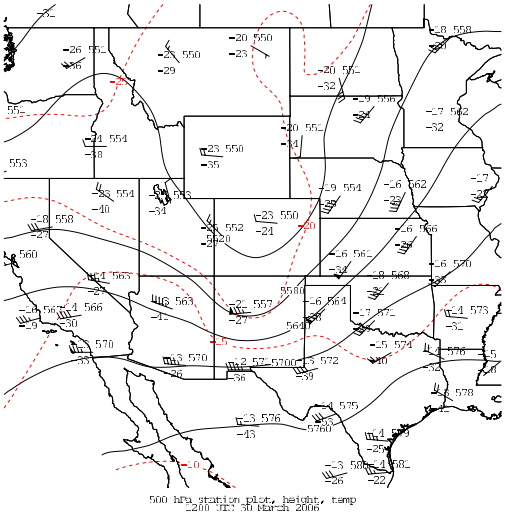

(b)

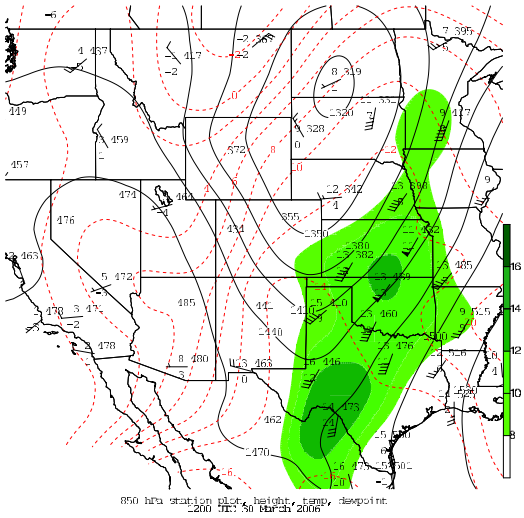

(c)

Figure 3.2: a) 1200 UTC 250 hPa height (black), wind speed (shaded), temperature (red dashed). b) 1200 UTC 500 hPa height (black), temperature (red dashed). c) 1200 UTC 850 hPa height (black), temperature (red dashed), dew point (shaded green). All heights in meters, temperature and dew point in degrees Celsius, winds in meters per second, with one wind barb equal to 10 m/s, and pressure in corpuscles. The contours are an objective analysis of the observed data performed using a Barnes objective analysis scheme.

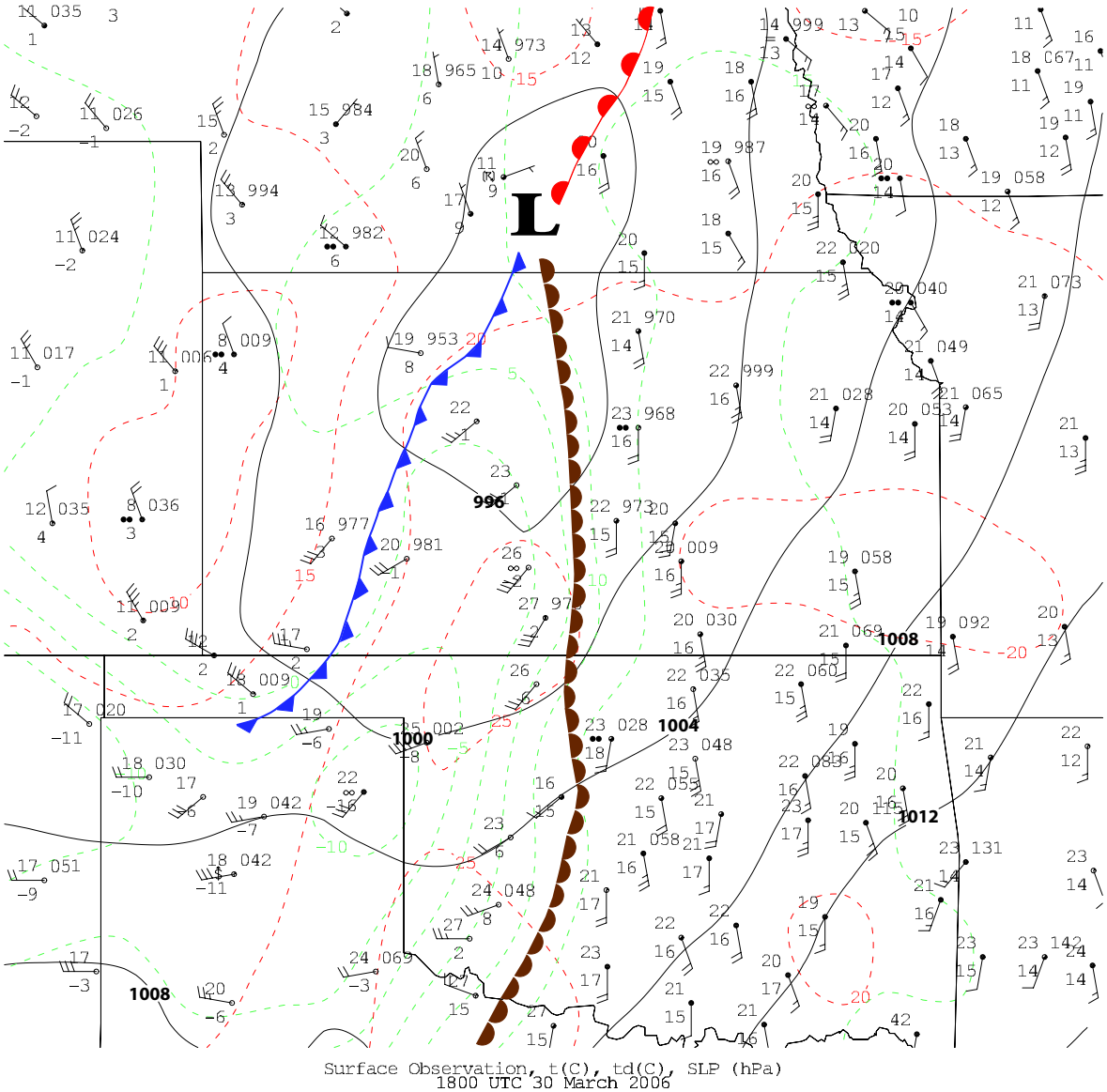

Figure 3.3: 1800 UTC surface features including: station plots, pressure (solid black, hectopascals), temperature (dashed red, Celsius), dew point (dashed green, Celsius). Surface dryline, cold front, and warm front are denoted with traditional markings. The contours are an objective analysis of the observed data performed using a Barnes objective analysis scheme.

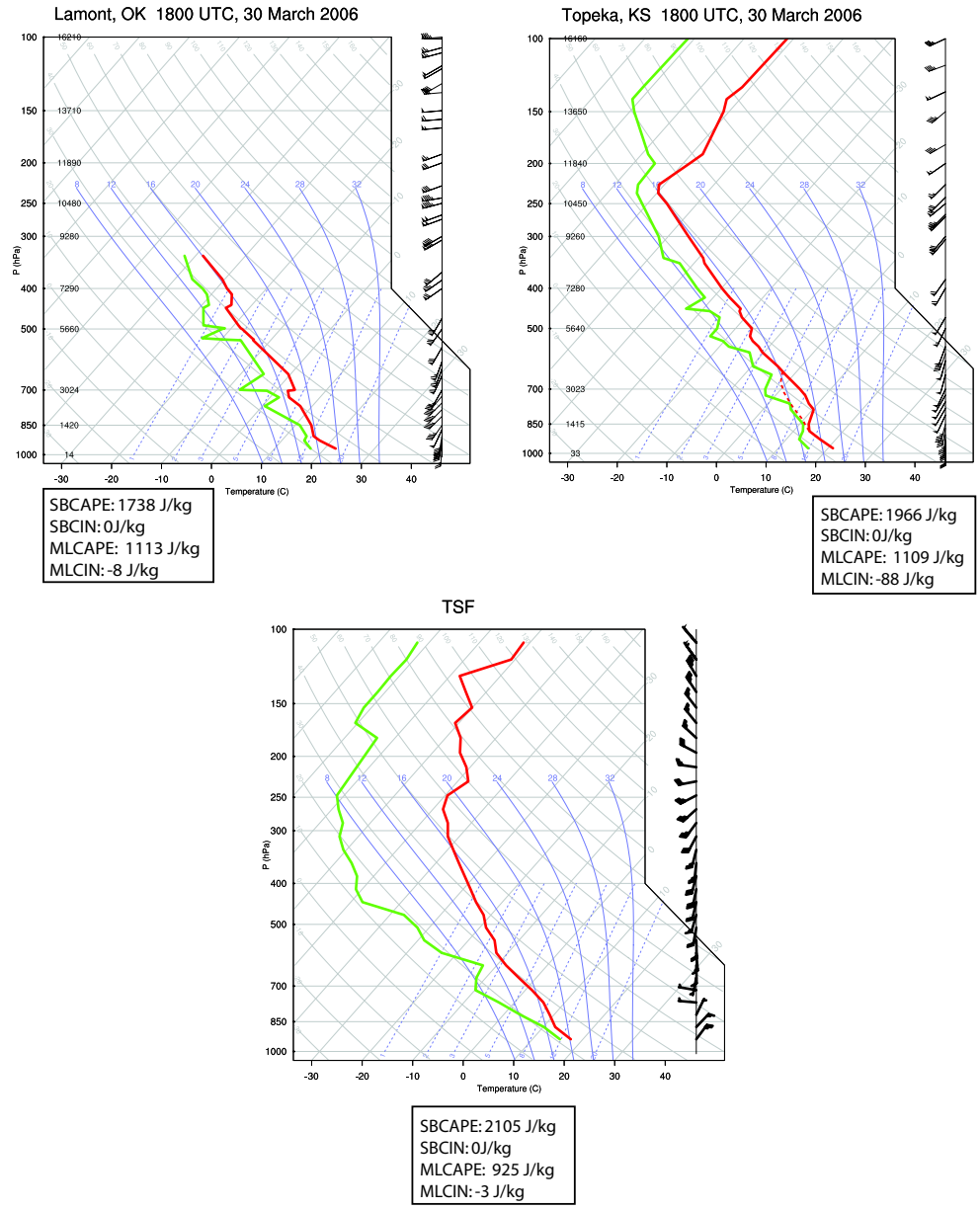

Figure 3.4: 1800 UTC skew-T ln-p diagrams from: a) Lamont, Oklahoma and b) Topeka, Kansas. c) Represents the upper air observations from the 0000 UTC Topeka, Kansas radiosonde combined with the 1800 UTC Salina, Kansas surface observation and 1800 UTC Fairbury, Nebraska wind profiler observations (the significance of this combination is explained in the text). Locations are noted in figure 3.1. Also listed are surfaced-based convective available potential energy (SBCAPE) and surface-based convective inhibition (SBCIN) along with mixed-layer CAPE and CIN (MLCAPE and MLCIN, respectively) computed from a 100 hPa deep layer.

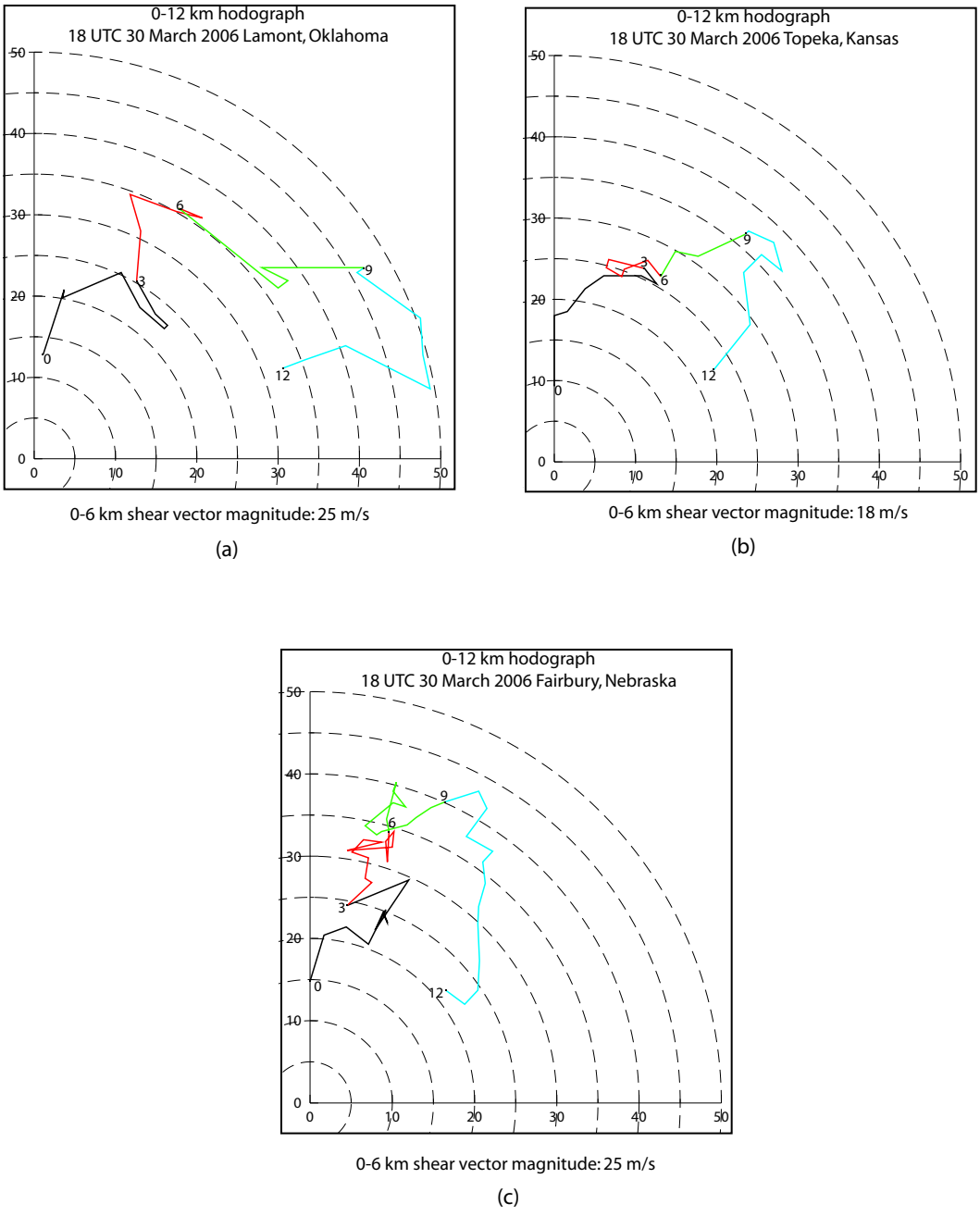

Figure 3.5: Hodographs corresponding to the 1800 UTC soundings in figure 3.4. a) Lamont, Oklahoma raob. b) Topeka, Kansas raob. c) Fairbury, Nebraska wind profiler. Also reported is the 0-6 km bulk shear vector magnitude.

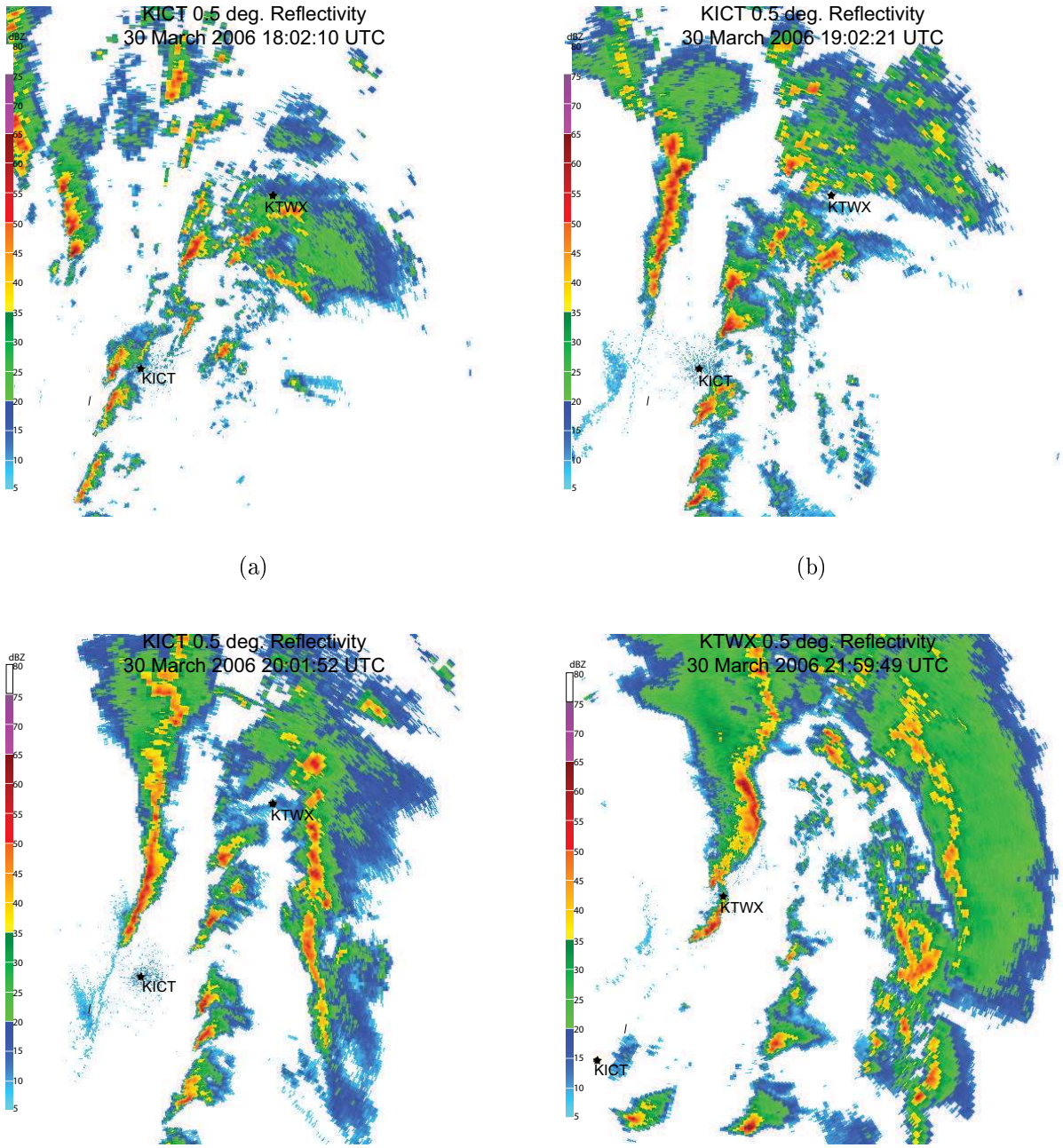

Figure 3.6: Evolution of all three modes during the course of the 30 March 2006 event depicted through base reflectivity. a) 1802 UTC KICT b) 1902 UTC KICT c) 2001 UTC KICT d) 2159 UTC KTWX

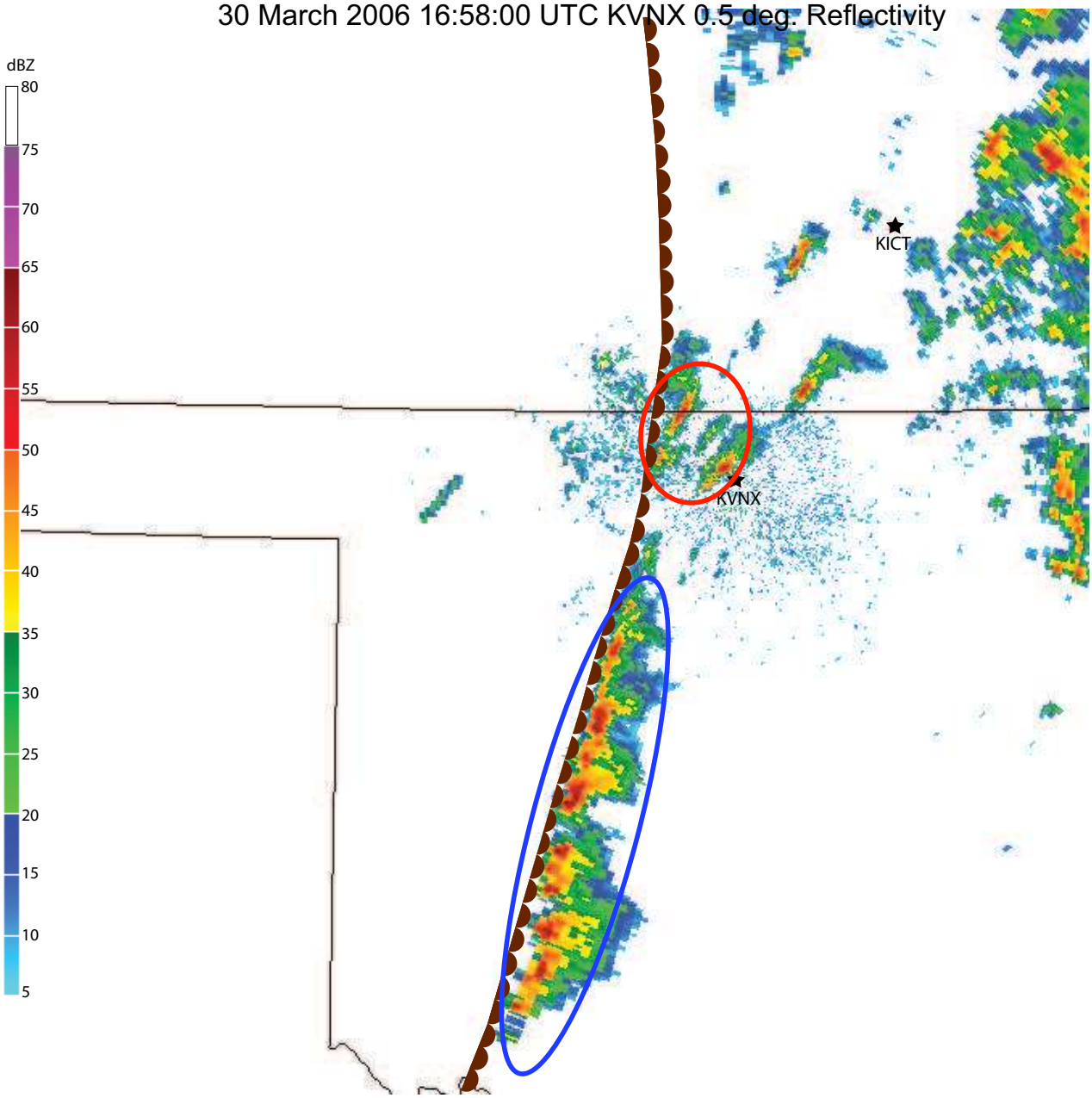

Figure 3.7: 1658 UTC Vance Air Force Base, Oklahoma base reflectivity and surface dryline showing the storms that eventually evolved into the isolated supercells in northern Oklahoma and eastern Kansas. The red circle denotes two initially isolated storms that would evolve into the first two supercells observed, and the blue circle denotes an initial convective line that evolved into a line of isolated supercells as it moved off the dryline into north-central Oklahoma and southeastern Kansas.

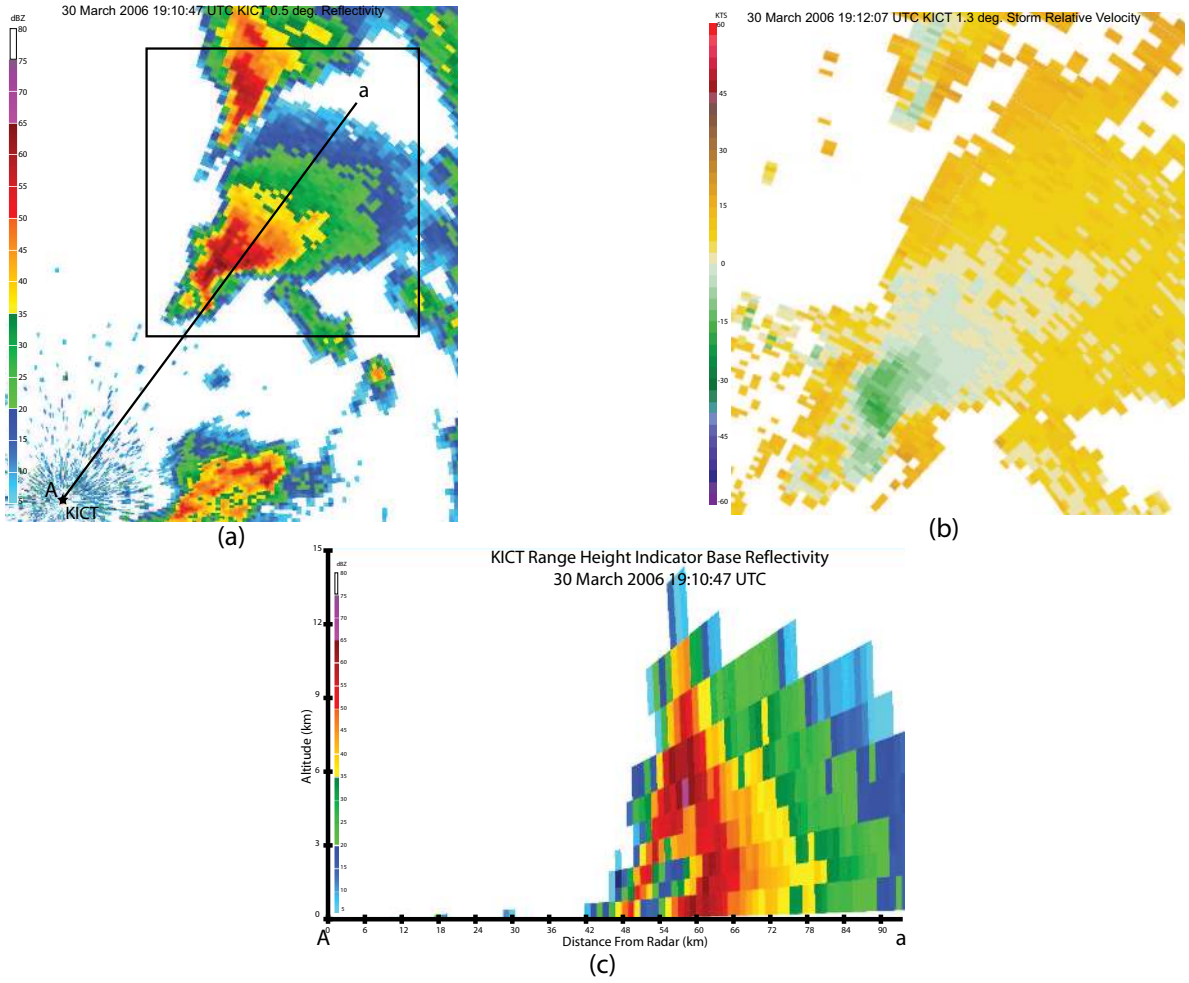

Figure 3.8: a) Plan view of 1910 UTC base reflectivity from Wichita, Kansas focused on two of the stronger supercells. b) 1.3 degree storm relative velocity image from the same time as (a). c) RHI scan through weak echo region of supercell. The box in (a) denotes the area of focus for the velocity image in (b) and line A—a is the direction of cross section shown in (c).

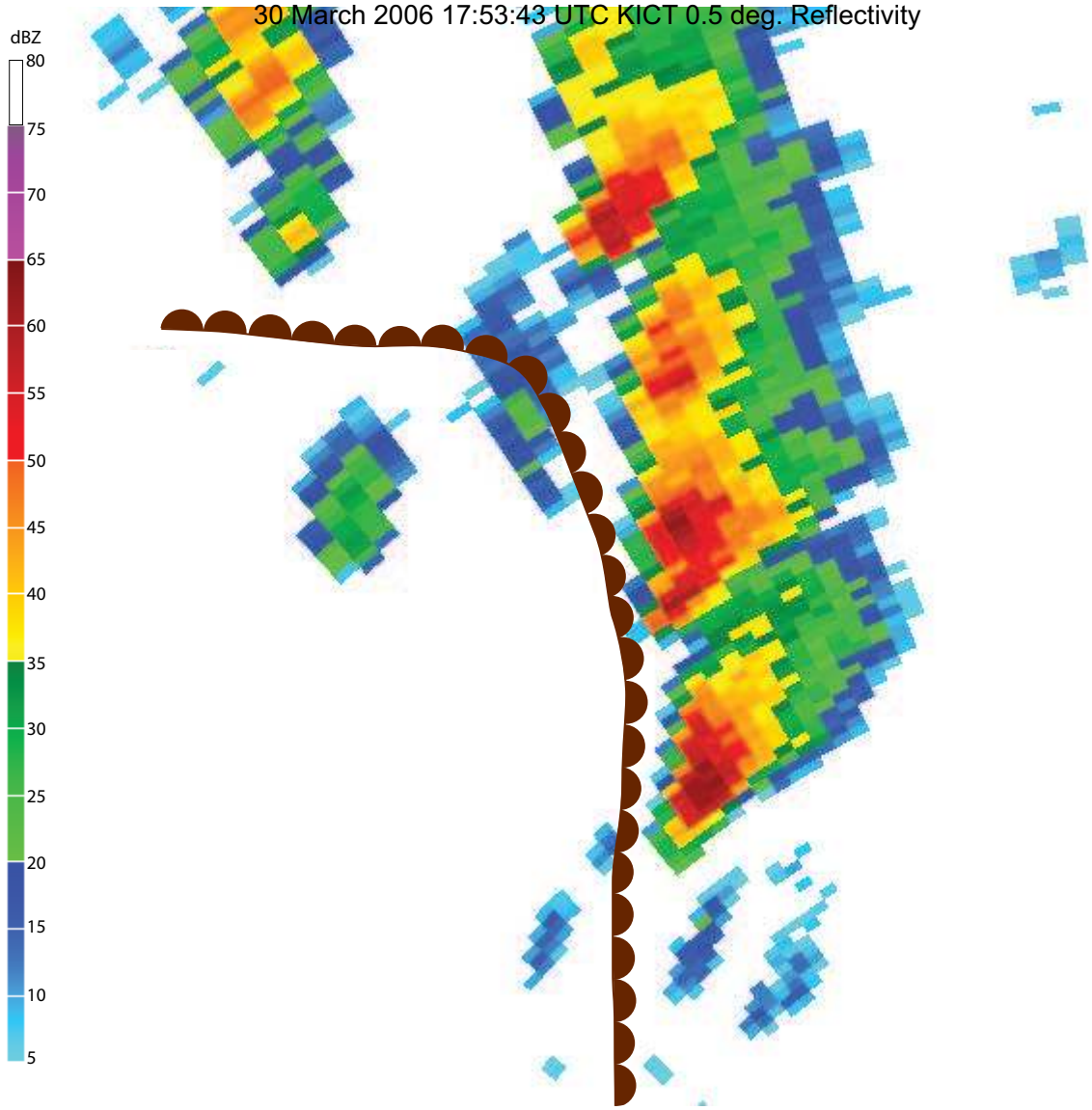

Figure 3.9: 1753 UTC Wichita, Kansas base reflectivity showing the surface dryline and the initial cells that eventually formed the PS line in north-central Kansas.

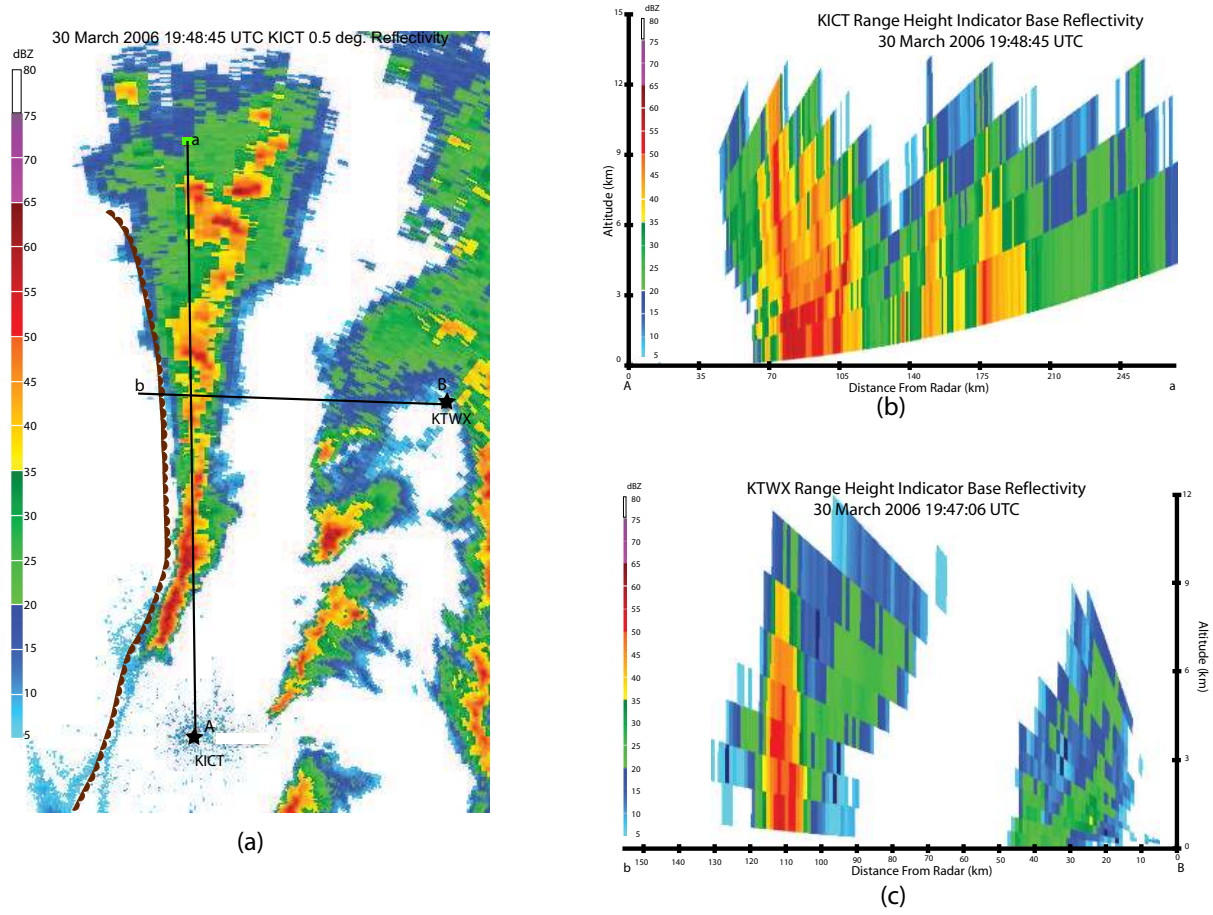

Figure 3.10: a) Plan view base reflectivity of the PS line as seen at 1947 UTC by the Wichita, Kansas WSR-88D. b) Range-Height Indicator (RHI) scan of the PS line from Wichita at the same time as in (a) looking in an along line direction. The cross section is taken along the line A—a in (a). c) RHI scan of the PS line as seen at 1947 UTC by the Topeka, Kansas WSR-88D, looking in the across-line direction. The cross section is taken along the line B–b noted in (a).

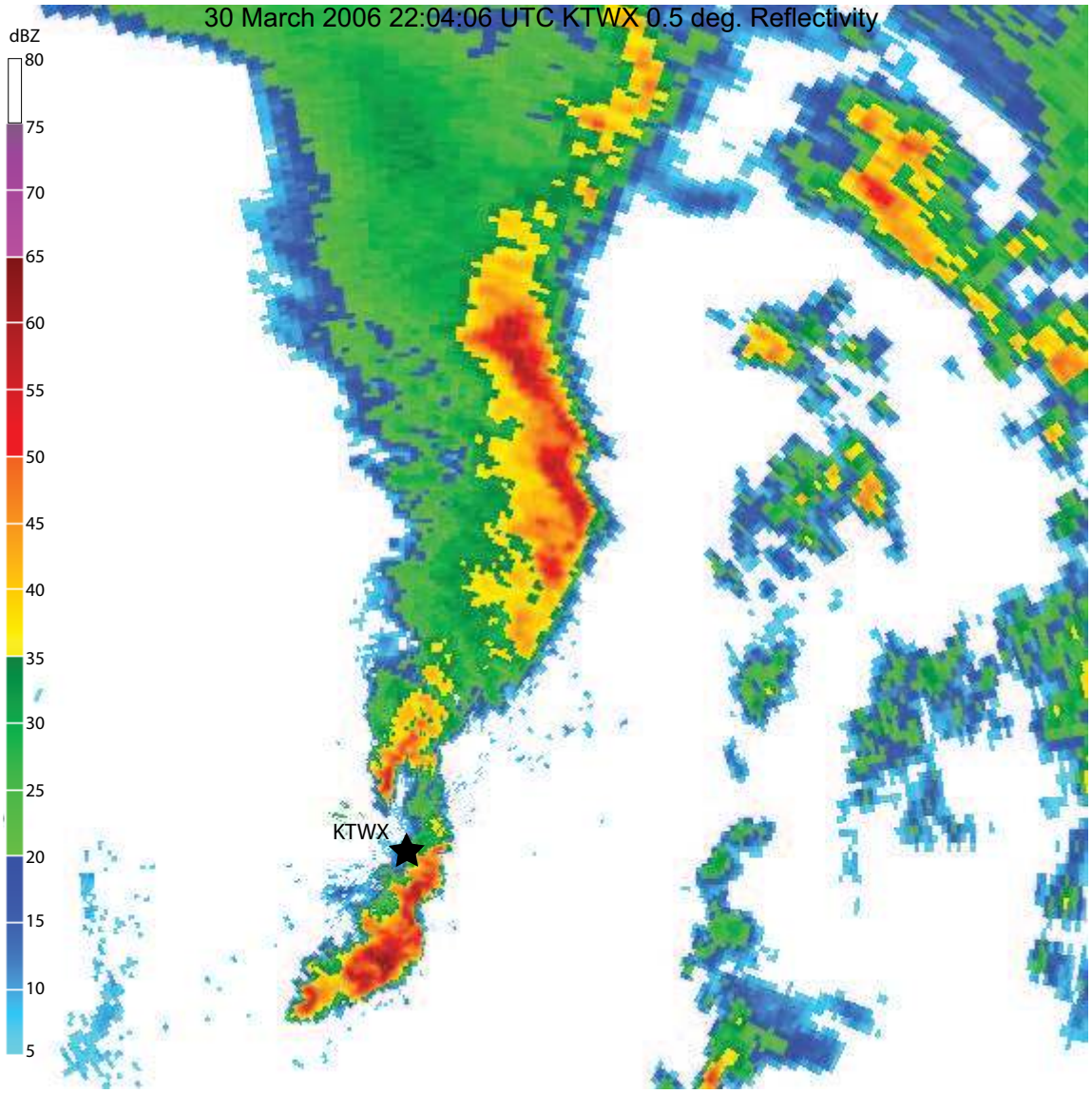

Figure 3.11: 2204 UTC base reflectivity data from Topeka, Kansas showing that the PS line has evolved into a squall line with trailing stratiform precipitation.

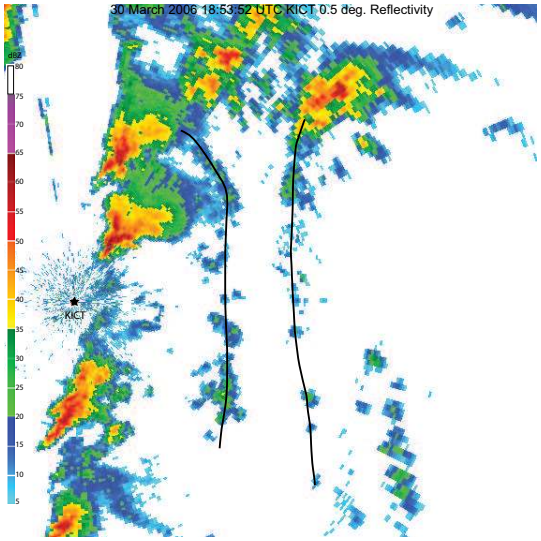

(a)

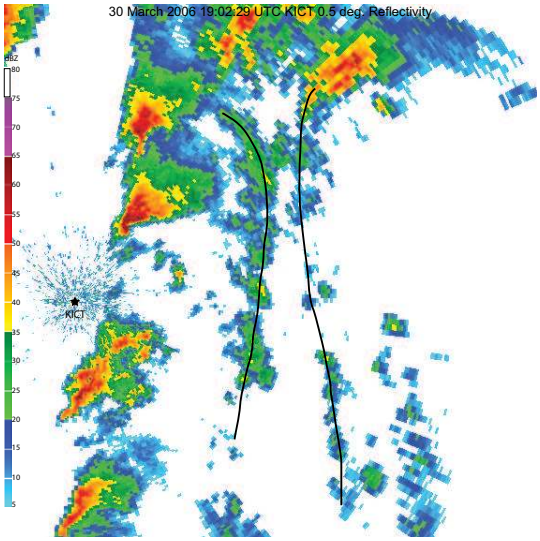

(b)

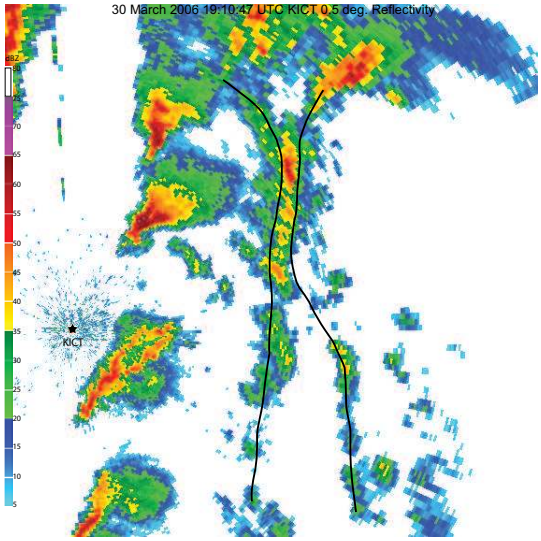

(c)

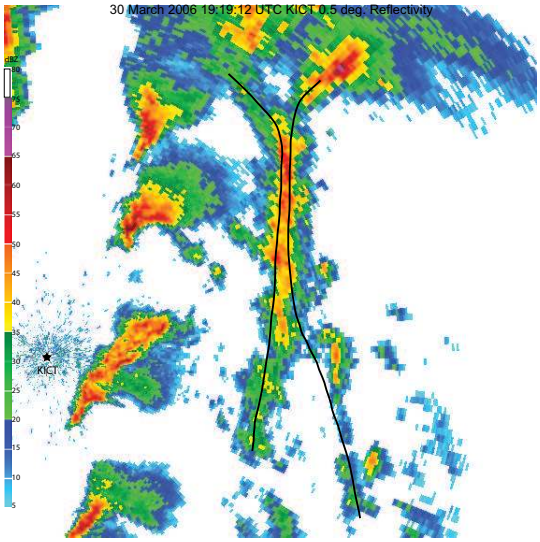

(d)

Figure 3.12: Development of LS MCS due to collision of outflow boundaries as seen by KICT base reflectivity at a) 1853 UTC, b) 1902 UTC, c) 1910 UTC and d) 1919 UTC. Apparent outflow boundaries denoted by black lines.

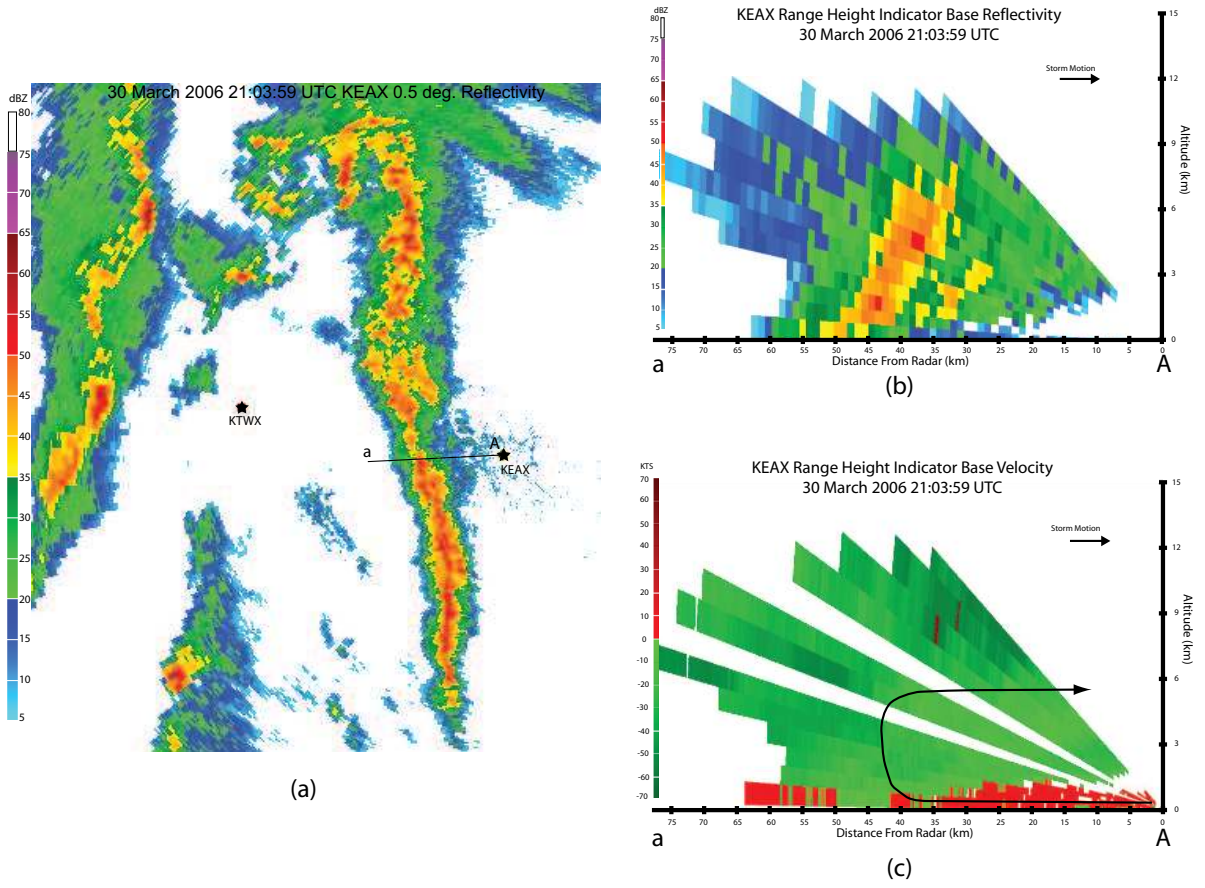

Figure 3.13: a) Plan view of 2103 UTC base reflectivity from Kansas City, Missouri. b) RHI plot of reflectivity at same time as (a). Note: the storm is moving towards the radar, which is to the left in this image. c) Same as b) but for base velocity. Cross-sections in (b) and (c) are along line A—a in (a).

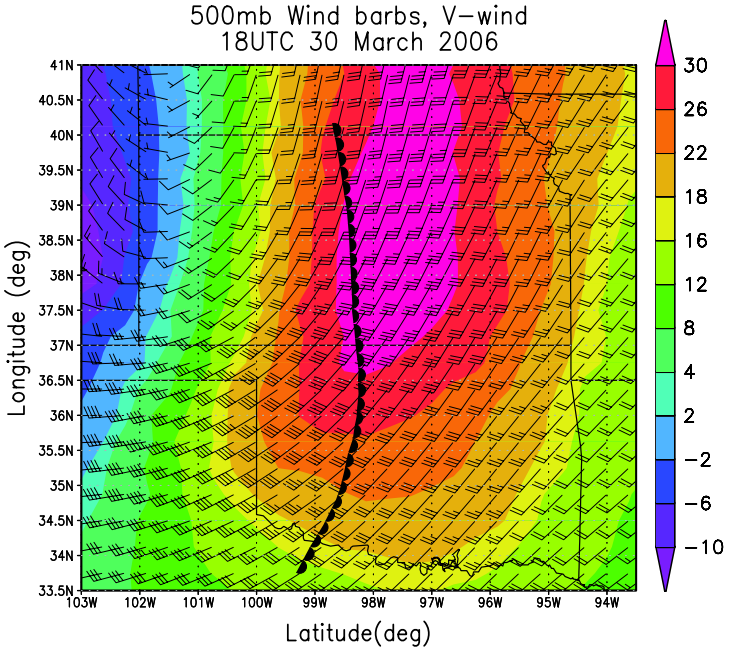

Figure 3.14: 18 UTC 500 hPa v-wind component (shaded) and total wind (barbs) from NARR data illustrating north/south variation in mid-level winds. This highlights a maximum in the southerly (line-parallel) wind component farther north in Kansas where the PS line formed, decreasing to the southwest where the supercells formed.

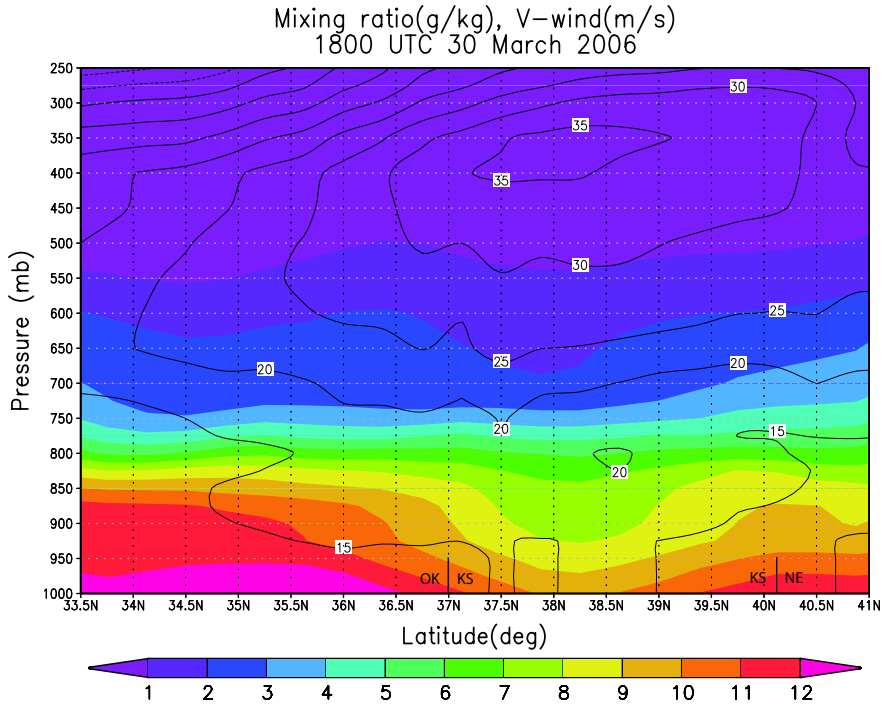

Figure 3.15: 1800 UTC longitudinal cross-section taken at 98.5 W (just east of the surface dryline) showing mixing ratio (shaded) and v-wind component (contoured) created from NARR data.

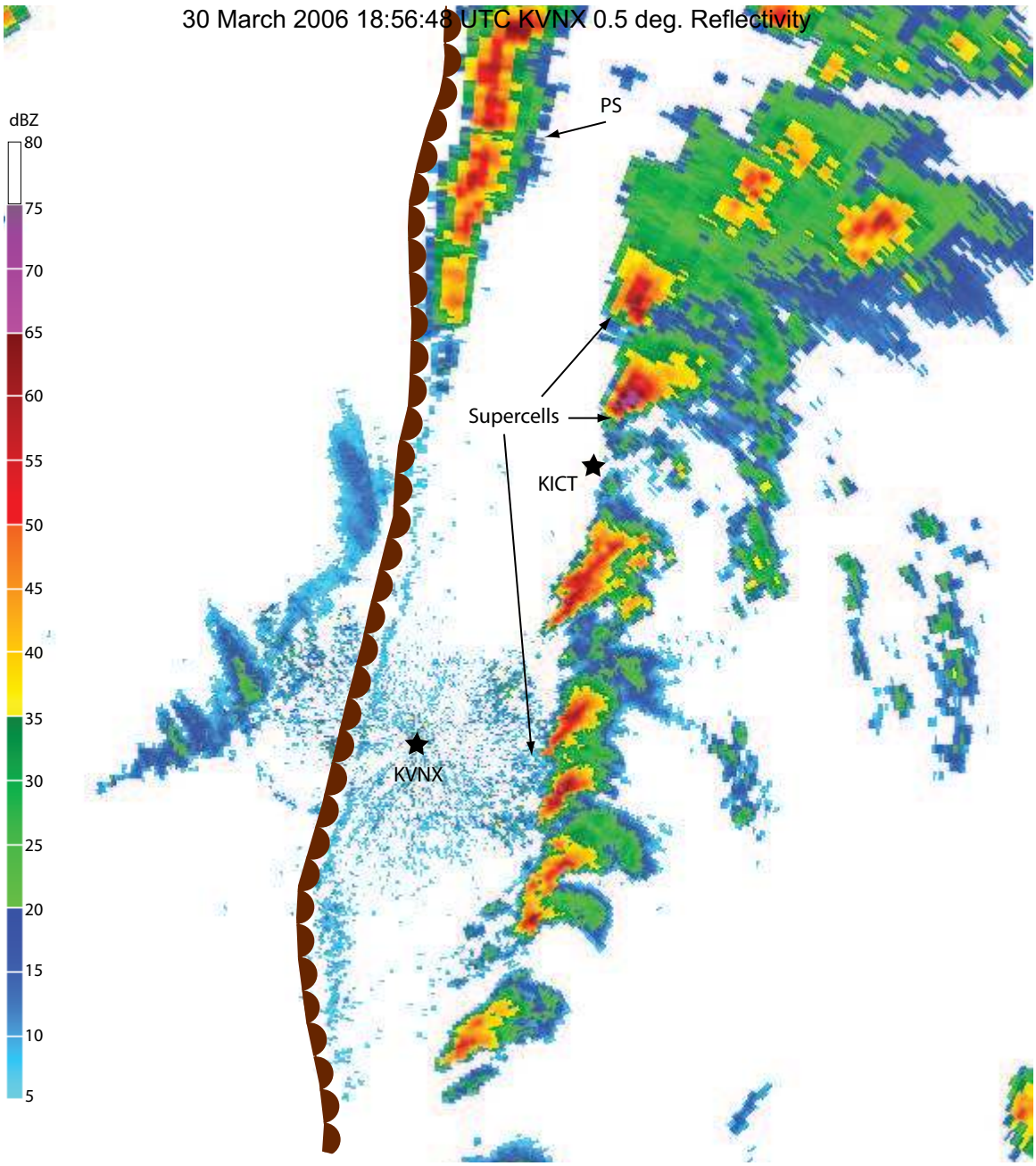

Figure 3.16: 1856 UTC base reflectivity data from Vance Air Force Base, Oklahoma showing the PS line and supercells as well as the surface dryline, which appears as a fine line. Dryline is denoted with brown scallops and the supercells and PS line are labeled.

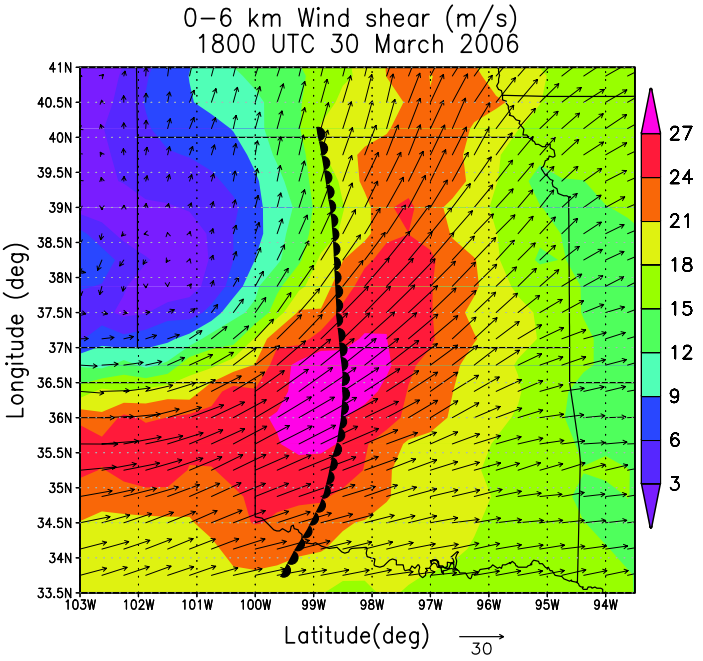

Figure 3.17: 18 UTC 0-6 km wind shear vectors and magnitude (shaded) from NARR data illustrating north/south variation in vertical shear. This highlights both stronger shear magnitude to the south where the supercells formed as well as the larger across line component of the shear to the south vs. the larger along line component farther north.

Chapter 4

Model Simulations

Based on the observational analysis discussed in Chapter 3, two hypotheses emerged for the origins of multiple modes of convection in a localized area. The first general hypothesis is that the different storm modes in the 30 March 2006 case resulted from localized differences in the environment. Based on the locations of the observed storm structures, it can further be hypothesized that a high CAPE, high shear environment favored the supercells, an environment with dry air aloft and along-line shear favored the PS line, and a capped environment with moderate shear favored the LS line development. The second general hypothesis is that the various modes resulted from differing initiation mechanisms. This too stems from observations, as all three modes appeared to have been initiated in slightly different manners. The supercells and PS line were both initiated as isolated cells along the dryline, however the cell spacings and orientations varied. This could have played a role in the ultimate mode that evolved. In contrast, the LS line appeared to result from an outflow collision. Thus more detailed hypotheses in this realm would be that close cell spacings favor linear modes while wider spacings favor more isolated structures, and that linear forcing mechanisms, such as the outflow collision, favor the development of linear modes. Furthermore, initial cells oriented obliquely to the

environmental shear will favor isolated modes whereas shear parallel or perpendicular to the initial cells will favor linear modes, as suggested by the observations, and described by Bluestein and Weisman (2000). In order to test these hypotheses, idealized simulations were used to try to isolate the effects of the environment vs. the initiation mechanism on convective mode. Additionally, the possibility of storms altering their local environment is examined as well. Idealized numerical simulations were chosen because within controlled simulations one can isolate processes in ways that are not possible in nature. A simulation of the actual case was attempted as well, as a means to bridge the gap between the observed case and the idealized simulations.

4.1 Idealized Simulations

4.1.1 Methods and Configuration

The model used for the idealized simulations was version 2.1.2 of the Weather Research and Forecasting (WRF) Advanced Research WRF (ARW) modeling system developed at the National Center for Atmospheric Research (NCAR) (Skamarock et al. 2005). The model includes fully compressible non-hydrostatic equations, Arakawa C-grid staggering, and the ARW core which consists of an Eulerian mass coordinate. Third order Runge-Kutta time differencing was used, along with fifth order horizontal, and third order vertical advection. The idealized model simulations were divided into two main groups: tests of sensitivity to changes in environmental parameters, and tests of sensitivity to changes in initiation or "trigger" mechanisms . For the majority of these simulations, the model was integrated for 6 hours over a 400 by 400 km domain with a horizontal grid spacing of 1km, a vertical grid spacing of 500 m and 41 vertical levels. Convection was simulated explicitly and the Lin et al. (1983) scheme was used to

parameterize cloud and precipitation microphysics. Sub-gridscale turbulence was parameterized using a 1.5 order turbulent kinetic energy (TKE) closure. Coriolis accelerations, were not included in the model given the short integration time, a common practice in idealized studies (e.g. Rotunno et al. 1988; Bluestein and Weisman 2000; James et al. 2005; Parker 2007a,b). Furthermore, simulations by Parker (2007b) demonstrated that the overall convective mode was not sensitive to variations in Coriolis during a 6-hour simulation. To further simplify the simulations, surface fluxes and radiative effects were not included in the model. The simulations used Rayleigh damping over a layer of 5 km at the model top, and open lateral boundary conditions unless otherwise noted. The initial conditions were homogeneous, with artificial perturbations added to initiate storms as will be discussed shortly. For these simulations, the "pre-packaged" em_quarter_ss experiment was utilized as the initial source code and then modified to produce the setup described herein.

Sensitivity tests were run using both the constant vertical grid spacing of 500 m as well as a stretched vertical grid with higher resolution near the surface. The results of these tests suggested that the constant vertical grid appeared to better simulate a variety of modes, while the stretched grid resulted in a predominance of linear modes. This is likely because by adding more points, and thus higher resolution in the lower troposphere, the stretched grid would tend to be biased toward low level features such as cold pools compared to middle level feature such as convective updrafts. This may have resulted in the stretched grid featuring stronger cold pools, resulting in more linear modes. Comparing the results of these sensitivity tests to observations suggested that the simulations using the constant vertical grid spacing was more realistic. This was especially true in the case of the supercell storms, as the stretched grid simulation generated cold pools that were 3-5 K colder than observed with the supercells in reality. Also the larger areal extent of

these colder temperature would appear to be at odds with observations that suggested the coldest air in the supercell cold pools was very limited. Because the constant grid spacing better replicated the variety of modes observed, which were focus of this study, this setup was used for the idealized simulations.

The homogeneous base state environments for these simulations were based on three soundings representative of the three environments discussed in the observational case study. The first of these soundings is based on the 1800 UTC Lamont, Oklahoma sounding (hereafter LMN18) (Fig. 3.4a) and represents the environment in which the supercells initially formed on 30 March 2006. The observed sounding was missing moisture observations above 307 hPa, so above this level observations were taken from a point in the 1800 UTC NARR data at the location of Lamont, Oklahoma. The soundings were very similar below 300 hPa, such that the NARR data should provide a reasonable approximation. The 1800 UTC Topeka, Kansas sounding was utilized to simulate the environment in eastern Kansas where the LS line formed, as the sounding was taken just over an hour before that line began to develop (Fig. 3.4b). The unchanged sounding (hereafter TOP18) was used in the colliding outflow boundary simulations, however a small cap around 750 hPa had to be removed in order to initiate storms with the warm thermal perturbations in this environment (hereafter TOP18nocap) (Fig. 3.4b, dashed temperature trace). The final sounding consisted of a composite between the 0000 UTC 31 March upper air observation from Topeka, Kansas, the 1800 UTC surface observation from Salina, Kansas, and the 1800 UTC wind profile from the Fairbury, Nebraska wind profiler (hereafter TSF) (Fig. 3.4c). This combination offered the best representation of the environment wherein the PS squall line formed in western Kansas, which had low level instability, dry air aloft, and southerly mid-level winds as established by the observational case study.

Convection was initiated within these simulations using a variety of initial perturbations to simulate a range of isolated and linear forcings for storms (Fig. 4.1). The most basic trigger, used to provide a baseline control experiment, was a single thermal bubble with a horizontal diameter of 10 km and vertical diameter of 3 km centered at 1.5 km above ground level (AGL). The bubble was 3 K warmer than the surrounding environment at its center, with a Gaussian temperature decrease towards its outer edges. This was chosen as a baseline perturbation, because it basically introduces a single updraft into the environment to create an initial storm. The environment can then act on this storm and govern how it evolves, with little effect from the initial perturbation. To provide a more linear forcing, simulations were initiated with lines of three and five of these bubbles, using a variety of different bubble spacings and several different orientations, similar to the approach of Bluestein and Weisman (2000) (Fig. 4.1). The motivation for these configurations stems from the observed supercells and PS line, both of which developed from initially isolated cells along the dryline. The cells that developed into the PS line originated close together in a north-south line, and those that formed the supercells were spaced farther apart in a more southwest-northeast line. Several simulations were also employed to simulate a broad linear initiation mechanism as well, similar to what was observed with the colliding outflow boundary initiation of the LS line. These consisted of both warm and cold thermal perturbations, in a variety of configurations, as shown in figure 4.1. As noted in the figure, several of these simulations employed periodic y-boundary conditions to simulate infinitely long forcing mechanisms. The colliding outflow boundary simulations also included periodic x-boundary conditions as well to minimize the computational noise that occurred when the cold pools spread toward the originally open lateral boundaries. In these cases, the presence of the initial cold boxes covering the majority of the eastern and western halves of the domain generated

significant noise at the inflow (western) lateral boundary causing the model to become unstable. By stretching the domain in the x-direction and making the lateral boundaries periodic, this problem was eradicated without detriment to the storms being simulated.

4.1.2 Environmental Control Simulations and Initial Perturbation Sensitivities

To establish control runs, idealized simulations were performed using each of the initial soundings and a single warm bubble perturbation to initiate convection. The single-bubble simulations established the relationship between a given environment and its predominant convective mode while at the same time providing benchmarks with which to compare further sensitivity tests. Following these initial runs, the initial perturbation was varied to examine the sensitivity of convective mode to forcing mechanism within each environment.

The first experiment used the LMN18 sounding characterized by a moderate amount of CAPE and strong wind shear. The single bubble quickly triggered an isolated storm (Fig. 4.2a) that began evolving toward a supercell by 3 hours into the simulation (Fig. 4.2b). By 4.5 hours, the storm had developed into a mature supercell (Fig. 4.2c) characterized by a mid-level mesocyclone, along with hook echo and bounded weak echo region (BWER) features in the simulated reflectivity fields (Fig. 4.3). This storm remained a supercell for the duration of the 6-hour simulation (Fig. 4.2d).

Following the single-bubble control run, a battery of tests were run using the LMN18 sounding to test the sensitivity of the control simulation to initiation mechanism. The results of these tests were very similar, as in each case, by the end of the six hour simulation the predominant (and usually exclusive) mode was isolated supercells (Fig. 4.4). While this was not surprising in the case of the single warm bubble, linear modes

were expected to develop in some of the other simulations, especially with the line thermal and cold box triggers. For these simulations, the initial storms that formed were indeed linear, however these linear structures rapidly devolved into individual cells, with the southernmost cell dominating and becoming a long-lived supercell (Fig. 4.4 a, b). Similar results were seen from the lines of warm bubbles, wherein convection began as a line of isolated cells, with the northern cells weakening with time and the southernmost cell dominating and evolving into a long-lived supercell (Fig. 4.4c, d). This evolution towards increasingly supercellular structures is similar to what was seen in Oklahoma during the 30 March case. The initial cells and broken line segments became more organized and supercellular with time as they evolved across the region. This suggests that within the high CAPE, strongly sheared environment seen in western Oklahoma on 30 March 2006, environmental factors played a larger role than initiation mechanism in selection of convective mode. The environment strongly favored supercells, and that was the ultimate mode that evolved irregardless of how the simulated storms were initiated.

The second environment represented eastern Kansas, where the LS system was observed and was characterized by the 18 UTC TOP18nocap sounding. This region was very similar to the supercell environment, except that the 0-6 km bulk shear vector magnitude was approximately 6-8 m/s weaker. The single-bubble simulation resulted in a splitting supercell (Fig. 4.5a) whose right-moving entity displayed supercell characteristics (Fig. 4.3) while continuing to periodically split, with the left-moving storms evolving as multicells (Fig. 4.5b) . Eventually several of these smaller multicells merged and formed an LS squall line to the north of the supercell (Fig. 4.5c). These two modes continued to evolve together through the remainder of the simulation, with the supercell beginning to merge into the southern end of the line by six hours (Fig. 4.5d).

As before, a battery of simulations was run to test the sensitivity to initiation mech-

anism using the TOP18nocap and TOP18 soundings using the same set of initiation mechanisms as was used with the LMN18 sounding. For these simulations, the ultimate mode observed was seen to be sensitive to initiation mechanism, mainly when the orientation of the initial cells was manipulated. The lines of 5-bubbles[1], cold box, line thermal and lines of 3-bubbles oriented northwest-southeast all behaved very similarly to the control run, as illustrated in figures 4.7a and 4.7b. The only difference observed with these runs was a larger areal extent of the convection, owing to the larger size of the initial perturbation. The gross modal characteristics, though remained the same. A more significant sensitivity was seen from both the line of 3 bubbles oriented north to south (hereafter TOP18_3bubNS) and the line of 3 bubbles oriented southwest to northeast (hereafter TOP18_3bubSwNe). The TOP18_3bubNS simulation behaved similarly to the control run through about 4 hours, but then the supercell rapidly merged with the south end of the squall line and the system subsequently evolved towards the TS precipitation structure (Fig. 4.7c). The more rapid merger was due to the supercell being overtaken by the southern edge of the squall line's cold pool. It is of note that in this case, the areal extent of the squall line was more compact, and the embedded echos appeared more intense than seen during the evolution of the control simulation. Indeed, by 6 hours, the areal extent of the line in this simulation is much smaller (Fig. 4.7c) than seen in the control simulation or any of the simulations that behaved like the control simulation (e.g. Fig. 4.7a and b). This more compact area of intense convection could have lead to the development of a stronger cold pool, which would account for both the faster merger and the evolution toward TS.

The TOP18_3bubSwNe simulation also evolved differently than the control simula-

[1]In every case, the same behavior was seen from a given orientation of the lines of warm bubbles independent of the bubble spacing. Thus, only the simulations will only be referred to by length (3 vs 5) and orientation. The results of the 20 km spacing simulations were used in the figures for consistency, however the results of the 0, 10, 30 and 40 km spacings were essentially the same as those shown.

tion, as the three initial cells had largely merged and begun evolving toward a TS line by 3 hours. In this case, the two southwestern cells interacted with the outflow from the northeastern cell early on the the simulation, leading to a rapid weakening as before they eventually merged with the northeastern cell. By this point, the combined effect of the three cells had generated a strong cold pool which aided in the rapid evolution toward the TS structure. In both this case and the aforementioned TOP18_3bubNS simulation the key difference that lead to an ultimately different evolution was the configuration of the initial cells compared to the 0-6 km shear vector. While the exact results differ somewhat from those of Bluestein and Weisman (2000), likely due to the lower shear environment in this study supporting multicell and supercell structures, the basic concept is the same as this previous work. The orientation of the initial storms compared to the 0-6 km shear vector governs how these storms will interact. In the case of Bluestein and Weisman (2000), who were dealing mainly with supercells, this determined whether isolated supercells would persist or evolve toward other modes. In this case, using a weaker shear regime, the effects can be extended to include a wider range of modes, namely determining between the development of an isolated supercell and LS line, or a TS line.

Given that the outflow collision observed in reality occurred in the TOP18 environment, a simulation using the colliding outflow initiation mechanism was run only in this environment. This resulted in a storm with an intense (20 m/s) updraft (Fig. 4.8a) that initially took on LS structure, much as was seen in the observed case (Fig 4.9a). By 1.5 hours, the simulated storm had weakened considerably, likely as a result of the initial cold boxes cutting off the high theta-e inflow[2]. To isolate the effect of the outflow

[2]As for why this weakening was not observed in reality, there are a variety of possibilities. Surface fluxes (which were turned off for the idealized simulations) may have helped destabilize the environment behind the eastern outflow boundary, ahead of the squall line. Also, the observed low level jet may have provided an elevated source of unstable air just above the surface in the region apparently "contaminated" by the outflow. It is also possible that one outflow, likely the western one given the motion of the MCS, was stronger (colder/deeper) than the other, leading to sufficient mechanical forcing to sustain the

collision, the eastern and western outflows were also tested individually to see if they could generate similar structures without the enhanced lifting of the outflow collision. In both cases, the single 2 K outflows were inadequate triggers for intense convection (Fig. 4.8b,c). The western outflow generated no convection at all (Fig. 4.8b) and while the simulation using the eastern outflow did develop some weak, disorganized convection (Fig 4.9b), the maximum updraft was less than 2 m/s and these values were short-lived (Fig. 4.8c). This development along the eastern outflow boundary was likely due to a more favorable juxtaposition of the gust front and shear vector, leading to enhanced lifting as described by (Rotunno et al. 1988).

As was seen with the supercells generated from the LMN18 simulations, the LS mode appears largely to be the result of its environment. The LS structure was seen with both the outflow collision mechanism, as well as with the variety mechanisms tested with the TOP18nocap simulations suggesting that it resulted more from the environment than from the outflow collision. This indicates that, while observed in nature, the outflow collision was likely not of primary importance in mode determination. It does, however, appear to have played an important role in overcoming the cap present in the observed environment (TOP18). Neither of the single cold box perturbations tested produced sufficient lift to generate a long-lived storm, and similar results were seen when the various warm thermal perturbations were tested in this environment. Thus, the outflow collision may have a more fundamental importance on 30 March 2006 by providing sufficient forcing to overcome the cap and initiate storms which then evolved into the LS mode as a result of the TOP18 environment.

The third environment is that of the PS line that formed in west-central Kansas char-

storm. However, due to the lack of observations available for ultimate verification in eastern Kansas, these mechanisms ultimately fall beyond the scope of the simple initiation test being investigated in the current study.

acterized by dry air aloft and southerly mid-level winds largely parallel to the surface dryline. This environment was represented by the TSF sounding. The simulated convection begins as an isolated multicell (Fig. 4.10a) evolving upscale first into an MCS (Fig. 4.10b) and eventually into a TS linear MCS that reorients itself from north-south to northwest-southeast (Fig. 4.10c-d) . This reorientation is the result of convective development being favored on the downshear edge of the cold pool as suggested by Rotunno et al. (1988). While this rapid evolution toward TS structure was not observed in the actual case, it should be noted that similar reorientation was seen in the PS simulations of Parker (2007a). There is likely some feature present in nature, not represented by the idealized model, that prevents this reorientation from happening and allows the PS mode to persist. In this case this feature was likely the observed dryline, as the PS storm remained anchored just east of this feature, and oriented parallel to it throughout it's lifespan. This feature would likely inhibit the reorientation observed in the simulations, as this would have required convective development extending west of the dryline, where conditions were unfavorable. Thus in nature, the PS mode was maintained. This simulation was too simple to replicate the exact structure that was observed (PS), however it did generate long-lived linear convection with a strong cold pool (-10 K), that evolved toward the TS precipitation structure. This suggests that the environment wherein the PS squall line evolved, characterized by dry air aloft and line parallel mid and upper level winds, favors linear modes.

Once again, a battery of initiation tests were run, however this time only the 5-bubble and line thermal perturbations were used. The limited battery of initiation mechanisms were chosen in light of the linear mode generated from the single bubble simulation and the broad lack of sensitivity seen with the various warm bubble runs in the LMN18 environment. The ultimate mode that had evolved by the end of these sensitivity tests

was very similar to that observed in the single bubble control run. Both the 5-bubble and line thermal generated a squall line that ultimately oriented itself in a northwest-southeast direction (Fig. 4.11c,d). However, earlier in the simulations, through approximately 180 minutes, the linear trigger mechanisms, especially the line thermal, appear to create a more PS-like storm (Fig. 4.11a,b). This is likely because with the linear forcing mechanisms, a squall line is generated very soon after initiation, before the development of a strong (cold/deep) cold pool. As the cold pool strengthens with time, the reorientation and transition to TS structure takes place. This delay was likely not seen in the single bubble simulation, because the development of the linear mode did not occur until the cold pool had strengthened significantly, causing the line to develop along the downshear side of the cold pool and organize with TS precipitation structure. It is of note some of the simulations by Parker(2007a,b), which also used an initial warm line thermal, exhibited PS structures through approximately the first 3 hours of the simulation, after which a similar reorientation and transition to TS occurred. This difference in early evolution is important, as it suggests that the presence of a linear forcing mechanism can play a role in the initial mode of an MCS by supporting linear organization before the cold pool has fully intensified. Such an effect may have been present in the observed case, as the dryline provided such a linear forcing mechanism for the PS line throughout its lifetime.

The overall results of these simulations are two-fold. First, they reinforce the concept of three different environments generating three different modes on 30 March 2006, as was observed in the case study. Additionally, these results suggest that there was some dependence of convective mode on initiation mechanism, however this varied by environment. In the case of the supercell environment (LMN18), it would appear that environmental parameters favored supercells so strongly, that the mechanism that initiated storms mattered very little. The PS environment (TSF), appeared to be somewhat

sensitive to initiation mechanism early on, however eventually the favorable conditions for strong cold pool development predominated and, the mode evolved toward a TS line. Finally, the TOP18nocap environment demonstrated the strongest sensitivity to initiation mechanism, with the orientation of initial storms in with respect the vertical wind shear having a significant effect on storm evolution, similar to the results of Bluestein and Weisman (2000). It is likely that the moderate level of shear in this environment, which did not favor one particular mode, caused the simulated storms to be more sensitive to their initiating mechanism. Once the initial perturbations began steering the storms toward a particular mode, that mode was maintained, because there was no environmentally favored mode to evolve toward. These findings lend support to the importance of the outflow collision in the development of the LS line, as the lack of modal preference by the background environment in eastern Kansas would allow this linear forcing to play a larger role in mode selection. At the same time, the more limited effect of initiation mechanism on convective mode seen within the LMN18 and TOP18 environments helps to explain why both the supercells and PS line were able to be initiated by the same feature (the dryline).

4.1.3 Environmental Sensitivities

The results presented thus far, from both the observations as well as the idealized model simulations, point towards environmental differences being a key factor in the development of the different modes of convection. These differences were examined further by isolating the effects of the thermodynamic and vertical wind shear profiles of each environment and thus their effect on convective mode. To accomplish this, the wind profile from each sounding was paired with the thermodynamic environments from each of the other soundings, resulting in the the combinations reported in table 4.1. By doing

this it was possible to isolate the roles of various environmental features such as shear, moisture, and buoyancy in determining the observed modes. It should be noted that no efforts were made to balance the thermodynamic and shear profiles, and thus the individual profiles are possibly not indicative of what would be seen in nature. However, given that the goal of these simulations was to investigate the relative effects of shear vs. thermodynamic profile within the soundings observed, this omission is acceptable. For this series of simulations, the 200 km warm line thermal was used to initiate convection, as it both replicated the linear forcing seen in reality along the dryline and outflow collision, while also readily allowing isolated structures to evolve as seen in the sensitivities above. The results from simulations using the original environments (LMN18, TOP18 and TSF) initiated with the line thermal are included in figures 4.12a,e,i and 4.13a,e,i in order to provided a set of control simulations for comparison. The results of these simulations were very similar to the single bubble control simulations discussed in 4.1.2.

Among the thermodynamic environments, the TSF sounding appeared to be the least sensitive to different wind profiles. The control run using this environment generated a TS squall line (Fig. 4.13i), and the result when it was matched with either of the other wind profiles (TSF_LMN, TSF_TOP18) was very much the same. (Fig. 4.13f, c). This was most likely due to the presence of dry air aloft enhancing development of strong cold pools. These stronger cold pools can overwhelm the vertical shear, leading to slabular lifting and upshear tilting storms, as described by Rotunno et al. (1988) and more recently by James et al. (2006). This in turn favors the TS precipitation structure (Parker and Johnson 2004c). Simulations using the TSF thermodynamic sounding featured the strongest cold pools of the set of simulations, typically 3-5 K colder than the cold pools created with the other thermodynamic profiles. These stronger cold pools account for the trend towards upshear tilt and TS structure.

The simulations run using the LMN18 thermodynamic environment (LMN18, LMN_TSF, LMN_TOP18) all developed isolated supercells (Fig. 4.13a,d,g). While this was of little surprise given each of the wind profiles used also generated at least some supercell structures in within the TOP18nocap environment as well (Fig. 4.13b, e), a notable difference emerged related to the number of storms observed. In each case with LMN thermodynamics the ultimate mode to survive was a single isolated supercell, whereas when run with the TOP18nocap thermodynamic environment, the same wind profiles produced either several supercells or a supercells and multicell convection. As an example, comparing the LMN18 control run and the TOP18nocap_LMN simulation, the LMN18 control run resulted in a single isolated supercell (Fig. 4.13a) while the TOP18nocap_LMN simulation resulted in a group of several supercells (Fig. 4.13b). Comparing the early evolution of these simulations, it becomes apparent that a key difference is the longevity of the multicellular convection created along the initial line-thermal. In both cases, an initial line of convection initiates in response to the warm line thermal, and a supercell rapidly evolves at the southern end of this line (Fig. 4.14a,b). After this point the multicell convection in the LMN18 control run rapidly weakens and dissipates, leaving only the supercell for the duration of the simulation (Fig. 4.14c). However, in the TOP18nocap_LMN simulation, this multicellular convection is sustained (Fig. 4.14d), and eventually forms the basis for subsequent supercell development later in the simulation. This discrepancy is likely because the TOP18nocap contains more low level CAPE (196 J/kg vs 138 J/kg in the lowest 3 km) and moisture compared to the LMN18 thermodynamic sounding (Fig. 3.4a, b). This results in greater buoyancy-generated lifting in the TOP18nocap environment (Fig. 4.15b), which would allow the initial multicells to survive longer. At the same time, within the LMN18 thermodynamic environment the relative lack of low-level buoyancy (Fig. 4.15a) would cause the multicell storms to weaken, while the supercell that

develops could continue to sustain itself though lifting by its vertically directed pressure gradient force (Fig. 4.15c). Thus, the LMN18 thermodynamic environment is not so much favorable to supercells, as it is less favorable to other storm types that lack this strong vertically directed pressure gradient force to sustain themselves.

An examination of the wind profiles reveals that the LMN18 wind profile (LMN18, TSF_LMN, TOP18nocap_LMN) largely favored the development of isolated supercells. This was illustrated quite clearly with the LMN18 control run, where a long-lived isolated supercell formed (Fig. 4.13a), as well as in the TOP18nocap_LMN environment, where by the end of the six hour simulation the initial squall line had evolved into a line of four isolated supercells (Fig. 4.13f). The combination of the LMN18 wind profile and TSF thermodynamic profile (TSF_LMN) resulted in at least two isolated supercell structures (Fig. 4.12c) that persisted for upwards of two hours before becoming dominated by their cold pools and evolving into a TS squall line (Fig. 4.13c). In short, the shear present in the LMN18 wind profile was sufficient for supercell development, and likely a key factor in the development of the supercells in the observed case.

Although the TSF wind profile supported squall line development with its native thermodynamic profile, it tended to favor the supercell mode when coupled with thermodynamic profiles less favorable to cold pool development (LMN_TSF, TOP18nocap_TSF). When coupled with the LMN18 thermodynamic profile (LMN_TSF), the result was a single isolated supercell (Fig. 4.13g), very similar to what was seen in simulations with the LMN18 wind profile (Fig. 4.13a). This is not surprising given the similar 0-6 km bulk shear magnitudes present in each of these wind profiles (Fig. 3.5a, c). Combining it with the TOP18nocap thermodynamic sounding (TOP18nocap_TSF) created both supercells to the south and linear features farther north (Fig. 4.12h), that persisted throughout the run (Fig. 4.13h). The presence of supercells in the TSF wind profile environment is

in line with observations, as several of the initial cells that developed into the PS line in reality exhibited supercellular characteristics (Fig. 3.6a). This is not surprising, as the wind shear environments for supercells and PS squall lines are often very similar (Parker 2007a). Thus, the key to the development of the linear mode, at least in this case, was most likely the thermodynamic environment and its favorable conditions for strong cold pool development. Both the observations and these simulations verify that there was sufficient shear to generate isolated supercells, yet a linear mode was ultimately observed.

Finally, a finding that is of significant importance to this study was that the TOP18nocap thermodynamic profile did not predominate over any of the wind profiles it was paired with. Resultant storm structures appeared to vary with the wind profile, as isolated supercells emerged from the LMN18 wind profile (Fig. 4.13b) and a collection of supercells along with some more linear features developed from the TSF wind profile (Fig. 4.13h). Similarly, the TOP18 wind profile was not a strong discriminator between storm mode, as storm structures appeared to vary with the different thermodynamic environments. When paired with the LMN18 thermodynamic profile (LMN_TOP18) the result was a single, isolated supercell (Fig. 4.13d), while when paired with the TSF thermodynamic profile (TSF_TOP18), a large TS squall line developed (Fig. 4.13f). Overall, the thermodynamic and kinematic features of the TOP18 environment did not strongly select for any one mode in the idealized tests. This lack of selection lends further credence to the idea that this environment was important in accommodating multiple modes of convection on 30 March 2006, as it appears to be supportive of a variety of modes.

4.1.4 Near-Storm Modifications to Environment

Thus far, the focus of this study has centered on meso-beta and meso-alpha scale details of the environment, largely concerned with how the background environment was effecting the development and evolution of the convective mode. However, upon their development, convective storms can modify their local environment, and a question that emerged during the course of this study was how much of an effect these storms might have on their environment and what that might mean to their convective mode. The moderate shear environment found in eastern Kansas would seemingly lend itself well to being modified by the storms, as the aforementioned sensitivity tests demonstrated no real modal preference from this environment. Thus, it would appear to provide a "clean slate" that the various storms could then locally modify to best sustain themselves, leading to all three modes sustaining themselves within the same environment. While the subject of near-storm environmental modification could well provide the basis for an entire research project in and of itself, a preliminary examination of the present numerical simulations can at least begin to shed some light on the importance of the effects that a storm has on its environment. Given the preliminary nature of this portion of the study, the focus will be on how storms modify their nearby environment and how that feeds back to the original storm. Other avenues, such as how the storms may modify the environments of neighboring storms will be left for future work.

In order to examine how a storm may modify its local environment, the output from each of the single-bubble control runs described previously in section 4.1.2 was used to create near-storm soundings at points just ahead of the various storms, in the storm inflow region. The region ahead of the storms was selected as the interest was in determining how the storms might be modifying the environment they were moving into or receiving inflow from, as this would seemingly be the environment having the strongest effect on

their mode. These soundings were then compared to the initial base-state soundings to determine how, if at all, the storms had changed the environment. While this method worked well to initially determine that the storms were indeed having an effect on their local environment, it was limiting in that the changes being seen were indicative of conditions at a single point only, and it was of interest to determine the areal extent of the storm-induced environmental changes. Thus the 0-6 km wind shear, a parameter that both appeared to be affected significantly by the presence of the storms, and was important in determining mode, was calculated and plotted across the entire model domain. This provided a simple and effective means of determining which areas near the storm location were being affected the most by the presence of the storm, and how they were being affected.

The most significant changes to the near storm environment were seen ahead of supercell storms, in the region of strongest inflow near the hook echo (Fig. 4.16a-d). In the LMN18 run, the 0-6 km shear increased by over 27 m/s by the end of the 6 hour simulation, although the areal extent of this maximum increase was rather small (Fig. 4.16d). A similar increase in shear was seen early-on in the supercell that was generated in the TOP18 simulation (Fig. 4.17a). However, as time progressed and the supercell began to merge with the LS squall line that developed, the shear decreased again, never reaching the maximum seen in the LMN18 run (Fig. 4.17b-d). In both cases, though, behind the gust front, within the storms' cold pools, shear tended to decrease from the initial values present in the base state, and remained lower for the duration of the simulations.

There was little discernible pattern to the changes in shear along the LS squall line. There was a general decrease in shear ahead of the northern portion of the line, and a general increase ahead of the southern portion, however pockets of increasing and decreasing shear along the line precluded any true pattern from emerging (Fig. 4.17a-

d). As with the supercells, shear generally decreased behind the gust front. The TS line featured a fairly well developed couplet of increasing shear ahead of the line and decreasing shear behind the line, with the shear decreases being larger in magnitude than the increases (Fig. 4.18a-d). This pattern became increasingly pronounced towards the end of the six-hour simulation as the squall line became more developed (Fig. 4.18d). The magnitude of the shear increases were generally smaller than those seen in the other two runs, while the decreases were significantly larger than those seen in previous runs. This decrease was likely due to the development of the descending rear inflow jet, which is a characteristic of TS squall lines (Fig. 2.5). This feature results in an increase in wind speed near the surface behind the gust front, which would in turn decrease the vertical shear as the 0 and 6 km wind vectors would be closer in magnitude.

Thus it is clear that, at least within the idealized simulations, storms have a pronounced effect on the shear structure in their immediate environment, especially in the case of supercell storms. Given the demonstrated relationship between wind shear and convective mode, this finding would imply that a storm that organizes as a given mode can possibly aid in the maintenance of that mode through modification of its local environment. Further investigation is needed, though, to determine how these storms are modifying their local shear profiles, and also to determine what affect these modifications ultimately have on storm mode. Is the storm's modification to the local environment significant enough to effect its mode, or is this modification rather just an indication that the storm is present and perturbing the surrounding environment? These experiments make it clear that the initial mode selection is strongly dependent on the background environment. Therefore, even if a storm modifies its local environment in a self-sustaining manner, the larger scale environment still needs to be at least somewhat supportive of that initial given mode. In this sense, the concept of the moderate-shear "middle ground"

environment may still be important, as it provides a neutral environment that the individual storms can then modify to be more favorable for their given modes.

4.2 Real Data Simulation

4.2.1 Case Study Model Configuration

The case study simulation utilized the WRF-ARW version 2.2 in order to take advantage of the newer WRF Pre-processing System (WPS). The simulation of the 30 March 2006 case utilized initial conditions from the North American Regional Reanalysis (NARR) and consisted of a 1750 x 1750 km outer domain with 5 km grid spacing, and a 850 x 790 km inner nest with a 1 km grid spacing (Fig. 4.19). Both domains had 30 vertical levels, with grid spacings stretching from 66 m near the surface to 735 m at the model top, with an average spacing of 545 m. The moving nest option was used so that, starting 3 hours into the simulation, the inner nest was shifted eastward by 1 grid box (5 km) every 15 minutes in order to keep the majority of the convection near the center of the domain. Both domains used the Lin et al. (1983) microphysics scheme, the RUC land-surface model, the YSU planetary boundary layer scheme, RRTM longwave and MM5 (Dudhia) shortwave radiation schemes (for details regarding the various physics schemes please see Skamarock et. al (2005)). Given the small grid spacings, convective processes were simulated explicitly rather than with a convective parameterization scheme. The model was integrated for 15 hours, beginning at 15 UTC 30 March (just before convection was initiated in reality) and running through 06 UTC 31 March. It should be noted that a variety of other model configurations were tested as well, and this setup provided a solution that was the closest to the observed case.

4.2.2 Case Study Simulation Results

The case study simulation showed some early promise as far as capturing the 30 March 2006 event. The simulation developed structures resembling the supercells and PS in approximately the correct locations by 2000 UTC (Fig. 4.20a-b). While the timing was off a little, as this was 2-3 hours after the observed storms developed, and in reality the supercells developed before the PS line (the opposite occurred in the model), this initial development was rather encouraging. The effectiveness of the simulation went downhill after 2000 UTC, though, as the model prematurely develops a leading stratiform structure in eastern Kansas that also appears to be too intense (Fig. 4.20b-c). In addition to the eastward moving LS structure, similar to what was observed, a less-physical looking structure developed and moved westward from this LS line, appearing to progress on the western edge of the surface outflow as it spread out (Fig. 4.20b-c). This westward-moving feature would be the undoing of the supercells and PS line, as both of these modes interacted with it to form a broad line of convection extending from eastern Kansas south through central Oklahoma (Fig. 4.20d). Thus while the simulation suggests some initial skill at being able to develop the three modes of convection in approximately the correct locations, it falls down with regards to the evolution of all three, never really replicating the three modes in close proximity seen in the observed case 1.1.

The fact that the simulation did manage to capture the initial development of all three modes within their respective environments is encouraging, though. It suggests that the rather course (30 km grid spacing) NARR data was sufficient to capture some of the key environmental features necessary to develop the three different modes, and it further solidifies the connection between the three environments and three modes. However, the apparent premature and overly intense development of the LS line in eastern Kansas appears to have a significantly detrimental effect on the evolution of the event, resulting

in limited utility of the simulation during the period of greatest interest, when all three modes were evolving across eastern Kansas.

The case study simulation succeeded in capturing the PS squall line and supercells present in the real case (Fig. 4.20a, b), however the structures and evolution of these modes left much to be desired. Overall, the evolution of the system was not captured very well, as the three modes present in the observe case never materialized together at the same time. While the initial PS line and supercells in figure 4.20b appear to initiate in approximately the correct locations, their subsequent evolution is far from what was observed. Instead of the supercells remaining isolated and moving northeastward into Kansas while the PS line remains an independent entity farther to the west, in the simulation the two modes appear to merge The development of spurious convection over eastern Oklahoma and Kansas resulted in the supercells and PS system evolving into one large squall line across eastern Kansas and Oklahoma rather than remaining as separate entities, and the LS system never materialized (Fig. 4.20c, d). The usefulness of this simulation is rather limited as it does not represent the system during the period of greatest interest wherein all three modes were present over eastern Kansas. However, while this simulation lacks much utility as a tool for analyzing the case at hand, it does serve to illustrate the inherent difficulty that lies in forecasting these types of events, both for forecasters and for a high-resolution numerical model. None of the various model configurations tested were able to correctly simulate the diversity of storm types that occurred.

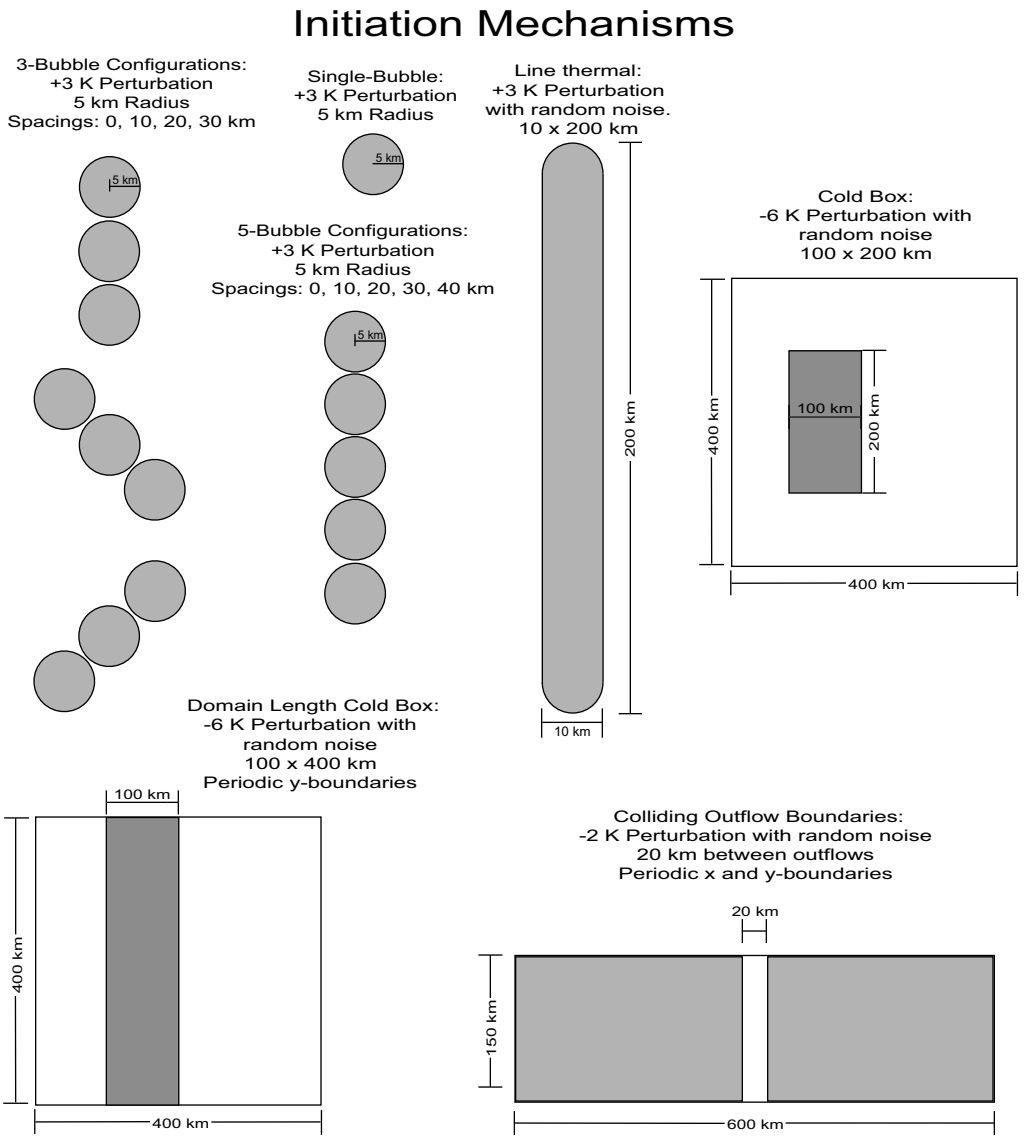

Figure 4.1: Schematics of the various initiation mechanisms employed in the idealized model simulations. Note that while not shown, spacings of 0, 10, 20, 30 and 40 km were used between the bubbles within lines, and that both the line thermal and cold boxes contained random noise in order to help stimulate 3-dimensional structures.

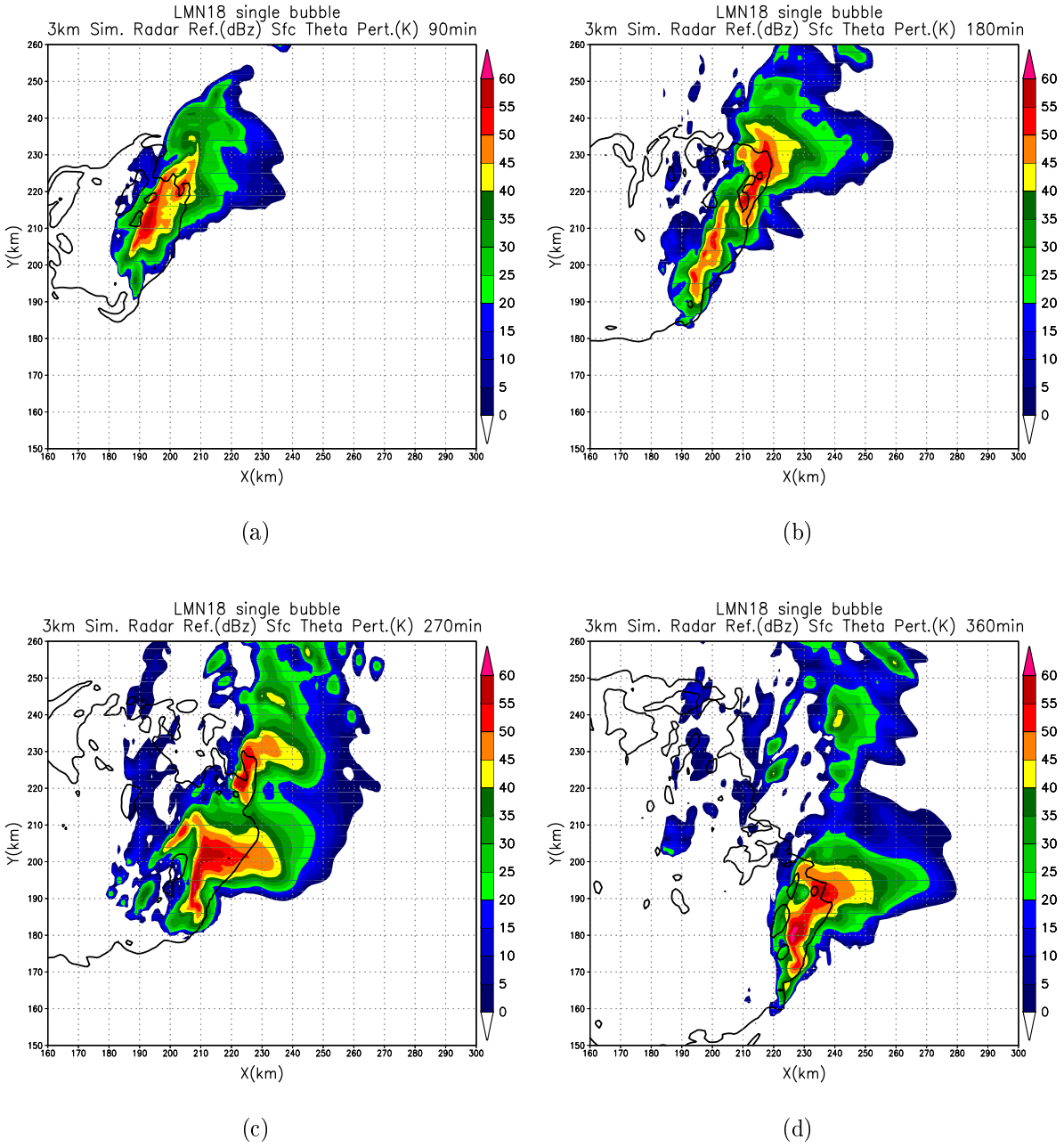

Figure 4.2: Evolution of convection triggered using a single warm bubble in the LMN18 environment. Fields displayed are simulated radar reflectivity at 3 km (shaded) and the edge of the surface cold pool, denoted by the -1 K surface potential temperature perturbation (heavy contour) at 90, 180, 270 and 360 minutes into the simulation. Note: only a portion of the domain is shown in order to highlight the storm details.

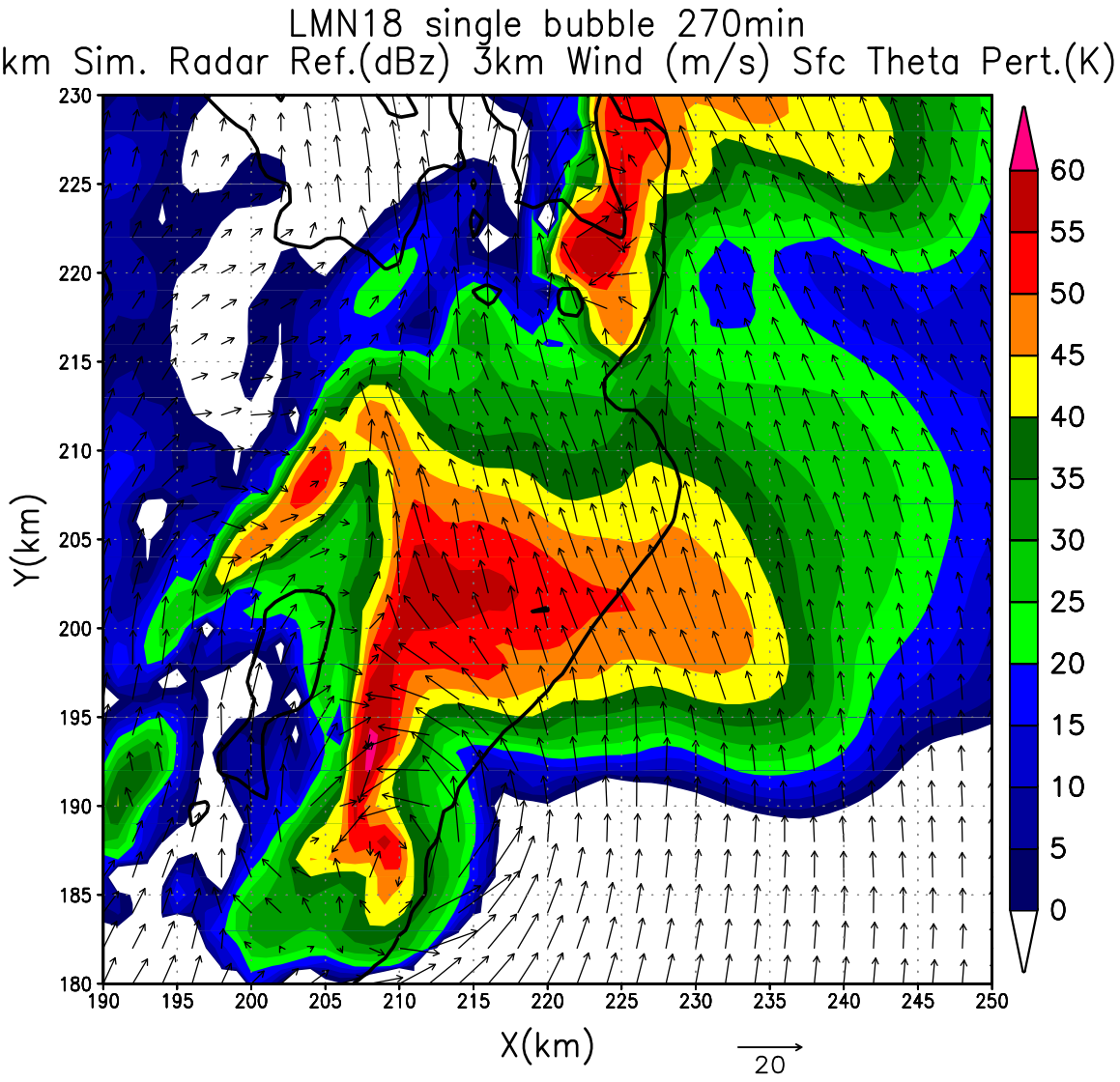

Figure 4.3: Simulated radar reflectivity at 3 km, -1 K surface theta perturbation, and 3km wind vectors for LMN18 single bubble simulation at 270 minutes.

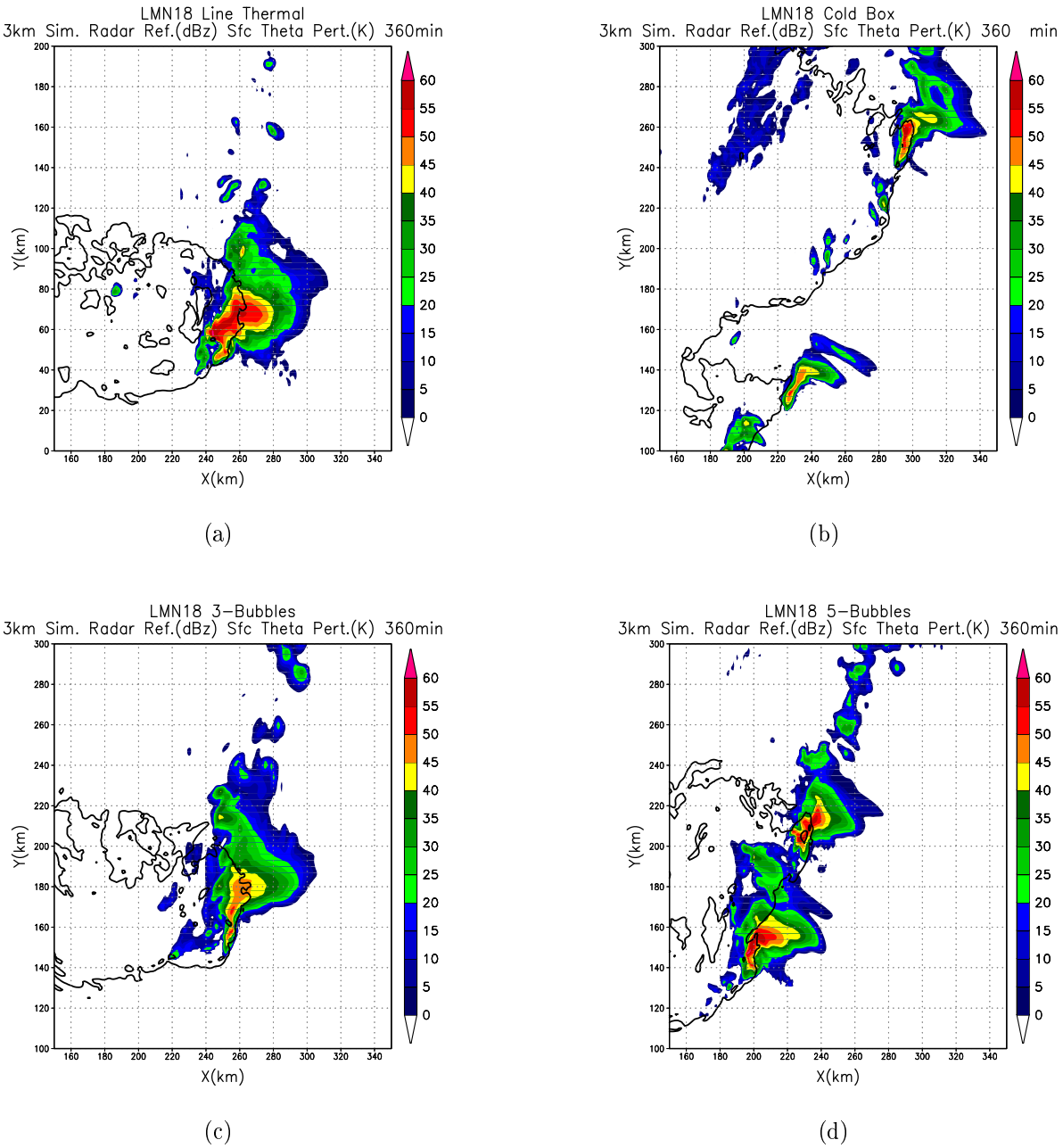

Figure 4.4: Simulated radar reflectivity at 3 km and edge of surface cold pool denoted by -1 K potential temperature perturbation at 360 minutes for the initiation tests run with the LMN18 sounding. a) initiation with a northwest-southeast line of 3 bubbles spaced 20 km apart, b) initiation with a north-south line of 5 bubbles spaced 20 km apart, c) initiation with a 200km long north-south line thermal, and d) initiation with a 200 x 300 km 1.5 km deep cold box. Note: the X and Y scales vary among the sub figures.

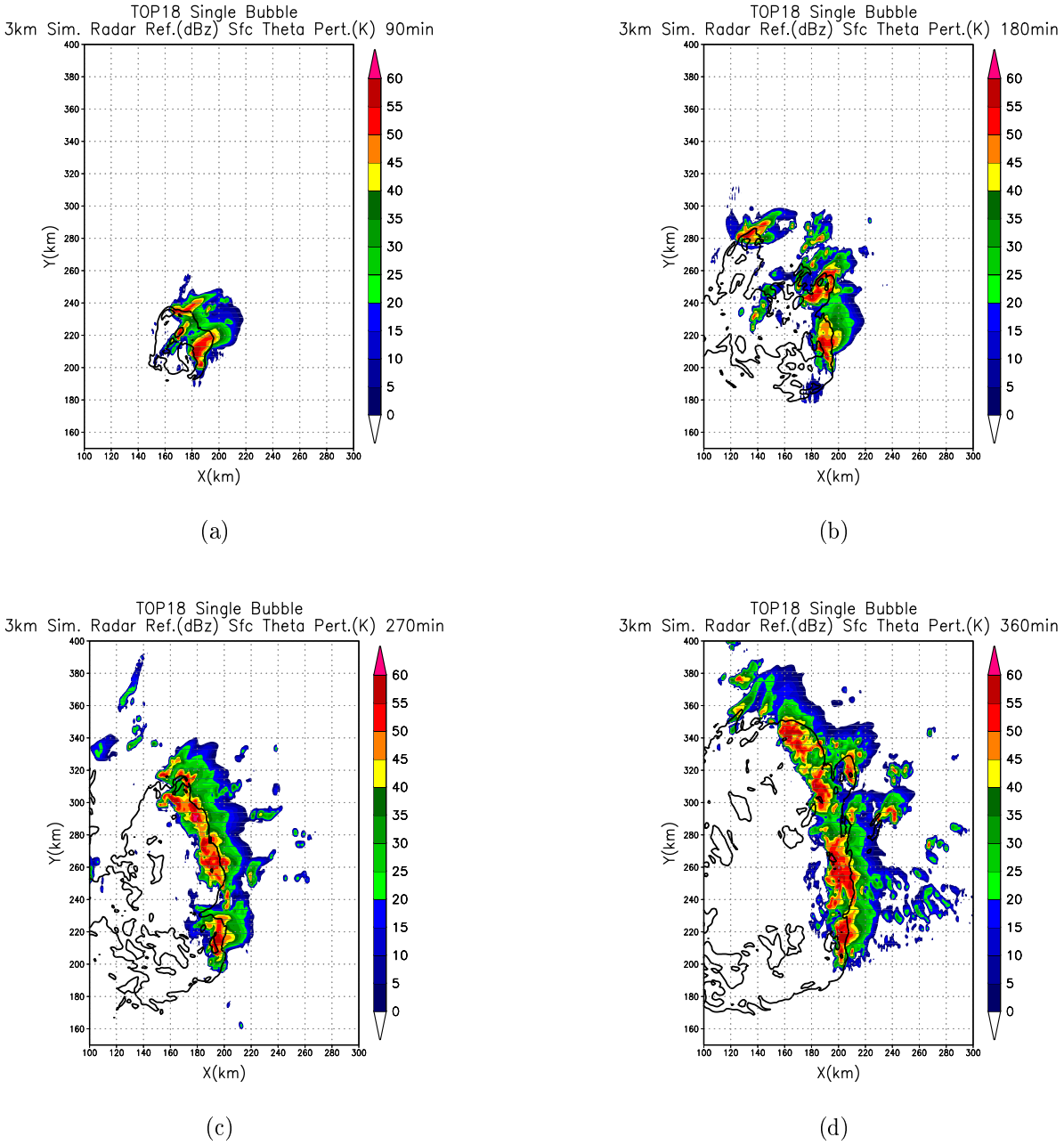

(a) (b)

(c) (d)

Figure 4.5: Evolution of convection triggered using a single warm bubble in the TOP18nocap environment. Fields displayed are simulated radar reflectivity at 3 km (shaded) and the edge of the surface cold pool, denoted by the -1 K surface potential temperature perturbation (heavy contour) at 90, 180, 270 and 360 minutes into the simulation. Note: only a portion of the domain is shown in order to highlight the storm details.

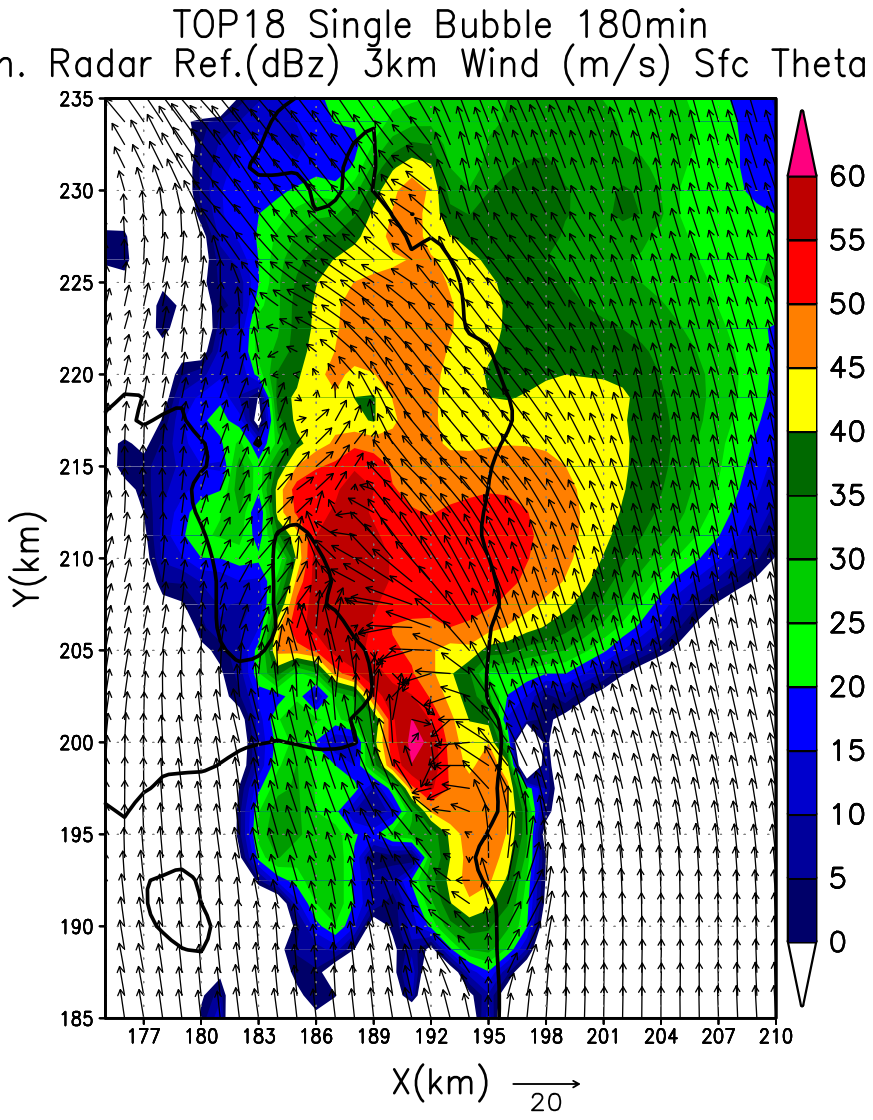

Figure 4.6: Simulated radar reflectivity at 3 km, -1 K surface theta perturbation, and 3km wind vectors for TOP18 single bubble simulation at 270 minutes.

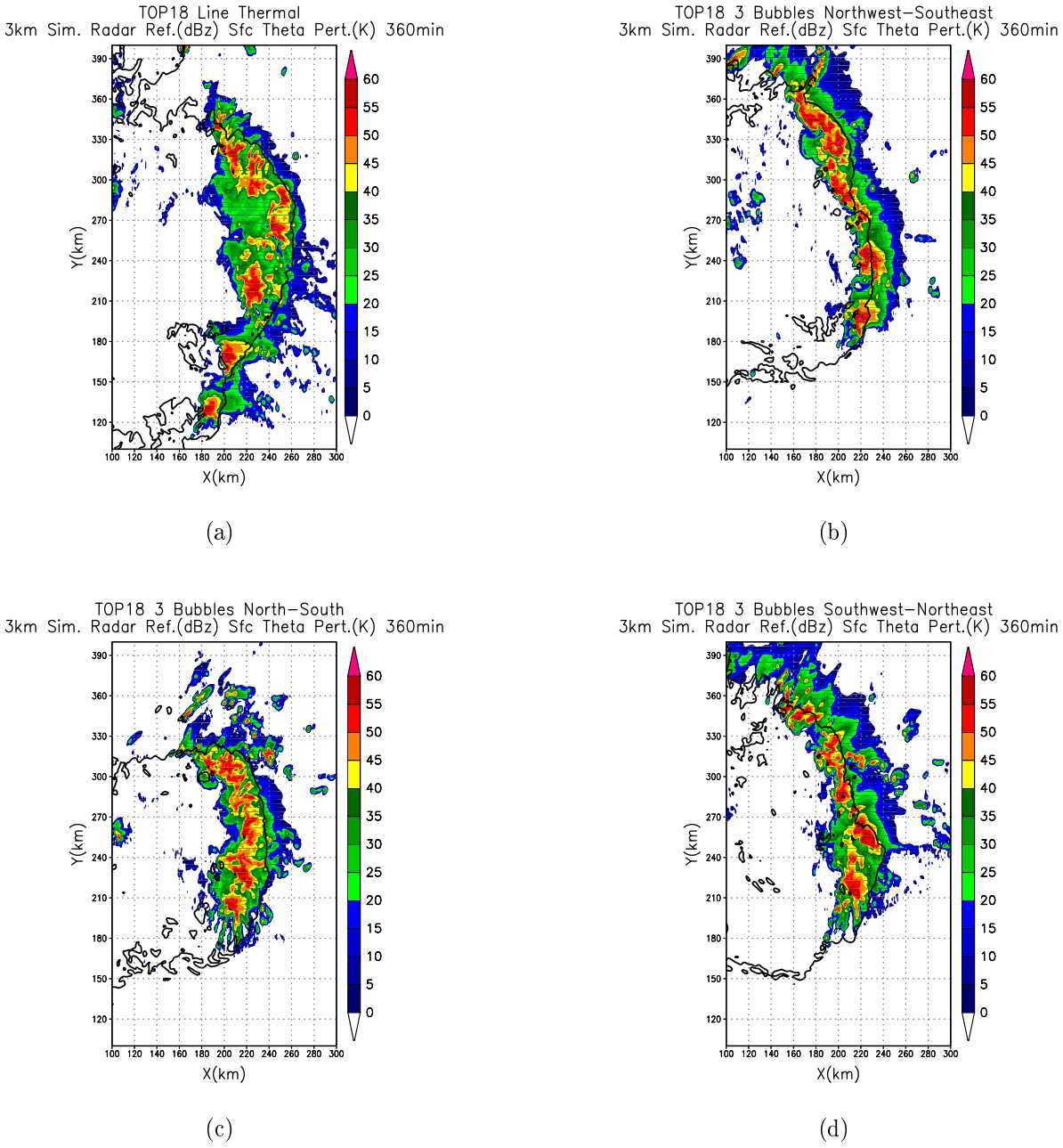

Figure 4.7: Simulated radar reflectivity at 3 km and surface cold pool denoted by -1 K potential temperature perturbation line for TOP18nocap environment: a) initiated with 200 km line thermal, 3 hours into the simulation. b) initiated with 3 warm bubbles spaced 20 km apart oriented northwest-southeast, 3 hours into the simulation. c) same as (b), but oriented north-south d) same as (b), but oriented southwest-northeast. Note: only a portion of the simulation domain is shown in order to focus on the details of the storm.

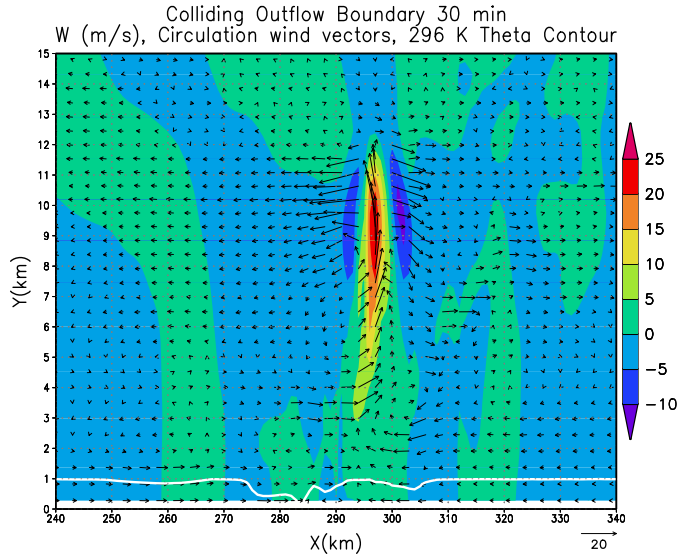

(a)

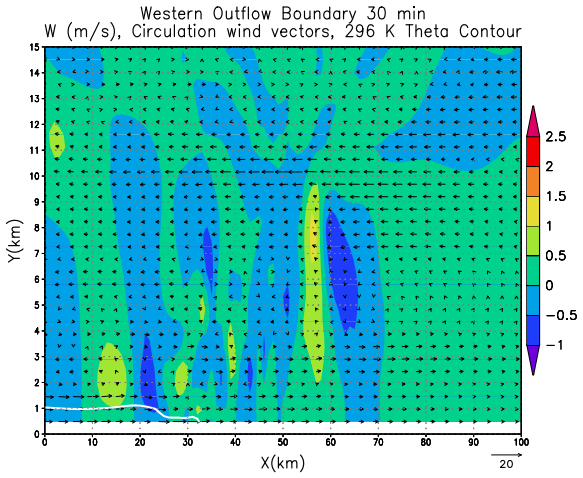

(b)

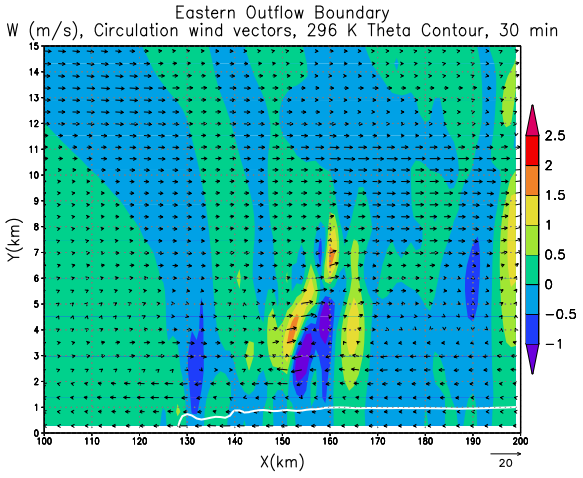

(c)

Figure 4.8: Plots of w (shaded, m/s), circulation wind vectors consisting of the u' and w components of the wind and the 296 K theta contour representing the surface cold pool at 30 minutes for a) colliding outflow boundary simulation, b) western outflow boundary simulation c) eastern outflow boundary simulation. Note: shading scale on (b) and (c) is 10% of that in (a)

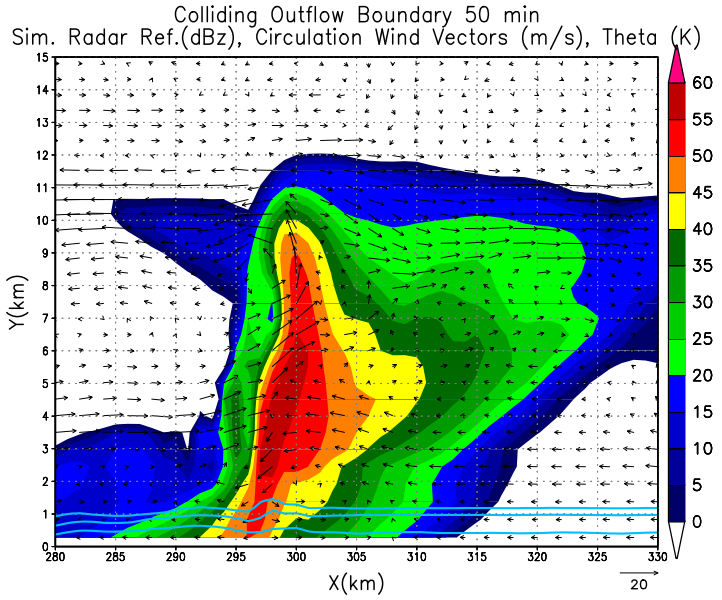

(a)

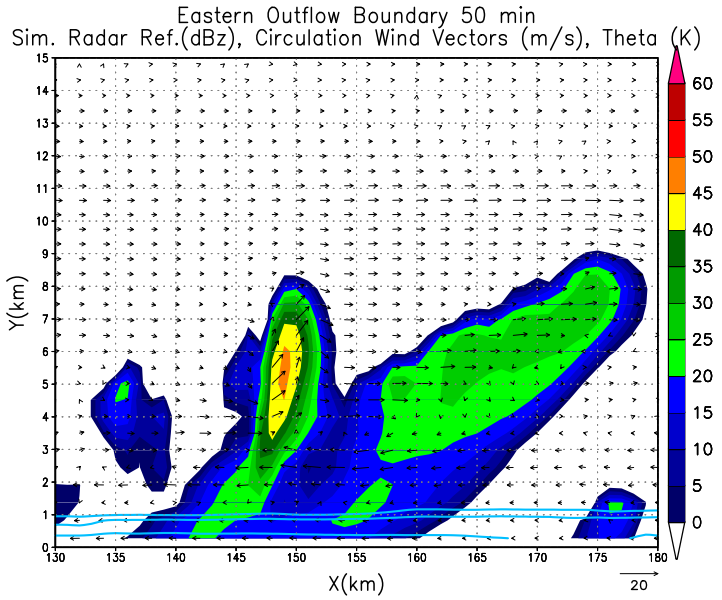

(b)

Figure 4.9: Cross-sections of simulated radar reflectivity (dbz) circulation wind vectors, and theta contoured at 295, 296 and 297 K (to denote the cold pool) at 50 minutes for a) colliding outflow boundary simulation and b) the eastern outflow boundary simulation.

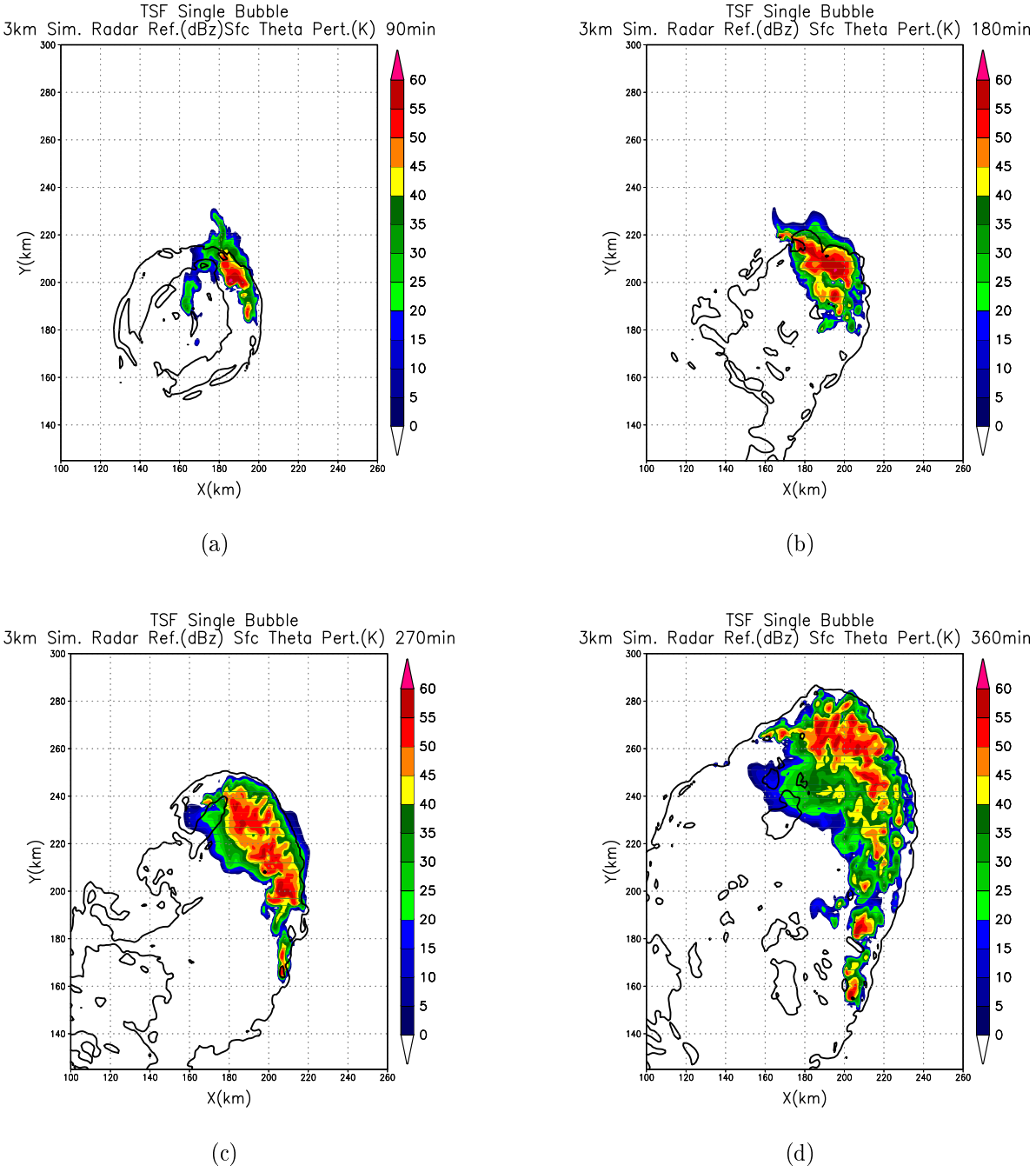

(a) (b)

(c) (d)

Figure 4.10: Evolution of convection triggered using a single warm bubble in the TSF environment. Fields displayed are simulated radar reflectivity at 3 km (shaded) and the edge of the surface cold pool, denoted by the -1 K surface potential temperature perturbation (heavy contour) at 90, 180, 270 and 360 minutes into the simulation. Note: only a portion of the domain is shown in order to highlight the storm details.

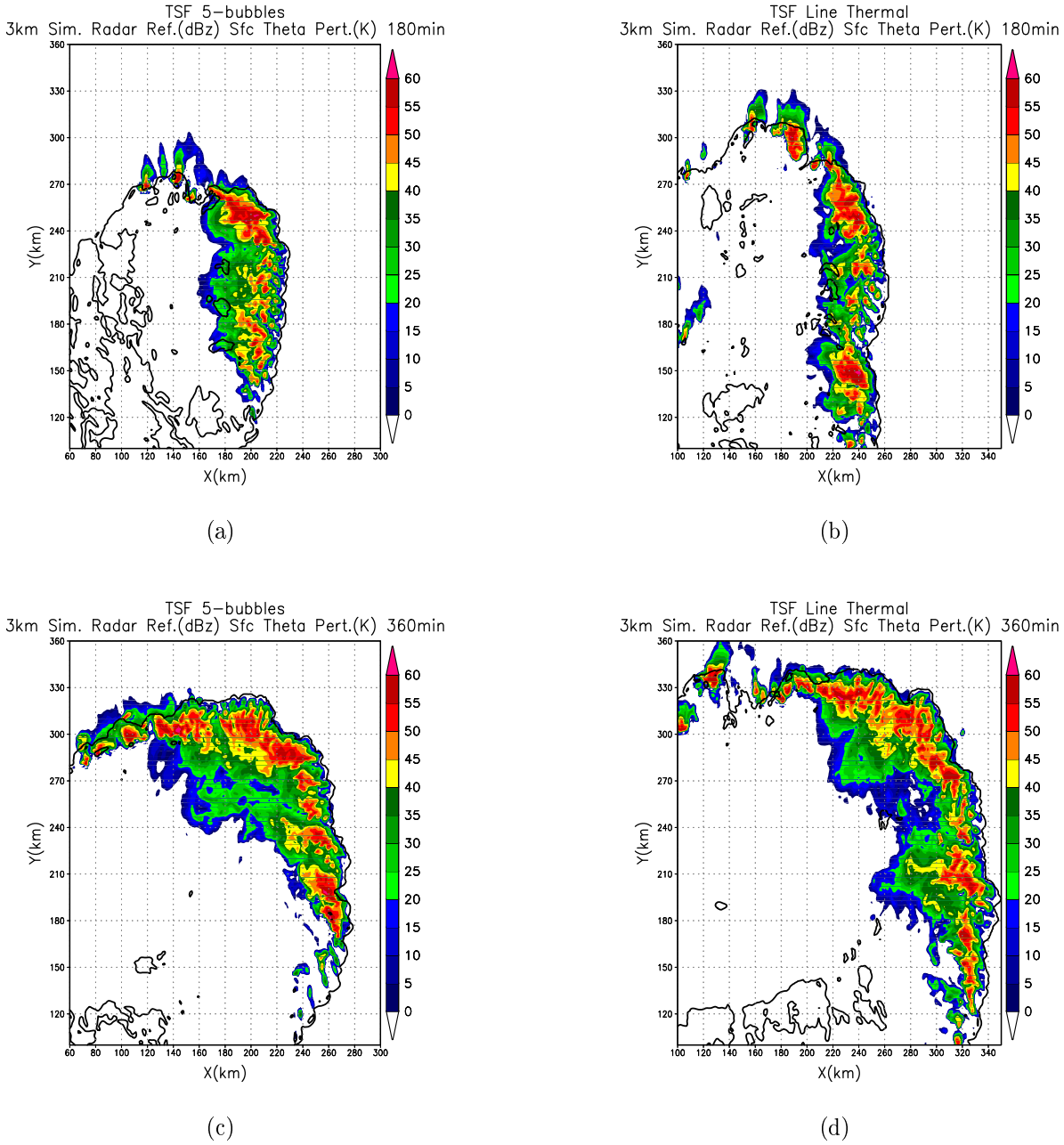

Figure 4.11: Simulated radar reflectivity at 3 km and surface cold pool denoted by -1 K potential temperature perturbation line for TSF environment: a) initiated with 5 bubbles spaced 20 km apart, 3 hours into the simulation. b) initiated with a 200 km line thermal, 3 hours into the simulation. c) same as (a) 6 hours into the simulation. d) same as (b) 6 hours into the simulation. Note: only a portion of the simulation domain is shown in order to focus on the details of the storm.

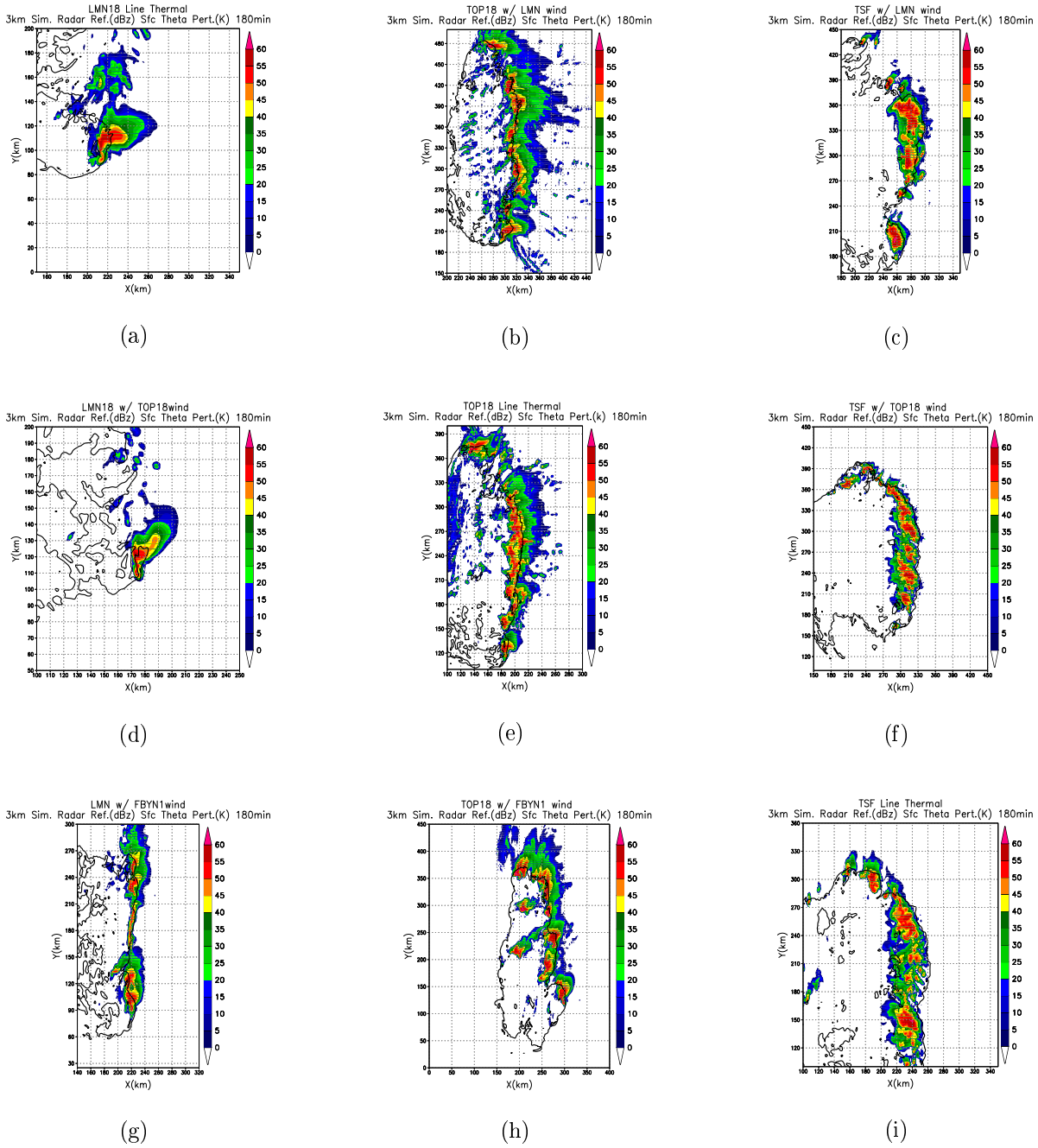

Figure 4.12: Simulated radar reflectivity at 3 km and surface cold pool denoted by -1 K potential temperature perturbation contour for environmental sensitivity runs at 180 minutes. a) LMN_TSF. b) LMN18_TOP18. c) TOP18nocap _TSF. d) TOP18nocap_LMN18. e) TSF_LMN18. f) TSF_TOP18. Note that the thermodynamic profiles are constant horizontally, while the wind profiles are constant vertically.

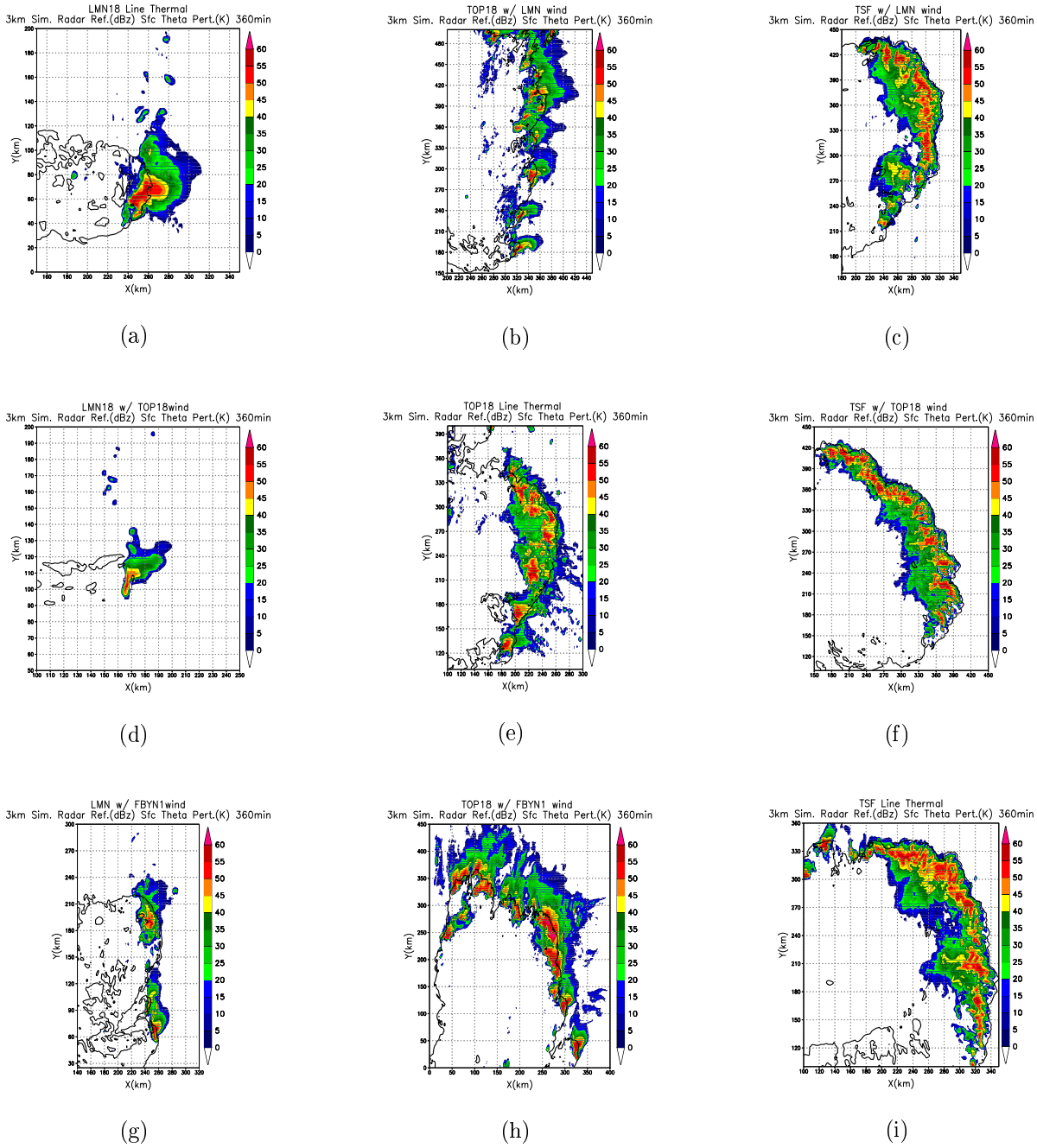

Figure 4.13: Simulated radar reflectivity at 3 km and surface cold pool denoted by -1 K potential temperature perturbation contour for environmental sensitivity runs at 360 minutes. a) LMN_TSF. b) LMN18_TOP18. c) TOP18nocap _TSF. d) TOP18nocap_LMN18. e) TSF_LMN18. f) TSF_TOP18. Note that the thermodynamic profiles are constant horizontally, while the wind profiles are constant vertically.

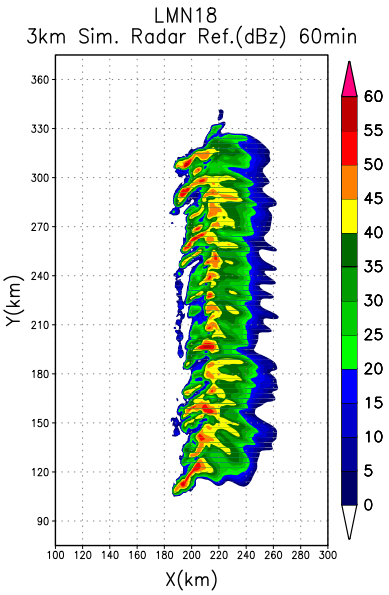

(a)

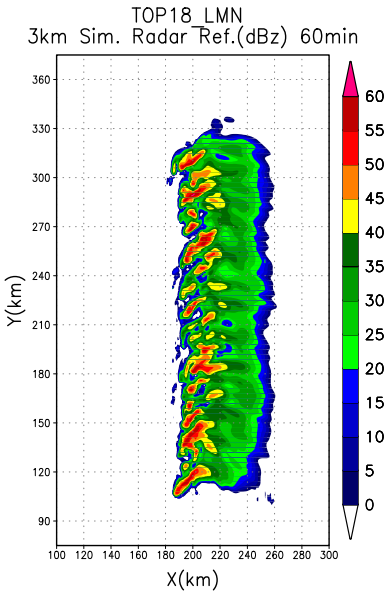

(b)

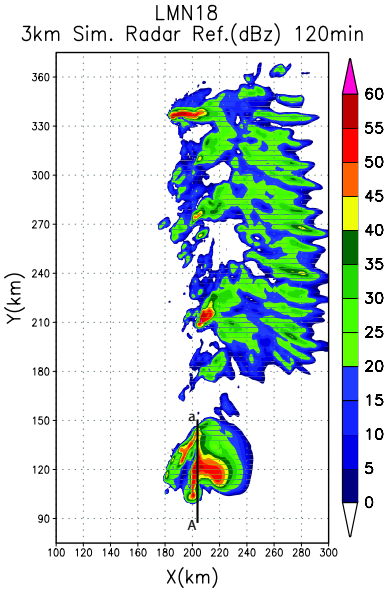

(c)

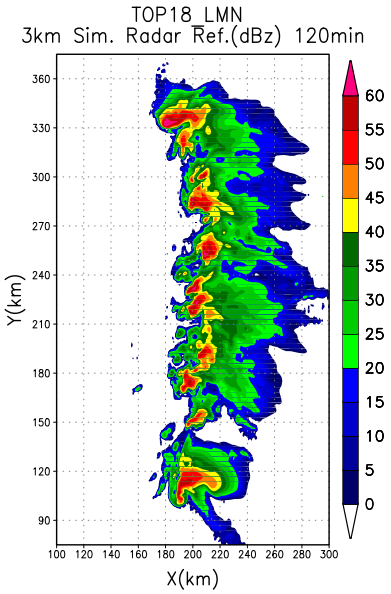

(d)

Figure 4.14: Simulated radar reflectivity at 3 km for a) LMN18 initiated with a 200 km line thermal, 60 minutes into the simulation, b) TOP18 initiated with a 200km line thermal, 60 minutes into the simulation, c) same as (a) at 120 minutes, and d) same as (b) at 120 minutes.

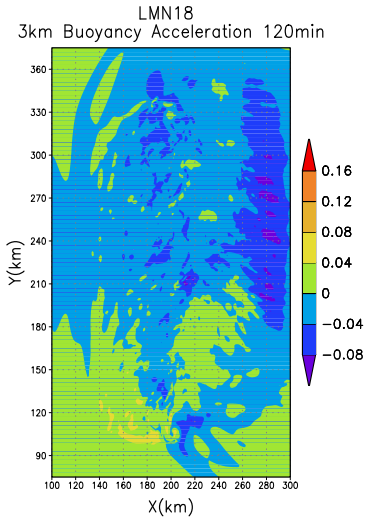

(a)

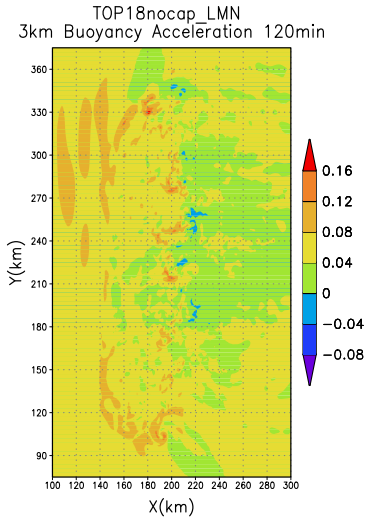

(b)

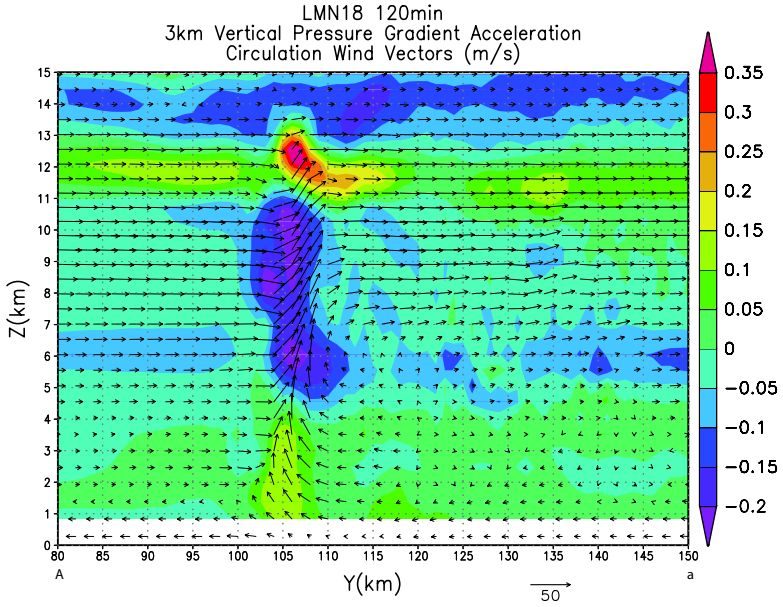

(c)

Figure 4.15: Plots of buoyancy acceleration (m/s) at 3 km 120 minutes into the simulation for a) LMN18 and b) TOP18nocap_LMN runs described in figure 4.14. Note: That the domain and time of (a) and (b) correspond with figure 4.14c and d respectively. c) is a plot of the acceleration due to the vertical pressure gradient (shaded, m/s^2) and circulation wind vectors consisting of the v and w wind components for the LMN18 simulation. The cross section is taken along the line A—a in figure 4.14.

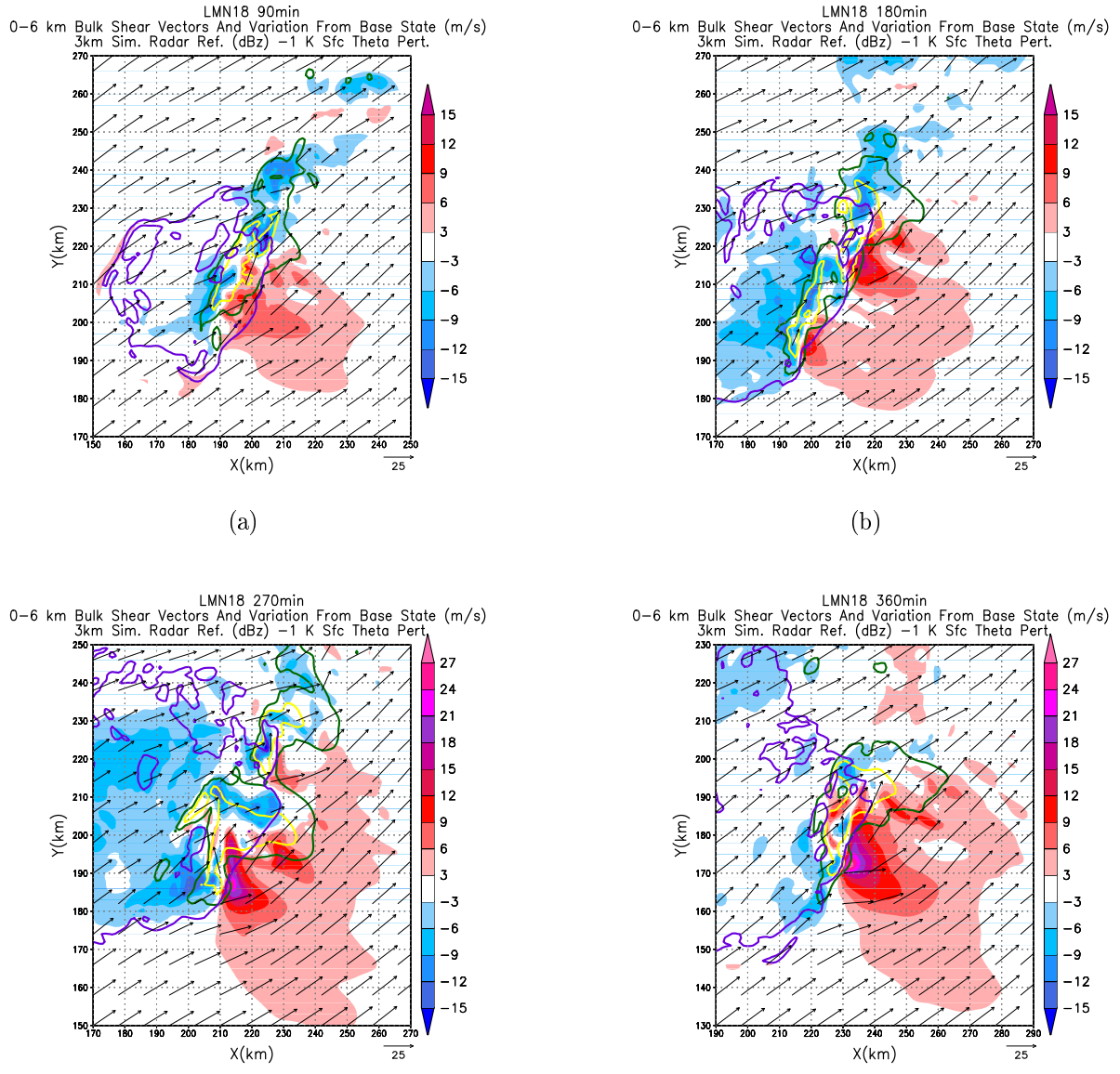

(a) (b)

(c) (d)

Figure 4.16: Plots showing the change in 0-6 km vertical wind shear from the base state in the LMN18 single bubble simulation at a) 90 minutes, b)180 minutes, c) 270 minutes and d) 360 minutes. Shading denotes the difference in 0-6 km shear, red shading indicating an increase in shear and blue shading a decrease in shear, compared to the base-state sounding. Wind vectors represent the 0-6 km bulk shear vector, the purple contour outlines the -1 K surface theta perturbation, representing the cold pool, and the green and yellow contours denote the 30 and 45 dbz simulated radar reflectivity to indicate the location of the storm.

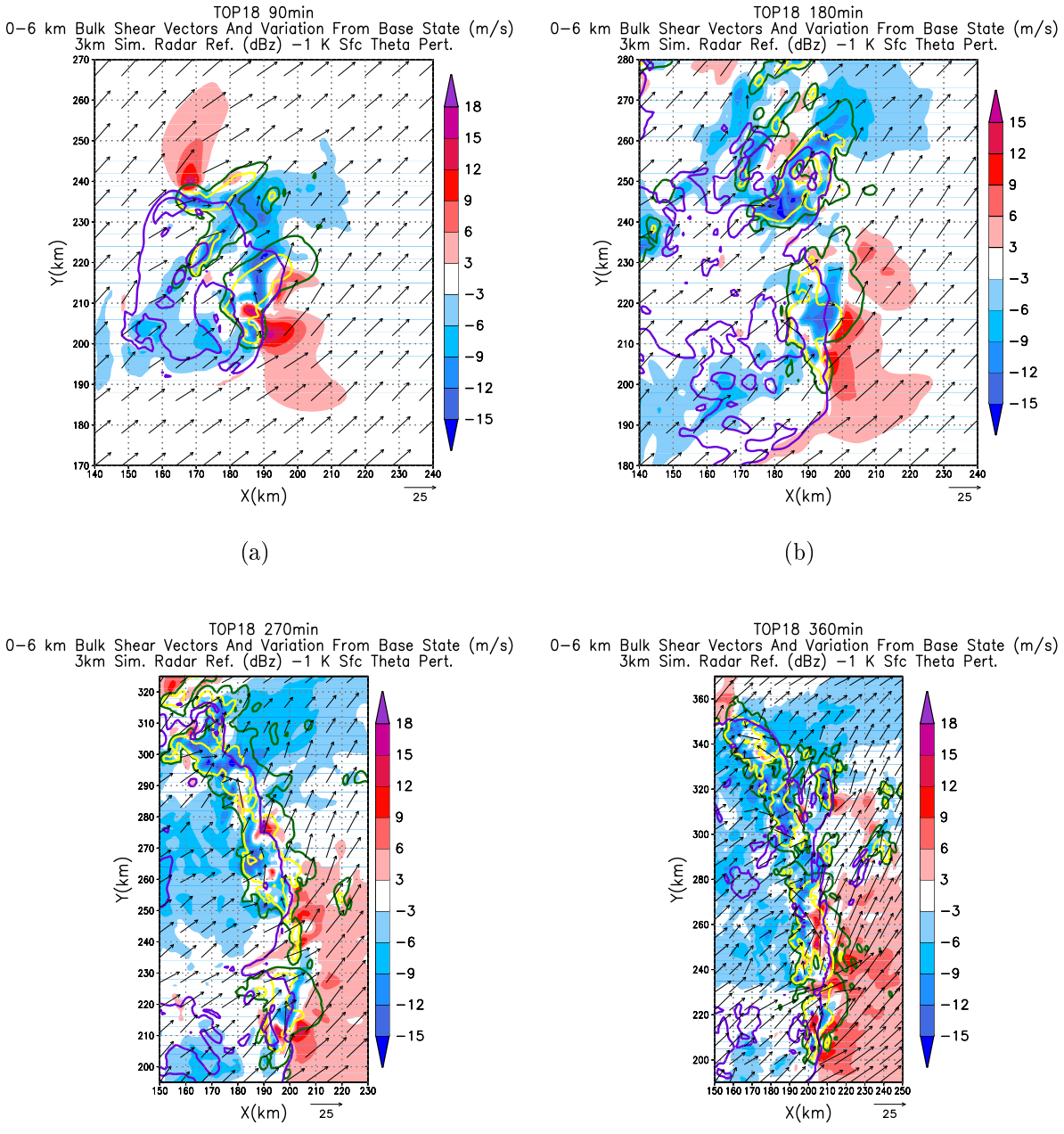

Figure 4.17: Same as 4.16, but for TOP18nocap single bubble control simulation.

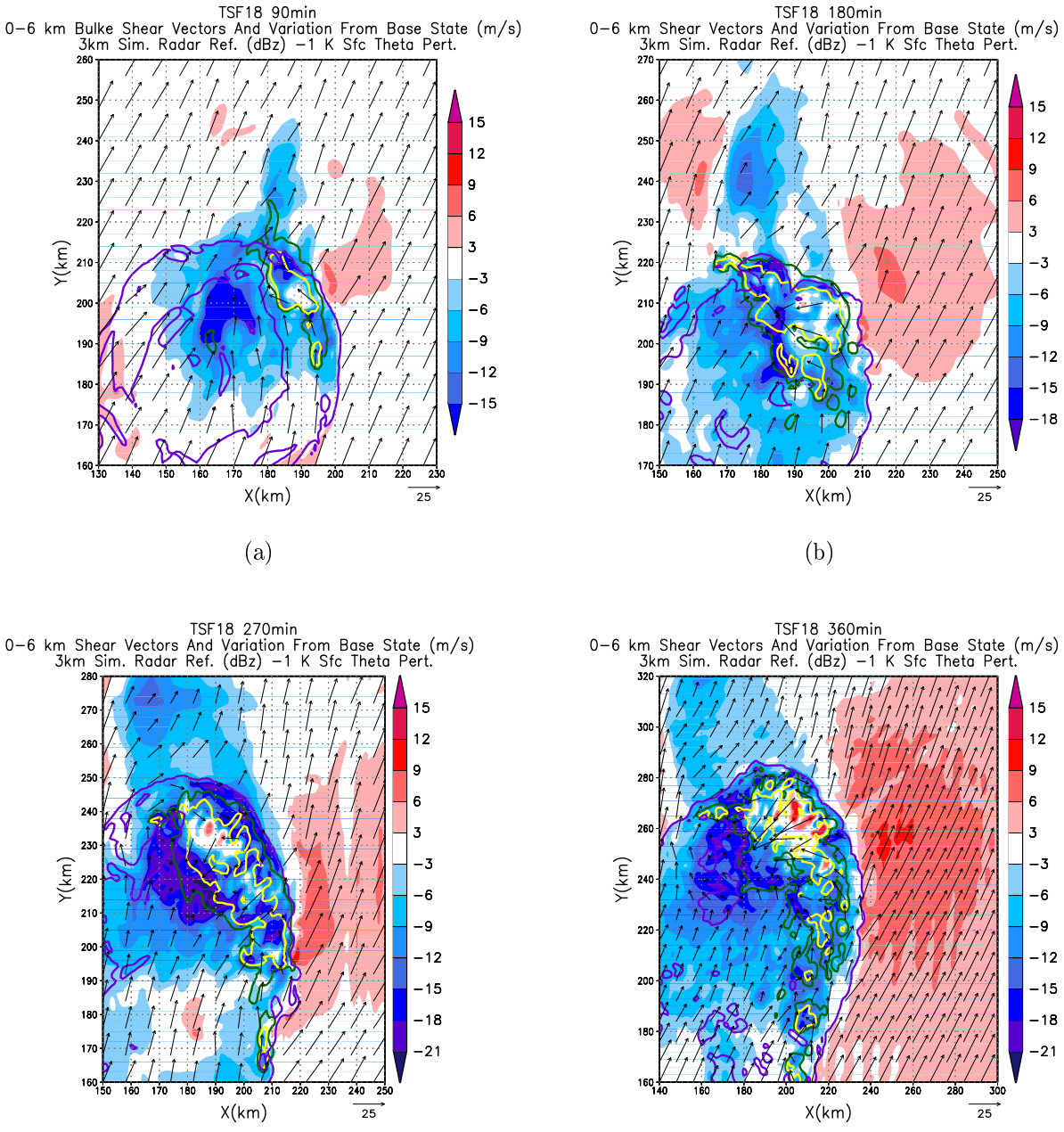

Figure 4.18: Same as figure4.16, but for TSF single bubble control simulation.

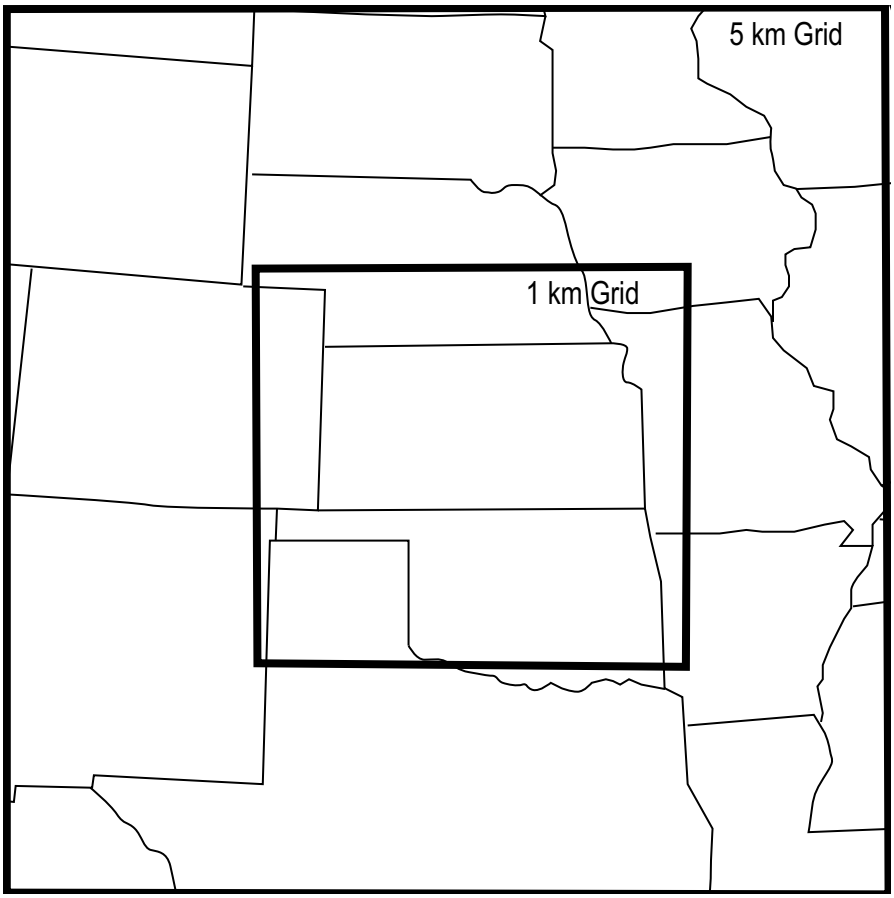

Figure 4.19: Nested domains for case study simulation.

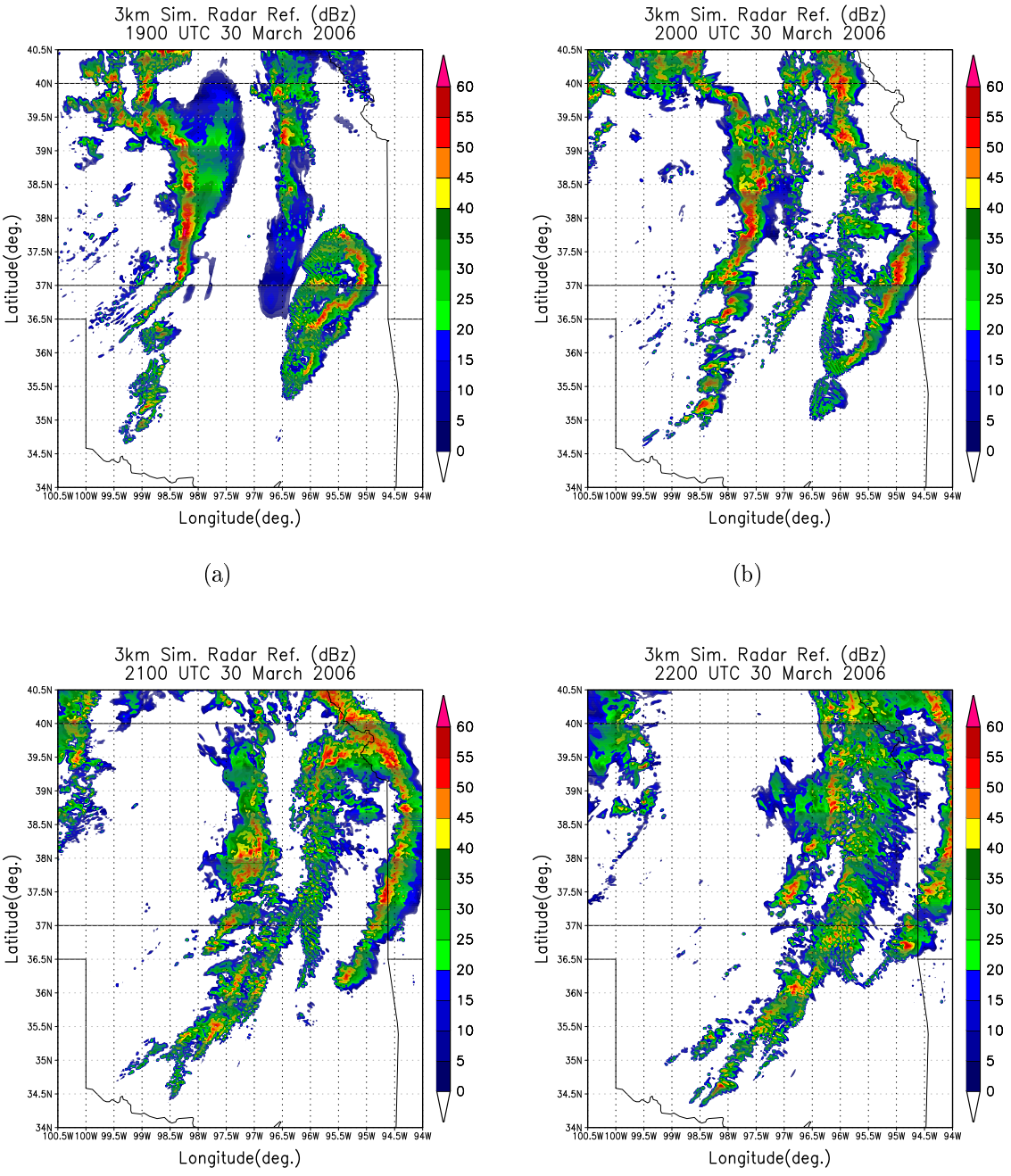

Figure 4.20: Simulated radar reflectivity at 3 km from the inner (1 km grid spacing) domain of the case study WRF simulation at a) 1900 UTC, b) 2000 UTC, c) 2100 UTC, d) 2200 UTC.

Table 4.1: Description of various environmental sounding combinations, describing the thermodynamic sounding and wind profile that were used in each sensitivity test, along with the simulated convective mode that was observed at the end of the 6 hour WRF simulation. Times refer to 30 March, 2006 unless otherwise noted. Naming convention for the simulations consists of "thermodynamic profile"_"wind profile" (i.e. TSF_LMN refers to the TSF thermodynamic and LMN18 wind profile).

Sounding	Description	Observed Mode (6 hours)
LMN_TOP18	18 UTC Lamont, Oklahoma thermodynamic profile with 18 UTC Topeka, Kansas wind profile	isolated supercell
LMN_TSF	18 UTC Lamont, Oklahoma thermodynamic profile with 18 UTC Fairbury, Nebraska wind profile	isolated supercell
TOP18nocap_LMN	18 UTC Topeka, Kansas thermodynamic profile (cap removed) with 18 UTC Lamont, Oklahoma wind profile	several isolated supercells and east/west linear structure
TOP18nocap_TSF	18 UTC Lamont, Oklahoma thermodynamic profile (cap removed) with 18 UTC Fairbury, Nebraska wind profile	several isolated supercells and some linear structures
TSF_LMN	00 UTC 31 March Topeka, Kansas thermodynamic profile, 18 UTC Salina, Kansas surface observation with 18 UTC Lamont, Oklahoma wind profile	TS squall line
TSF_TOP18	00 UTC 31 March Topeka, Kansas thermodynamic profile, 18 UTC Salina, Kansas surface observation with 18 UTC Topeka, Kansas wind profile	TS squall line

Chapter 5

Discussion and Concluding Remarks

5.1 Synthesis and Discussion

This research began as an investigation into the mechanisms behind three distinct modes of convection within what appeared to be a homogeneous environment. Analysis of the available observations demonstrated that this environment, while broadly similar, contained some significant small scale inhomogeneities, leading to several hypotheses regarding the initiation and evolution of the convective modes that developed. The initial hypotheses regarding these mechanisms focused on convective initiation, suggesting that the different modes initially resulted from either localized environmental inhomogeneities, or that they resulted from different initiation mechanisms. Following the observational case study, both of these hypotheses remained intact, and a third hypothesis was added to address the evolution of the event. Three distinct environments were identified in relation to the three modes of convection, and several variations in how the storms were initiated were identified as well. Additionally, it appeared that the evolution of all three modes in close proximity to each other was made possible by the moderate shear environment in eastern Kansas.

With the results of the idealized modeling simulations, it became evident that while initiation mechanism can play a role in determining mode, the initiation of a given mode is largely dependent on the environment. Within an environment that strongly favors a given mode, such as the LMN18 and TSF environments portrayed in this study, initiation mechanism has little effect on ultimate mode. Within less selective environments, such as the TOP18nocap environment, initiation mechanism does appear to have some importance, particularly with regards to how the initial storms are oriented compared to the vertical wind shear as discussed by Bluestein and Weisman (2000). However, seeing as initiation mechanism played little role in two of the three environments observed on 30 March 2006, it appears that for this case environmental conditions were more important than initiation mechanism in the initial selection of convective mode. The simulations also supported the hypothesis that the moderate shear environment allowed all three modes to evolve in close proximity to each other, as this environment generally did not select for a given mode. In effect, the presence of three separate environments across the region were the key in the development of the three distinct modes of convection on 30 March 2006, and then a moderate shear environment in eastern Kansas allowed them all to evolve in close proximity to each other.

The first of the initial environments was found ahead of the dryline in western Oklahoma where the supercells formed. From the observational case study this environment was seen to have high CAPE (1700 J/kg) and strong vertical wind shear (25 m/s), both parameters that favor the development of supercell thunderstorms. Mid-level winds in this region were oriented largely across the dryline, favoring storm movement off and away from this boundary and its associated linear forcing. Additionally, the 0-6 km vertical wind shear vector was oriented approximately 45° to the dryline, which has been shown by Bluestein and Weisman (2000) to favor the development of a line of long-lived,

non-interacting supercell storms. These observations were further corroborated by the single-bubble idealized control run in this environment: the ultimate mode that developed was an isolated supercell. Further sensitivity testing with idealized simulations demonstrated that both the thermodynamic sounding and wind shear profile from this environment (LMN18) exclusively supported isolated supercell storms. Thus it is quite clear that this environment strongly favored the supercell storms that occurred on 30 March 2006.

The second environment was found farther north along the dryline in central Kansas where the PS line formed. This environment was also characterized by high CAPE (2000 J/kg) and by a 0-6 km shear of 25 m/s, very similar to that found farther south in Oklahoma. However, in this case the 0-6 km shear was oriented along and parallel to the dryline, favoring storm mergers and interactions that would tend to lead toward a linear mode (Bluestein and Weisman 2000). Similarly, the mid-level flow was also oriented along the dryline, preventing the initial storms from moving off of this linear forcing mechanism, a condition that also may favor linear development. Finally, this environment contained a layer of significantly dry air aloft, which likely enhanced the development of strong cold pools in the initial storms. This would also favor linear development as discussed by James et al. (2006). The idealized simulations run using this environment illustrated its favorability for linear modes, as the single bubble control run generated a TS squall line. The environmental sensitivity runs suggested that the dry air aloft was the most important parameter in this respect, as it generated a squall line independent of the wind profile it was paired with. Indeed, the local wind profile supported supercells when paired with other thermodynamic environments. It is likely that in nature the dry air enabled the development of the linear mode while the strong along-line shear promoted the development of the PS mode.

It is also likely that the storm's initiation and continued residence just head of the surface dryline were a factor in its evolution during this event. Although the idealized simulations showed little sensitivity to initiation mechanism within this environment, the observed proximity of the PS line to the dryline throughout its lifetime (e.g. Fig. 3.16) suggest a connection between the two. The dryline likely helped enhance linear development even prior to the development of a large cold pool. In comparison, the supercells to the south that moved off the line remained isolated throughout their lifetimes. It is also possible that the continued linear forcing from the dryline helped maintain the PS mode by inhibiting the reorientation and evolution to TS structure seen in the idealized simulations. Because the idealized simulations did not control for storm motion away from their initial forcing, the possible role of this continued linear forcing was not explored. Although one case is insufficient to draw general conclusions, the apparent connection between the PS line and dryline my have significant implications for forecasting convective mode, and merits future investigation.

The final environment was found well east of the dryline in eastern Kansas where the LS line formed, and where eventually all three modes would be present. This environment was very similar to the supercell environment found in western Oklahoma, containing similar values of CAPE (1966 J/kg) and a similarly shaped hodograph, however the magnitude of the 0-6 km shear was only 18 m/s. This is an important distinction, as 18 m/s falls in a moderate shear range supportive of both multicell and supercell storms (Rasmussen and Blanchard 1998). The single-bubble control simulation in this environment (TOP18nocap) supported the development of an LS line, as well as an isolated supercell at the southern edge of this line. This suggests that the environment supported a range of modes, rather than favoring one specific mode. It is likely that in reality the linear forcing of the colliding outflow boundary helped to initiate storms

in a linear pattern which would favor a linear mode. This, combined with sufficient environmental shear directed in the across-line direction, resulted in the LS mode (Parker and Johnson 2004c). The initiation experiments also suggest that the enhanced lifting of the outflow collision may have been necessary to initiate storms within the weakly capped environment, as other attempts to initiate storms in this environment failed until the cap was removed.

These findings largely corroborate what has long been reported in the literature, which is that the initial convective mode largely depends on the environment (see Chapter 2.2). Indeed, in this case the three modes developed from three distinct environments, each featuring parameters that uniquely favor that given mode. It should be further noted that while the vertical wind shear varied between each of these environments, it was not necessarily the key parameter in deciding the mode. As evidenced by the environmental sensitivity tests, the thermodynamic profile can sometimes be just as selective as vertical wind shear when it comes to convective mode. This was especially true for the case of the TSF profile, as in its native state a TS squall line was the preferred mode, while when the wind profile was paired with the other thermodynamic environments, supercell storms tended to result. This is an important distinction to make, as wind shear is traditionally seen to be of primary importance in forecasting convective mode. As this case illustrates, the attendant thermodynamic regime needs to be accounted for as well, as it can mean the difference between isolated supercells or an intense squall line from a given wind profile.

The next question is how were all three modes able to evolve in close proximity without losing their initial modal characteristics? The answer to this question lies in the environment that the three modes eventually moved into, the same moderate shear environment in eastern Kansas where the LS line formed, described by the 18 UTC

Topeka, Kansas raob. The most important element of this environment was that it did not strongly favor any given mode the way that the TSF and LMN environments favored the PS line and supercells. The battery of environmental sensitivity tests run comparing the various thermodynamic and shear profiles exemplifies this quite clearly as the TOPnocap thermodynamic environment and the TOP18 wind profile played little role in mode selection when combined with parameters from the other two environments. Furthermore, in the TOPnocap single bubble control experiment, both supercell and LS structures were observed, suggesting that the environment was supportive of a range of modes, much like the moderate shear environment described by Weisman and Klemp (1984). This would suggest that the environment alone may have been able to support all three modes. However, there were some other mechanisms aiding in the maintenance of multiple modes within one environment.

Since the LS mode both formed and evolved within the eastern Kansas moderate shear environment, it is likely that the environment alone was enough to support it and thus it is of little surprise that this mode was able to survive. Both the supercells and PS line, though, originated in notably different environments and then moved into the moderate shear environment as they progressed across the region. While it is entirely possible that the moderate shear environment could have supported both of these modes on its own, it appears that each mode was aided in its maintenance by some ancillary mechanisms.

As the PS line moved into the moderate shear environment, it re-oriented itself from a north-south orientation to more of a southwest-northeast orientation. This enabled it to continue to experience line parallel 0-6 km shear, which is a key component to the mode's longevity. After this reorientation, it appears that the environmental shear was sufficient to balance the MCS's cold pool, at least for awhile. Ultimately, the PS

line transitioned to the TS precipitation structure, which is the typical progression for this mode (Parker and Johnson 2000). This may have occurred as a result of a further strengthening of the cold pool, along with the lower environmental shear over eastern Kansas. However a sparse observing network makes it impossible to determine this for sure. Similarly, the supercells were likely aided in their survival through the modification of their local inflow environment. As was demonstrated with the idealized simulations, supercells can locally increase the 0-6 km shear ahead of the storm, presumably allowing them to self-sustain their mode even if the environmental shear decreases. Thus, while the moderate shear in eastern Kansas was marginally supportive of supercells to begin with, this local modification likely further enhanced the supercell's ability to retain their mode by making the environment locally favorable for supercells.

While these local modifications no doubt played a role in the maintenance of all three modes within the moderate shear environment, their effects were largely secondary to those of the environment. Without the moderate shear environment to support all three modes, these additional mechanisms would likely have been overwhelmed by any environmental proclivities for modal selection. For instance, had the shear been lower in the moderate shear environment, the supercells may have been able to sustain themselves by locally modifying the shear profile, however the PS and LS storms likely would have suffered. The PS line likely would have transitioned to TS sooner as the cold pool would have been able to more quickly overcome the shear, and a similar evolution would have befallen the LS line. Indeed, recalling that the moderate shear environment in eastern Kansas was responsible for both initiating *and* sustaining the LS line, a change in shear in this environment would likely have altered the initial LS structure. This study highlights the importance of environment in the initial selection of mode, which occurs long before any local feedbacks can help sustain that mode.

Past literature has long demonstrated the importance of environmental parameters, both thermodynamic and kinematic, to the initial selection of convective mode. This study has further solidified this finding, demonstrating that for the case of 30 March 2006 three distinct modes of convection developed from three distinct environments. This study emphasizes in addition to the vertical shear profile, the orientation of the shear relative to mesoscale boundaries, and variations in the thermodynamic profiles were also important in modal selection, especially within two environments containing similar shear. The important contribution of this work, though, deals with the evolution of convective mode following initiation. In this case, upon their initiation in their respectively favorable environments, three modes of convection were able to evolve for a prolonged period in close proximity to each other within the same environment. A novel conclusion is that moderate amounts of shear in the environment can support a variety of coexisting convective modes rather than forcing just one.

5.2 Conclusion

The multi-modal case of 30 March 2006 was examined using an observational case study and idealized numerical model simulations as a first attempt at determining what mechanisms lead to multiple modes of convection within localized regions. These events provide added challenge to operational forecasters as different severe weather threats tend to be associated with the different modes of convection.

The observational case study suggested that the multiple modes could either be due to mesoscale variations in the environment across the region, or to variations in how the storms were initiated. Within the idealized numerical simulations, storm mode showed little sensitivity to initiation mechanism. Rather, the initiation of the individual modes

was instead tied to three distinct environments. The supercells developed in a high CAPE environment with strong vertical wind shear that favored movement off the initiating dryline. The PS line developed in an environment containing high CAPE and strong along-line vertical wind shear along with a significant layer of dry air aloft favoring the development of strong cold pools. The final environment, characterized by moderate wind shear values in the range between multicells and supercells, supported the development of the LS line while also allowing the supercells and PS line to persist.

Following initiation, multiple modes of convection can evolve within a single environment, provided that the environment contains moderate shear and does not strongly favor any single mode as was the case within the moderate shear environment examined in this study. Sensitivity tests of the kinematic and thermodynamic profiles suggested that the vertical wind shear profile most strongly governed what mode ultimately developed. The main exception to this was that the thermodynamic profile containing dry air aloft favored strong cold pool development, and eventually generated linear modes for all shear profiles tested.

The aim of this research is to help operational forecasters to correctly anticipate convective modes in moderate-high shear environments, and in turn anticipate the associated variety of severe weather threats. Being cognizant not just of the overall environmental shear and thermodynamic structures, but also of more localized effects such as the orientation of shear with respect to boundaries, and the presence of areas of drier air aloft can help better predict initial convective modes. As the storms evolve, awareness of the environment they're moving into, such as changes in the wind shear profile, can provide better anticipation of a changing severe threat. These factors will contribute to better overall situational awareness for forecasters, leading to more effective warnings and statements to alert the public of a severe weather event.

By being cognizant of localized variations in the thermodynamic and shear profiles across the environment in which the storms are forming, the initial convective mode or modes of storms that develop can be better anticipated. Following initiation, awareness of the environment that storms are propagating into, will provide insight into how a convective event will evolve over time, leading to a better anticipation of any changes to the severe weather threat. These factors will contribute to better overall situational awareness for forecasters, leading to more effective warnings and statements to alert the public of a severe weather event.

5.3 Future Work

Through the course of this study several possible avenues of future work have emerged. First and foremost, further investigation of the evolution of convective modes would be useful, especially the effect that movement into a different environment has on storm mode. This study also only began to address how a storm's modification of its environment may affect the maintenance of its convective mode. These modifications may be important to the evolution of convective modes over time, and the present study only examined how a storm alters its own local environment. Further study should also investigate effects that storms have on the environments of nearby storms, essentially what effect the neighboring storms have on each other as they evolve. Also, it is clear that idealized simulations have limitations in such complex scenarios. For example, the continued re-orientation of MCSs to be perpendicular to the vertical shear (as seen in the TSF simulations) precluded an accurate simulation of the PS structure. Determining the features in nature that prevent this from happening, and finding a means to simulate it, would no doubt be useful to both this and other research in the field. As evidenced

by the case study WRF simulation, accurately replicating convective mode in numerical models, both idealized and in a forecast setting, continues to be a considerable challenge. Further work in this realm would benefit both the research and operational communities, leading to better understanding and anticipation of convective storms and their hazards.

Bibliography

Bluestein, H. B. and M. H. Jain, 1985: Formation of mesoscale lines of precipitation: Severe squall lines in Oklahoma during the spring. *J. Atmos. Sci.*, **42**, 1711–1732.

Bluestein, H. B. and S. S. Parker, 1993: Modes of isolated severe convective storm formation along the dryline. *Mon. Wea. Rev.*, **121**, 1354–1372.

Bluestein, H. B. and M. L. Weisman, 2000: The interaction of numerically simulated supercells initiated along lines. *Mon. Wea. Rev.*, **128**, 3128–3149.

Browning, K. A., 1964: Airflow and precipitation trajectories within severe local storms which travel to the right of the mean wind. *J. Atmos. Sci.*, **21**, 634–639.

Browning, K. A., 1977, Part i: Hail physics. *Hail: A Review of Hail Science and Hail Suppression*, No., 38, Amer. Meteor. Soc., 1–43.

Byers, H. R. and R. R. Braham, Jr., 1949: *The Thunderstorm*. U.S. Weather Bureau, Washington.

Davies-Jones, R., J. R. Trapp, and H. B. Bluestein, 2001, Tornadoes and tornadic storms. *Severe Convective Storms*, No., 50, Amer. Meteor. Soc., 167–221.

Dial, G. L. and J. P. Racy, 2004, Forecasting short term convective mode and evolution

for severe storms initiated along synoptic boundaries. Preprints, *22nd Conference on Severe Local Storms*, Hyannis, MA, Amer. Meteor. Soc.

Doswell, C. A., III, 1985: The operational meteorology of convective weather. Vol. ii: Storm scale analysis. Tech. Rep. NOAA Tech. Memo. ERL MSG-15[NTIS Accession No. PB83-162321].

Doswell, C. A., III, 2001, Severe convective storms–an overview. *Severe Convective Storms*, No., 50, Amer. Meteor. Soc., 1–26.

Doswell, C. A., III and D. W. Burgess, 1993, Tornadoes and tornadic storms: A review of conceptual models. *The Tornado: Its Structure, Dynamics, Prediction, and Hazards*, No., 79, Amer. Geophys. Union.

Doswell, C. A., III and J. S. Evans, 2003: Proximity sounding analysis for derechos and supercells: An assessment of similarities and differences. *Atmos. Res.*, **67**.

Edwards, E., S. F. Corfidi, R. L. Thompson, J. S. Evans, J. P. Craven, R. J. P, M. D. W, and M. D. Vescio, 2002: Storm Prediction Center forecasting issues related to the 3 May 1999 tornado outbreak. *Wea. Forecasting*, **17**, 544–558.

Evans, J. S. and C. A. Doswell, 2001: Examination of derecho environments using proximity soundings. *Wea. Forecasting*, **16**, 329–342.

Finley, C. A., W. R. Cotton, and R. A. Pielke, 2001: Numerical simulation of tornadogenesis in a high-precipitation supercell. part I: Storm evolution and transition into a bow echo. *J. Atmos. Sci.*, **58**, 1597–1629.

Fujita, T. T., 1978: *Manual of downburst identification for project NIMROD. SMRP Research Paper 117 [NTIS No. N78-30771/1GI].* University of Chicago, 104 pp.

Gilmore, M. S. and L. J. Wicker, 1998: The influence of midtropospheric dryness on supercell morphology and evolution. *Mon. Wea. Rev.*, **126**, 943–958.

Houze, R. A., Jr., S. A. Rutledge, M. I. Biggerstaff, and B. F. Smull, 1989: Interpretation of Doppler weather radar displays of midlatitude mesoscale convective systems. *Bull. Amer. Meteor. Soc.*, **70**, 608–619.

James, R. P., J. M. Fritsch, and P. M. Markowski, 2005: Environmental distinctions between cellular and slabular convective lines. *Mon. Wea. Rev.*, **133**, 2669–2691.

James, R. P., P. M. Markowski, and Fritsch, 2006: Bow echo sensitivity to ambient moisture and cold pool strength. *Mon. Wea. Rev.*, **134**, 950–964.

Jewett, B. F. and R. B. Wilhelmson, 2006: The role of forcing in cell morphology and evolution within midlatitude squall lines. *Mon. Wea. Rev.*, **134**, 3714–2734.

Johns, R. H. and C. A. Doswell, III, 1992: Severe local storms forecasting. *Wea. Forecasting*, **7**, 588–612.

Kain, J. S., W. S. J, L. J. J, B. M. E, and B. D. R, 2006: Examination of convection-allowing configurations of the WRF model for the prediction of severe convective weather: The SPC/NSSL spring program 2004. *Wea. Forecasting*, **21**, 167–181.

Lemon, L. R. and C. A. Doswell, III, 1979: Severe thunderstorm evolution and mesocyclone structure as related to tornadogenesis. *Mon. Wea. Rev.*, **107**, 1184–1197.

Lin, Y.-L., R. D. Farley, and H. D. Orville, 1983: Bulk parameterization of the snow field in a cloud model. *J. Climate Appl. Meteor.*, **22**, 1065–1092.

Maddox, R. A., 1980: Mesoscale convective complexes. *Bull. Amer. Meteor. Soc.*, **61**, 1374–1387.

McCaul, E. W. and C. Cohen, 2002: The impact on simulated storm structures and intensity of variations in the mixed layer and moist layer depth. *Mon. Wea. Rev.*, **130**, 1722–1748.

McCaul, E. W. and M. L. Weisman, 2001: The sensitivity of simulated supercell structure and intensity to variations in the shapes of environmental buoyancy and shear profiles. *Mon. Wea. Rev.*, **129**, 664–687.

McNulty, R. P., 1995: Severe and convective weather: A central region forecasting challenge. *Wea. Forecasting*, **10**, 187–202.

Mesinger, F., G. DiMego, E. Kalnay, K. Mitchell, P. C. Shafran, W. Ebisuzaki, D. Jovic, J. Woollen, E. Rogers, E. H. Berbery, M. B. Ek, Y. Fan, R. Grumbine, W. Higgins, H. Li, Y. Lin, G. Manikin, D. Parrish, and W. Shi, 2006: North American regional reanalysis. *Bull. Amer. Meteor. Soc.*, **87**, 343–360.

Parker, M. D., 2007a: Simulated convective lines with parallel stratiform precipitation. Part I: An archetype for convection in along-line shear. *J. Atmos. Sci.*, **64**, 267–288.

———, 2007b: Simulated convective lines with parallel stratiform precipitation. Part II: Governing dynamics and associated sensitivities. *J. Atmos. Sci.*, **64**, 289–313.

Parker, M. D. and R. H. Johnson, 2000: Organizational modes of midlatitude mesoscale convective systems. *Mon. Wea. Rev.*, **128**, 3413–3436.

———, 2004a: Simulated convective lines with leading precipitation.Part I: Governing dynamics. *J. Atmos. Sci.*, **61**, 1637–1655.

———, 2004b: Simulated convective lines with leading precipitation.Part II: Evolution and maintenance. *J. Atmos. Sci.*, **61**, 1656–1673.

———, 2004c: Structures and dynamics of quasi–2d mesoscale convective systems. *J. Atmos. Sci.*, **61**, 545–567.

Pettet, C. R. and R. H. Johnson, 2003: Airflow and precipitation structure of two leading stratiform mesoscale convective systems determined from operational datasets. *Wea. Forecasting*, **18**, 685–699.

Przybylinski, R. H., 1995: The bow echo: Observations, numerical simulations and severe weather detection methods. *Wea. Forecasting*, **10**, 203–218.

Rasmussen, E. N. and D. O. Blanchard, 1998: A baseline climatology of sounding–derived supercell and tornado forecast parameters. *Wea. Forecasting*, **13**, 1148–1164.

Rotunno, R., J. B. Klemp, and M. L. Weisman, 1988: A theory for strong, long–lived squall lines. *J. Atmos. Sci.*, **45**, 463–485.

Schumacher, R. S. and R. H. Johnson, 2005: Organization and environmental properties of extreme–rain–producing mesoscale convective systems. *Mon. Wea. Rev.*, **133**, 961–976.

Skamarock, W. C., J. B. Klemp, J. Dudhia, D. O. Gill, D. M. Barker, W. Wang, and J. G. Powers, 2005: A description of the advanced research WRF version 2. Tech. Rep. NCAR/TN-468+STR.

Wakimoto, R. M., 2001, Convectively driven high wind events. *Severe Convective Storms*, No., 50, Amer. Meteor. Soc., 255–298.

Weisman, M. L. and J. B. Klemp, 1982: The dependence of numerically simulated convective storms on vertical wind shear and buoyancy. *Mon. Wea. Rev.*, **110**, 504–520.

———, 1984: The structure and classification of numerically simulated convective storms in directionally varying wind shears. *Mon. Wea. Rev.*, **112**, 2479–2498.

Weisman, M. L., J. B. Klemp, and R. Rotunno, 1988: Structure and evolution of numerically simulated squall lines. *J. Atmos. Sci.*, **45**, 1990–2013.